Table of Contents

1. Capture Studies

1.1 Post Combustion Technology

1.1.1 Adsorption Technology

1.1.1.2 Radical Chemistry (Self Assembled Nanopourous Materials for CO_2 Capture)

Report Title

CO_2 Capture Project - An Integrated, Collaborative Technology Development Project for Next Generation CO_2 Separation, Capture and Geologic Sequestration

Radical Chemistry (Self Assembled Nanopourous Materials for CO_2 Capture)

Report Reference

1.1.1.2

Type of Report:	Semi-Annual Report
Reporting Period Start Date:	February 2003
Reporting Period End Date:	July 2003
Principal Author(s):	Ripudaman Malhotra, Albert S. Hirschon, and Anne Venturelli
Date Report was issued:	August 2003
DOE Award Number:	DE-FC26-01NT41145
Submitting Organization:	SRI International
Address:	333 Ravenswood Avenue Menlo Park, CA 94025 USA

1.1.1.2.1 Abstract

Under a contract with the CO_2 Capture Project (CCP), SRI International (SRI) has been conducting research on novel self-assembled nanoporous materials that could be used in a pressure-swing adsorption (PSA) system to capture CO_2 from flue gases of power plants. The materials SRI proposed to develop were inspired by the work of Seki who has shown that a range of structures can be built using copper salts of dicarboxylic acids. These materials have a square cavity whose dimensions can be controlled by the choice of the dicarboxylic acid. Solids with cavities large enough to accommodate four to five methane molecules were shown to have the highest capacity for methane. SRI proposed to synthesize and test these materials that would physisorb CO_2 by relatively weak van der Waals forces and that would have have a high adsorption capacity for CO_2. For structures that could accommodate multiple CO_2 molecules at each site, there is the possibility that the binding of CO_2 would be cooperative. Binding is considered cooperative when subsequent molecules of CO_2 adsorb onto the material with slightly greater heats of adsorption. In such a case, the PSA system would require less work to capture an equivalent amount of CO_2 than a noncooperative system. During 2002, we demonstrated the thermodynamic validity of our concept and also demonstrated the computational tools necessary for designing these materials. This year we embarked on a program of synthesizing, characterizing and testing a leading candidate, copper terephthalate, with the objective of providing a cost estimate for a PSA system that uses it as the sorbent. This report describes the progress made since March 2003 when this phase of the project began.

The procedure for the synthesis of the 3-D complexes as described by Seki in his papers and patents leaves out many details such the strength of formic acid, the order of addition as well as heat treatment details. We undertook a study of many of the synthesis variables in our attempt to optimize and scale-up the procedure. Over fifty different preparations were conducted, of which thirty-one were taken through the second stage to obtain the 3-D complexes. The surface areas of the complexes were determined by single-point BET measurements. The surface areas of the products ranged from 20 m^2/g to 1200 m^2/g. The total amount of product with surface area in excess of 900 m^2/g is about 10 g. We also received 300 g of the 3-D complex of copper terephthalate from Seki which had a surface area of 600 m^2/g. Samples (30 g) of the Seki product and pooled SRI product with surface area greater than 1000 m^2/g were sent to Adsorption Research Inc. (ARI) for further testing. We also characterized selected products by scanning-electron microscopy, X-Ray diffraction, and thermogravimetry.

ARI performed static absorption tests with the SRI product with CO_2 and N_2. They noted that the CO_2 isotherm did not level off even at the highest pressures they tested. This result is consistent with a very high capacity of the material to adsorb CO_2. They estimate the selectivity of the material for CO_2 over N_2 is about 8.

1.1.1.2.2 Table of Contents

1.1.1.2.3 List(s) of Graphical Materials

1.1.1.2.4 Introduction

Under a contract with the CO_2 Capture Project (CCP), SRI International (SRI) has been conducting research on novel self-assembled nanoporous materials that could be used in a pressure-swing adsorption (PSA) system to capture CO_2 from flue gases of power plants. For the purpose of minimizing wasted heat, it is desirable to operate the PSA system at low temperatures, preferably around 40°C. This requirement means that the heat of adsorption of CO_2 on the adsorbent should be only around 30 kJ/mol, and not much larger. SRI proposed to develop materials that would physisorb CO_2 by relatively weak van der Waals forces and that would have a high adsorption capacity for CO_2.

The nanoporous materials that we proposed to study were inspired by the work of Seki who has shown that a range of structures can be built using copper salts of dicarboxylic acids.[1,2] These materials have a square cavity whose dimensions can be controlled by the choice of the dicarboxylic acid. Further, these framework structures self-assemble upon mixing of the solutions of the metal ions and the dicarboxylic acid. Seki reports the adsorption capacity of the copper salt of biphenyl dicarboxylic acid to be 212 cc of methane (STP) per gram of the salt, which translates to 9.5 moles of gas per Kg solid.[3] This is a very high value, and in a review article for *Nature*, Davis writes that the adsorption capacity of the salts synthesized by Seki "exceeds that of any other known crystalline material.[4] The high adsorption capacity results from optimizing the pore size and wall surfaces. The pores are large enough to accommodate multiple methane molecules yet not too large that many methane molecules in the cavity are left without direct access to the walls. Figure 1.1.1.2.4*(1)* shows one layer of copper oxalate, a representative of this family of framework solids.

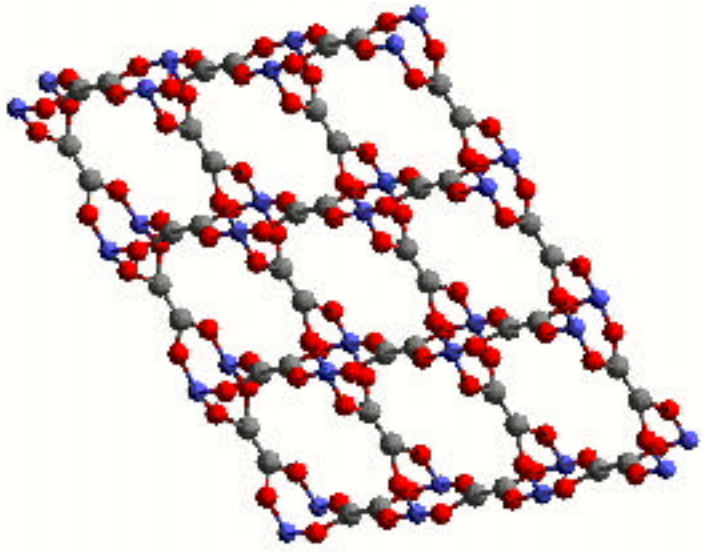

Figure 1.1.1.2.4 *(1)*. Simulated structure of copper oxalate.

We anticipated that the CO_2 molecules would be held in the cavities (i.e., cells where CO_2 can bind). The dimensions of the cavity could be tailored by the choice of the dicarboxylic acid. For structures that could accommodate multiple CO_2 molecules at each site, there is the possibility that the binding of CO_2 would be cooperative. Binding is considered cooperative when subsequent molecules of CO_2 adsorb onto the material with a slightly greater heats of adsorption. In such a case the PSA system would require less work to capture an equivalent amount of CO_2 than a non-cooperative system. Our original research program called for surveying many variants on these structures by molecular modeling and then preparing and testing those systems that showed the most promise.

During 2002, we worked on two tasks: thermodynamic validation and modeling tools. Under Task 1, we demonstrated the validity of the concept, including that of cooperative binding. The modeling tools needed for this work included those required for performing *ab-initio* quantum mechanical calculations on the structures, semi-empirical calculations for adsorption of CO_2 in the lattices, as well as fluid mechanics tools for calculating the breakthrough of CO_2 from packed beds. The objective of Task 2 was to demonstrate that all the modeling tools were functional by end of FY2002, and that we would conduct the exploration of various structures in FY2003. We have achieved our 2002 goal for this task, and have calculated the structures of copper oxalate and copper terephthalate. We have also calculated the heats of adsorption of CO_2 on these materials. In the case of copper terephthalate, which can accommodate four CO_2 molecules at each site, we have calculated the energetics of each additional CO_2 molecule. We have also obtained software to calculate the breakthrough curves for CO_2 through a packed bed, and determined flow conditions that would correspond with cycle times around 3-4 min and yet have sharp breakthroughs such that the entire bed will be used effectively.

However, in view of the fact that the CCP project will terminate in September 2003, by which time all the technologies must be evaluated, we proposed to conduct a focused effort on one system that had already shown some promise. Last September, we learned from Dr. Seki that the copper terephthalate system has a very high capacity for CO_2.[5] These preliminary studies have been conducted on a very small scale, and there are no data on how these materials perform in the presence of interfering gases. Accordingly, we undertook experimental studies on this material to obtain the necessary information to enable us to estimate the capital and operating expenses of a PSA system utilizing copper terephthalate.

A reliable cost comparison between systems inevitably requires the use of models. Models for full-scale PSA systems are complex, and they require as input operating conditions, adsorption coefficients, and mass-transfer coefficients, many of which depend on the size and shape of the unit. We will make the comparison with each system operating under its optimal conditions. The parameters to be used in the ASPEN (or similar) code will be extracted from experimental studies that will be conducted in a well-characterized test-bed under several conditions and ensure that we extract accurate mass transfer coefficients. We are teaming with Adsorption Research Inc. (ARI), a small business operated by Dr. Kent Knaebel, who is a world-renowned expert in this area. ARI is fully equipped to perform the tests with rapid turnaround time. This teaming arrangement will allow each party to focus on their respective strengths: SRI on the synthesis and characterization of the materials, and ARI on adsorption tests and PSA modeling. Finally, we will together perform the cost analysis based on a model developed by SRI's Process Economics Program.

1.1.1.2.5 Executive Summary

The procedure for the synthesis of the 3-D complexes as described by Seki in his papers and patents consists of two steps. In Step 1 a 2-D complex of copper terephthalate is formed. This intermediate is then pillarized with triethylenediamine (TED) to give the 3-D complex. However, the description leaves out many details such the strength of formic acid ,the order of addition, and the heat treatment conditions. Also, the amounts of solvents used were such that simple scaling would require prohibitively large volumes. For example in one procedure over 200 cc of methanol are used in the first step to prepare about 0.3 g the copper terephthalate. It also appeared to us that the second step, pillarization with TED, was the bottleneck in the production process. However, the patent also cautions that there are potential problems with byproducts at higher concentration, thus simply increasing the concentration to process a larger amount in a given auotoclave experiment was not an option.

We undertook a study of many of the process variables in our attempt to optimize and scale-up the synthesis. Over fifty different preparations were conducted, of which thirty-one were taken through the second stage to obtain the 3-D complexes. These experiments have led us to a preferred procedure, which is rapid and convenient. The synthesis procedure is still not optimized and there are factors that we do not fully understand that lead to variability in product quality.

The complexes were characterized by single-point BET surface area measurements. The surface areas of the products ranged from 20 m^2/g to 1200 m^2/g. We found that slow layering of a methanolic copper solution on top of a DMF solution of terephthalic acid and formic acid, generally correlated with higher surface areas. However, there were also a few runs in which the addition was rapid and yet the product had a high surface area in excess of 1000 m^2/g. Thus, slow layering, which was a tedious step, does not appear to be critical.

We determined the pore-size distribution for one sample. It had a surface area of 450 m^2/g, and more than 90% of the area was found to be in pores less than 20Å. This result is in accord with the molecular simulation conducted last year, which showed the cavities in copper terephthalate to be about 10Å. Further experiments with materials of surface areas greater than 1000 m^2/g have yet to conducted to insure that even in these materials most of the porosity is in the nanopores.

We characterized selected products by scanning-electron microscopy (SEM), X-Ray diffraction (XRD), and thermogravimetric analysis (TGA). Surface morphologies of the sample from Dr. Seki and a high surface area product from SRI were determined by SEM. Dr. Seki's sample has a cubic morphology but the SRI sample had many lamellar structures. The abundance of edge features is probably responsible for the relatively higher surface area of the SRI product.

XRD is an important diagnostic for determining crystallinity and nanoporosity. Seki had noted that intensity of the peak at $2\theta = 9°$ relative to that at 16° correlates with .the nanoporosity of the crystals. In this respect, the SRI product has a more intense peak at $2\theta = 9°$ than the Seki product, although it is not as intense as in the spectrum reported in the literature.

TGA of the Seki product shows weight loss beginning around 280°C and occurs in three stages with steepest losses at 332, 365 and 400°. The three stages probably correspond to the loss of loosely bound TED (pillaring material), tightly bound TED, and the organic matrix. The final residue is 30% of the original weight. SRI product #50A showed a very similar thermogram, albeit the proportion of weight losses in the three stages were somewhat different. Two of SRI products showed an additional weight loss peak at 200°C, and in these samples the residue is about 18%. We suspect that these samples wee not fully dried and had some solvent associated with them.

The total amount of product with surface area in excess of 900 m^2/g is about 10 g. We also received 300 g of the 3-D complex of Seki prepared copper terephthalate. This sample had a surface area of 600 m^2/g.

A sample (30 g) of the Seki product and several SRI products with surface area greater than 900 m^2/g were sent to Adsorption Research Inc. (ARI) for further testing.

ARI measured the absorption of CO_2 and N_2 on one of the SRI products. They noted that the CO_2 isotherm did not level off even at the highest pressures they tested (1 atm. CO_2, which corresponds to 20 atm flue gas containing 5% CO_2). This result is consistent with a very high capacity of the material to adsorb CO_2. They estimate the selectivity of the material for CO_2 over N_2 is about 8.

During the isotherm determination, some points were recorded during pressurization, while others during depressurization. The fact that both sets of points lie on the same line attests to fairly rapid diffusion and lack of any hysteresis. Both of these features bode well for a PSA application. Tests with the Seki product and a reference material, silicalite, are under way.

The next steps include conducting dynamic tests in which simulated flue gas will be flown through a bed packed with pressed pellets of the 3-D complex. We will monitor the breakthrough of CO_2 from the bed as a function of flow conditions. The data will yield parameters that will help us design a laboratory PSA system, whose performance will then be used in a process model to design and estimate the cost of a full scale PSA system. We have already received the flow conditions and product specifications from the CCP and expect to complete the tasks on time.

1.1.1.2.6 Experimental

1.1.1.2.6.1 Synthesis of the 3-D Complex of Copper Terephthalate • Triethylene Diamine

Papers and patents by Seki describe a general procedure for the synthesis of the complexes in a 2 to 5 g range. The synthesis consists of two steps. In Step 1 a 2-D complex of copper terephthalate is formed. This is then pillarized with triethylenediamine (TED) to give the 3-D complex. A typical synthesis consists of dissolving $CuSO_4 \bullet (H_2O)_5$ in methanol, and terephthalic and formic acids in DMF followed by slow addition of the copper solution to the acid solution. The mixture is left standing at 50°C over a period of several days a 2-D complex of copper terephthalate crystallizes out. The crystals are then heated to 160°C with TED in toluene in an autoclave to form the 3-D complex. A procedure that resulted in a high surface area product follows.

Copper sulfate pentahydrate (3.1g) was added to 50 mL of methanol and the flask was swirled to dissolve the solid. Terephthalic acid (2.1g) and formic acid (3.2mL) were added to 100 mL of DMF and dissolved with stirring. The blue copper methanolic solution was added in one portion to the DMF solution producing a momentary (~5seconds) homogeneous solution, which was followed by a slow precipitation. The mixture was placed in a 50°C water bath. After 13 days, the mixture was filtered, washed with methanol (3x250 mL) followed by of water (3x50 mL). The blue solid was transferred to an autoclave sleeve. TED (0.806g) was dissolved in 80mL of methanol and 40mL of toluene and added to sleeve. The mixture was placed in autoclave, purged with N_2, and heated to 161°C. After four hours at temperature, the mixture was cooled to room temperature, filtered, and washed with methanol to give a pale blue solid. The solid was dried at 100°C for four hours under vacuum. Yield 2.90 g.

1.1.1.2.6.2 Surface Area Determination

The surface areas of the product were determined on a Micrometrix Model TPD/TPR 2900 apparatus. Argon gas was adsorbed on 100 mg of sample at –186°C (bp of Ar) and desorbed by warming the sample to room temperature. The data were treated by the single-point BET algorithm.

1.1.1.2.6.3 Scanning Electron Microscopy

Powder samples were mounted on conducting carbon tape and gold sputter-coated to prevent charging of the samples. Imaging was performed with a LEO 435VP Scanning-Electron Microscope using a secondary electron detector, with excitation voltages of 20 kV and 30 kV.

1.1.1.2.6.4 X-Ray Diffraction

The X-ray diffraction spectra were obtained using a Philips X-ray diffractometer with a copper anode operating at 45 kV and 30 mA. The sample size was 2 cm x 2 cm. The incident X-rays were collimated and the diffracted X-ray signal was detected after monochromation with a Ge crystal, with a solid state detector. The spectra were recorded using a computer equipped with Radix data acquisition system. The data was analyzed using Jade X-ray analysis program.

1.1.1.2.6.5 Thermogravimetric Analysis

Thermogravimetric analysis of the samples was performed on a TA Instruments model 2050 TGA with a model 5200 controller. The TGA was calibrated for temperature and weight using the manufacturer procedures. Data analysis was performed using TA Instruments' Universal Analysis 2000 software. The TGA was purged thoroughly with argon prior to use. Purge rate for the sample runs was 100 ml/min argon. After auto-taring the TGA balance, 5 to 12 mg of sample was loaded into the TGA platinum pan. An initial weight stabilization period of 2 minutes was allowed. The sample was then heated from

ambient temperature to about 1000° C at 10° C/min. Data were acquired on the 5200 Controller and then analyzed.

1.1.1.2.6.6 Static Adsorption Tests

The apparatus for measuring the adsorption isotherms is shown in Figure 1.1.1.2.6*(1)*. These tests are conducted in a static mode. The adsorbent is loaded into the B cell inside a 25-µm filter. Unless severely agitated, the sample powder stayed inside the filter. We measured the solid density of the powder by pulling a vacuum on the entire cell. The assumption is that none of the helium is adsorbed by the adsorbent but it can reach all of the pores. The solid density is needed for calculating the isotherm.

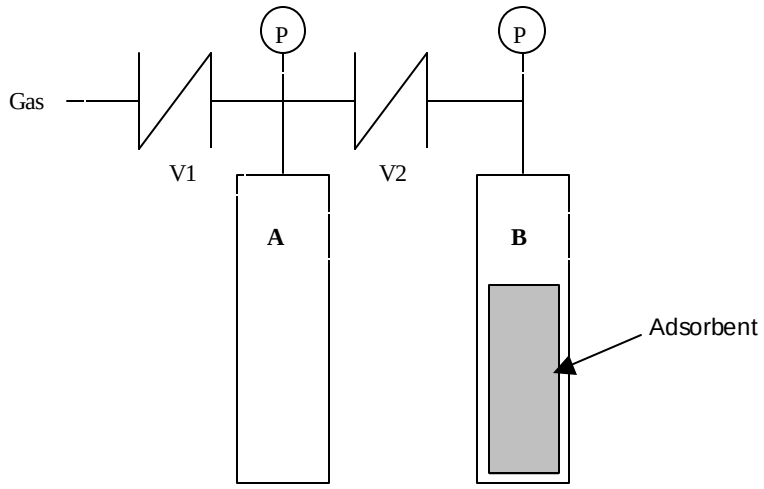

Figure 1.1.1.2.6*(1)*. Apparatus for static adsorption tests to determine isotherms.

Determination of each point on the isotherm uses the same basic procedure as measuring the solid density. Since the volumes of cells A and B are known as well as the mass and solid density of the adsorbent, we can use the ideal gas law to calculate how much gas must have been adsorbed by measuring the change in pressure in the cell. We start with a vacuum in the entire cell. With valve V2 closed cell A is "charged" with a certain volume of gas (initial pressure). Valve V1 is then closed, and we wait until the pressure reading is stable in cell A. Valve V2 is then opened and we again wait until the pressure is stabilized and that is the final pressure. Again, by using ideal gas law, we can compute the amount of gas in the vapor phase, and—from the difference between that and the initial charge—the amount adsorbed.

1.1.1.2.7 Results and Discussion

1.1.1.2.7.1 Material Synthesis

The procedure for the synthesis of the 3-D complexes as described by Seki in his papers and patents consists of two steps. In Step 1 a 2-D complex of copper terephthalate is formed. This intermediate is then pillarized with triethylenediamine (TED) to give the 3-D complex. However, the description leaves out many details such the strength of formic acid ,the order of addition, and the heat treatment conditions. Also, the volumes of solvents used are quite large and scaling the synthesis for larger preparations could cause difficulties. For example in one procedure over 200 cc of methanol was used in the first step to prepare about 0.3 g of the copper terephthalate. It also appeared to us that as described in the second step, pillarization with TED, was the bottleneck in the production process. However, the patent also cautions that there are potential problems with by products at higher concentration, thus simply increasing the concentration to process a larger amount in a given auotoclave experiment was not an option.

We undertook a study of many of the synthesis variables in our attempt to optimize the procedure. Some of the key questions that we considered include the following.

1. The procedure in the patent involves first making a solutions of copper sulfate and carboxylic acid, dripping or slowly adding the copper complex to the acid solution, and then letting the mixture sit for a number of days. Is the order of addition important? Is addition of copper solution to the solution of organic acid preferred over the addition of the organic acid to the copper solution?
2. Once the solutions are mixed, is there a reason for not stirring, or does it really make a difference?
3. What happens during the time that the mixture sits? Once a precipitate forms is there a continuation of reaction? Is there any advantage in waiting several days, and if so can the process be accelerated by heating?
4. The procedure calls for the use of copper sulfate as the copper salt, and it also uses a relatively large excess of formic acid? What is the purpose of formic acid? What happens if it is not added? What is the strength of the formic acid? It is available in two standard strengths of 96% and 88%. Is there a role of water?
5. In the preparation of the 3-D complex, it is not clear if the TED is added directly to the solution that had been standing for several days or if it is first filtered? If filtered, should it also be refortified with additional formic acid?
6. In the second step toluene is used as the solvent. However, methanol is also a very good solvent for TED. Does the toluene help in the pillaring with TED? Is there a problem with washing out the 2-D complex?
7. Is the autoclave used mainly for heating without solvent loss? Can we use a higher boiling solvent to pillar the complex with without an autoclave? Cumene, a higher homologue of toluene with similar solubility properties, has a boiling point of 152°C. Could we heat the 2-D complex with TED in cumene under reflux and obtain the 3-D complex?

We sent a message to Dr. Seki with our concerns and questions, but he was unable to answer them because of intellectual property considerations. He was however willing to send us a 300 g sample of his product so that we could conduct tests with his material. This material was recently received at SRI, and about 30 g of the product was sent to Adsorption Research Inc.

During the reporting period we conducted over fifty preparations by varying experimental parameters; thirty-one of these were taken through the second stage to yield the 3-D complexes. The runs were mostly on 3-6 g scale. The total amount of product with surface area in excess of 900 m^2/g is about 10 g, and it was sent to Adsorption Research Inc.

1.1.1.2.7.2 Product Characterization

1.1.1.2.7.2.1 Surface Area Measurements

The 3-D complexes showed a large variation in surface areas ranging from 20 m^2/g to 1200 m^2/g. Most of the low surface area products were obtained when we first began the work. We found that slow layering of cooper solution on top of a DMF solution of terephthalic acid and formic acid to generally correlate with higher surface areas. However, there were also a few runs in which the addition was rapid and yet the product had a high surface area in excess of 1000 m^2/g. Figure 1.1.1.2.*7(1)* shows a histogram of the number of preparations that resulted in samples with surface areas in various ranges for both slow-addition and rapid-mixing experiments. For one sample of surface area about 450 m^2/g, we also determined the pore-size distribution. Greater than 90% of the area was found to be in pores less than 20Å. This result is in accord with the molecular simulation conducted last year, which showed the cavities in copper terephthalate to be about 10Å. In order for the material to be effective in a PSA, we want most of the surface area in nanopores.

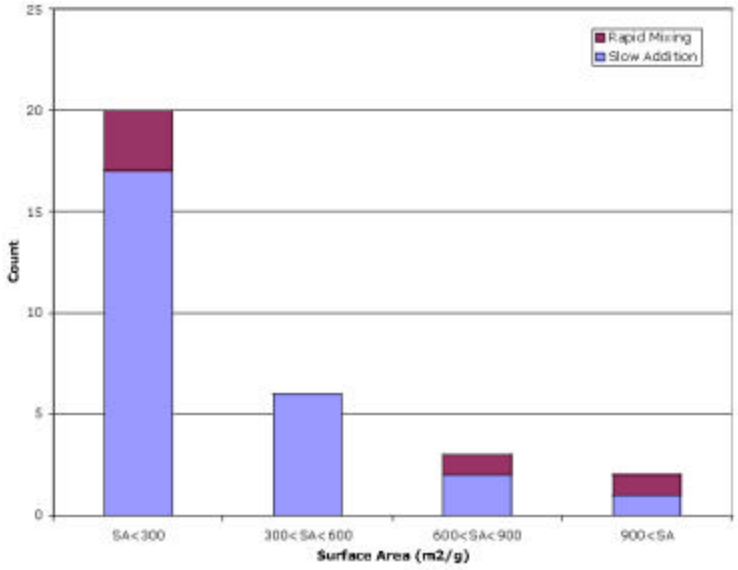

Figure 1.1.1.2.7 *(1)*. Distribution of surface areas of 3-D complexes.

1.1.1.2.7.2.2 Scanning-Electron Microscopy

Sample morphology was determined by using Scanning Electron Microscopy (SEM). Micrographs of the product from Dr. Seki and an SRI sample with high surface area are shown in Figures 1.1.1.2.7*(2)* and 1.1.1.2.7*(3)* respectively. Dr. Seki's sample has a cubic morphology but the SRI sample tends to show many lamellar structures, which could be responsible for the relatively higher surface area.

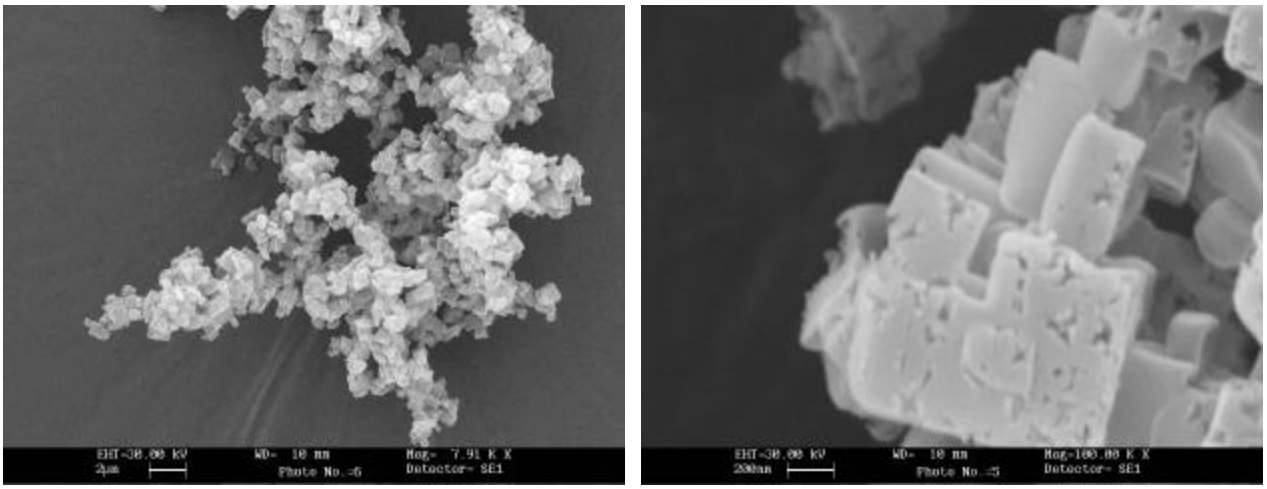

Figure 1.1.1.2.7 *(2)*. Scanning-electron micrographs of Seki product (Surface area: 600 m^2/g).

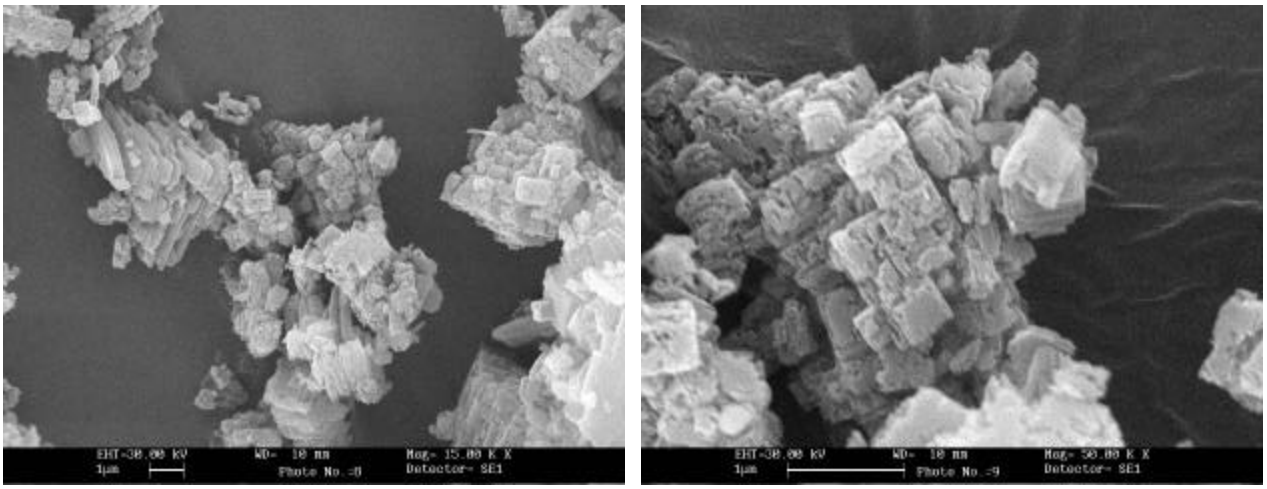

Figure 1.1.1.2.7 *(3)*. Scanning-electron micrographs of SRI product (Surface area: >1000 m^2/g).

1.1.1.2.7.2.3 X-Ray Diffraction

Seki has used XRD as an important diagnostic for the copper salts of dicarboxylic acids. In particular he has noted that intensity of the peak at $2\theta = 9°$ relative to that at 16° correlates with the nanoporosity of the crystals. The XRD spectra of the Seki product and the SRI products shown in Figures 1.1.1.2.7*(4)* and 1.1.1.2.7*(5)*. Both of these spectra were recorded at SRI. The SRI product has a more intense peak at $2\theta = 9°$, although it is not as intense as in the spectrum reported in the literature, which is reproduced in Figure 1.1.1.2.7*(6)*. Note that in this spectrum the peak at $2\theta = 9°$ is about twice as intense as the peak at $2\theta = 16°$.

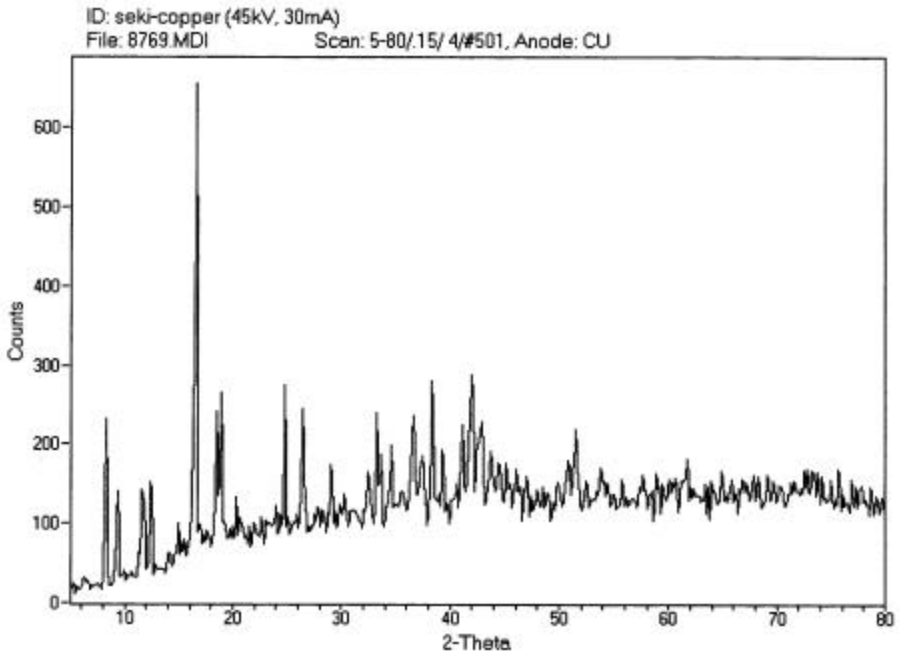

Figure 1.1.1.2.7 *(4)*. XRD spectrum of the Seki 3-D copper terephthalate•TED complex.

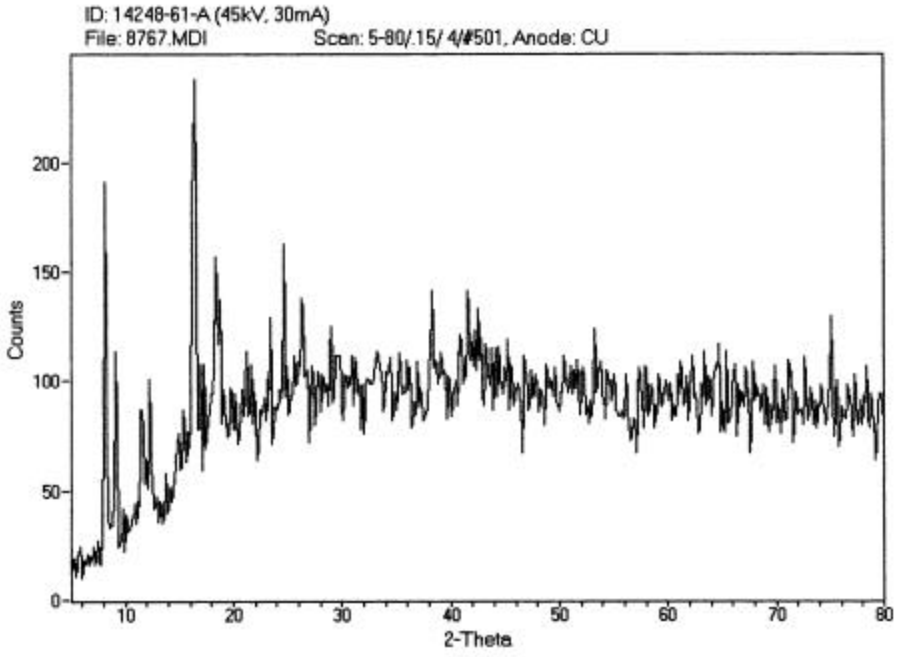

Figure 1.1.1.2.7 *(5)*. XRD spectrum of the SRI 3-D copper terephthalate•TED complex.

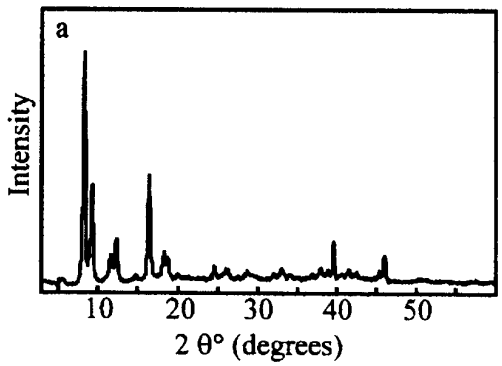

Figure 1.1.1.2.7 *(6)*. Published XRD spectrum of the 3-D Complex.

1.1.1.2.7.2.4 Thermogravimetry

The thermal stability of the Seki product along with several SRI products was assessed by thermogravimetric analysis. The TGA of the Seki product is shown in Figure 1.1.1.2.7*(7)*. The weight loss begins around 280°C and occurs in three sta ges with steepest losses at 332, 365 and 400°C as can be better seen in the differential plot (green). The three stages probably correspond to the loss of loosely bound TED (pillaring material), tightly bound TED, and the organic matrix. The final residue is 30% of the original weight. The SRI product 50A has a very similar thermogram, albeit the proportion of weight loss in the three stages is somewhat different (Figure 1.1.1.2.7*(8)*.. The final residue is again 30%. This product has a surface area 546 m^2/g which is comparable to that of the Seki product. However, this sample had a slightly greenish tint to it. As shown in Figures 1.1.1.2.7*(9)* and 1.1.1.2.7*(10)*, SRI samples 61A (surface area 1238 m^2/g) and 42A (surface area 669 m^2/g) show an additional weight loss peak at 200°C, and in these samples the residue is about 18%. We suspect that these samples were not fully dried and had some solvent associated with them.

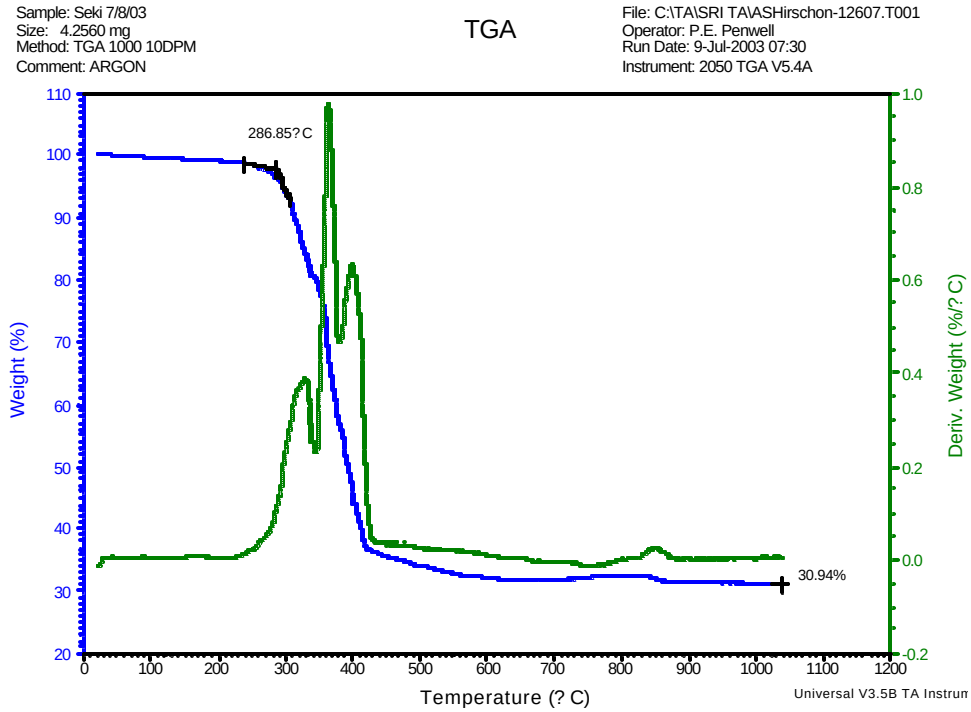

Figure 1.1.1.2.7 *(7)*. TGA of the Seki product.

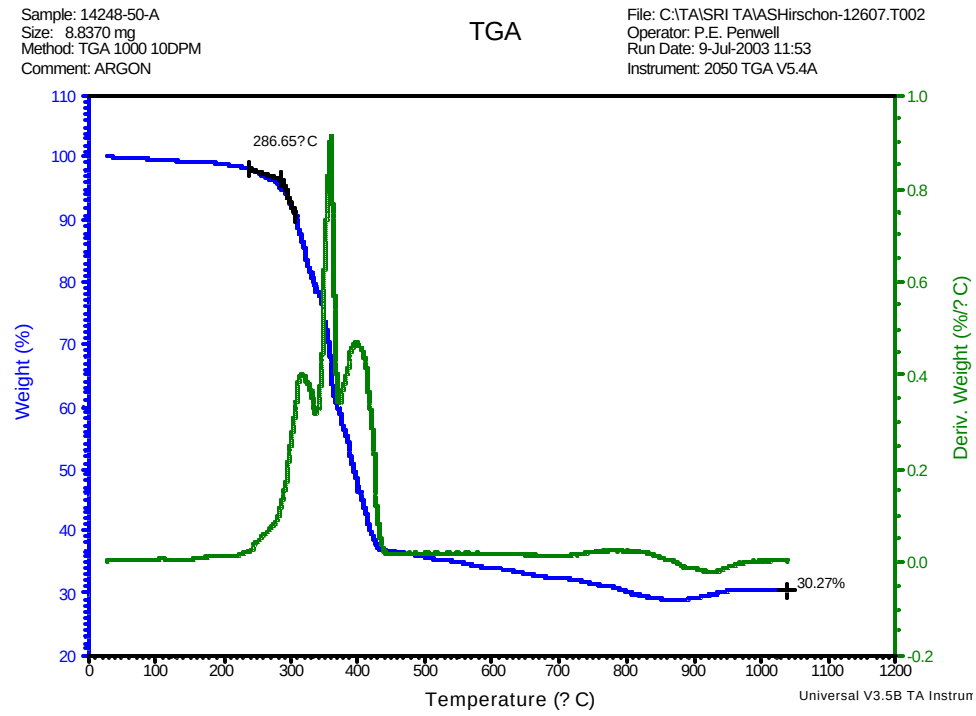

Figure 1.1.1.2.7 *(8)*. TGA of the SRI product 50A.

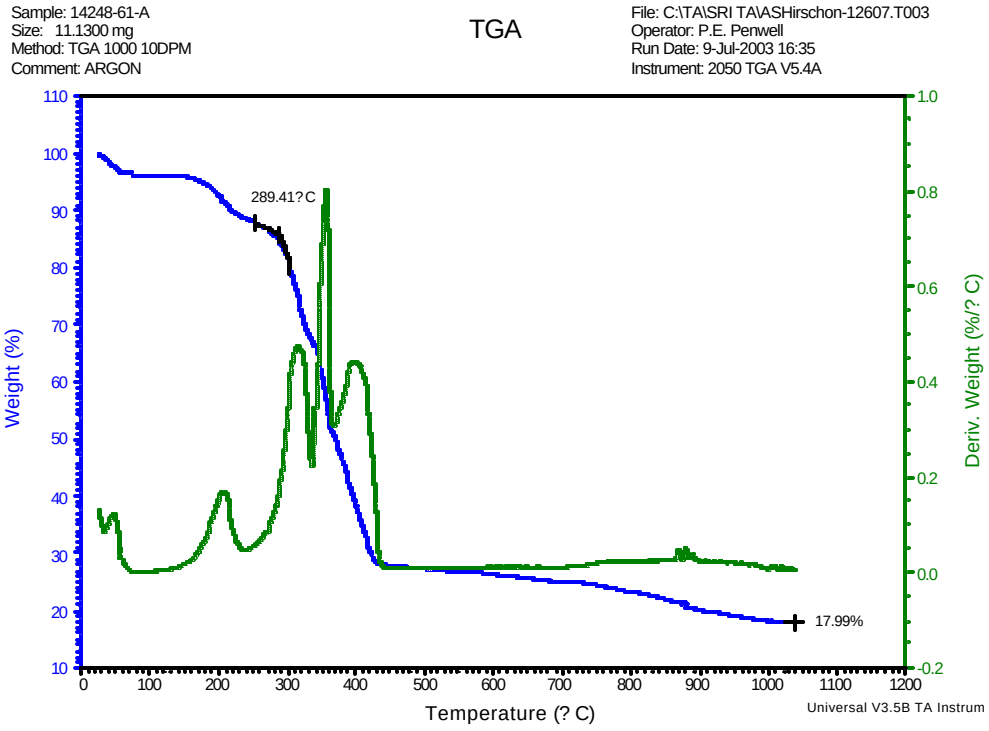

Figure 1.1.1.2.7 *(9)*. TGA of the SRI product 61A.

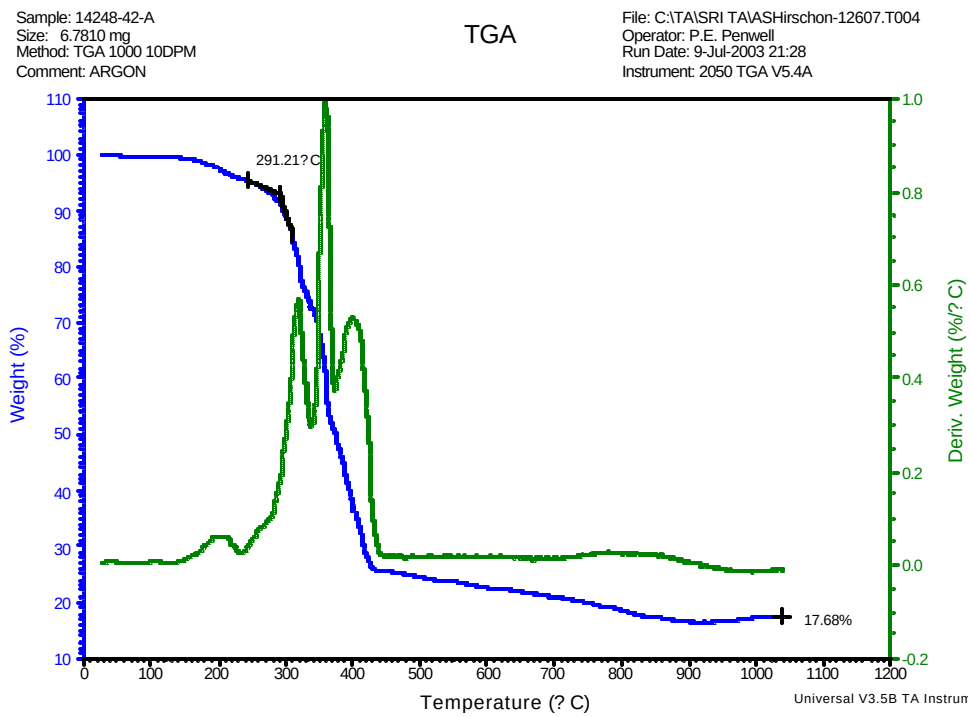

Figure 1.1.1.2.7 *(10)*. TGA of the SRI product 42A.

1.1.1.2.7.3 Static Adsorption Tests

Static Adsorption tests were conducted by Adsorption Research Inc., a subcontractor. Within the reporting period, adsorption isotherms for only one SRI sample was determined for CO_2 and N_2. The results are shown in Figure 1.1.1.2.7*(11)*. ARI noted that the CO_2 isotherm did not level off even at the highest pressures they tested (15 psia or 1 atm). Because flue gas contains about 5% CO_2, this pressure of CO_2 corresponds to pressurizing the flue gas to 20 atm. This result is consistent with a very high capacity of the material to adsorb CO_2. ARI estimates the selectivity of the material for CO_2 vs. N_2about 8. Some of the points in each of the isotherms were recorded during pressurization, while others during depressurization. The fact that both sets of points lie on the same line attests to fairly rapid diffusion and lack of any hysteresis. Both of these features bode well for a PSA application. Tests with the Seki product and a reference material, silicalite, are under way.

1.1.1.2.7.4 Next Steps

The next steps include conducting dynamic tests in which simulated flue gas will be flown through a bed packed with pressed pellets of the 3-D complex. We will monitor the breakthrough of CO_2 from the bed as a function of flow conditions. If we perform the breakthrough tests with powders, we are likely to encounter very large pressure drops and the results will not be relevant to a full-scale system that will likely use some kind of engineered pellets. Ceramic materials are often pelletized by blending them with organic binders, extruding them, and burning off the binder. This procedure leads to the development of meso and macropores that are essential for proper gas diffusion through the bed. However, we cannot use this method for copper terephthalate, because the material itself will be thermally degraded. Alternate strategies for pelletization include simple pressing into disks, or drying slurries into monolithic structures. For the present project, we will prepare pressed disks, which will be broken into pieces and sieved before packing them in beds for the breakthrough tests. We have prepared many disks by pressing the 3-D complex. The disks retain their integrity during shipment from SRI in California to ARI in Ohio. We therefore believe that simple pressing will be adequate at least for the laboratory tests.

The breakthrough tests data will yield parameters that will help us design a laboratory PSA system, whose performance will then be used in a process model to design and estimate the cost of a full scale PSA system. We have already received the flow conditions and product specifications from the CCP and expect to complete the tasks on time.

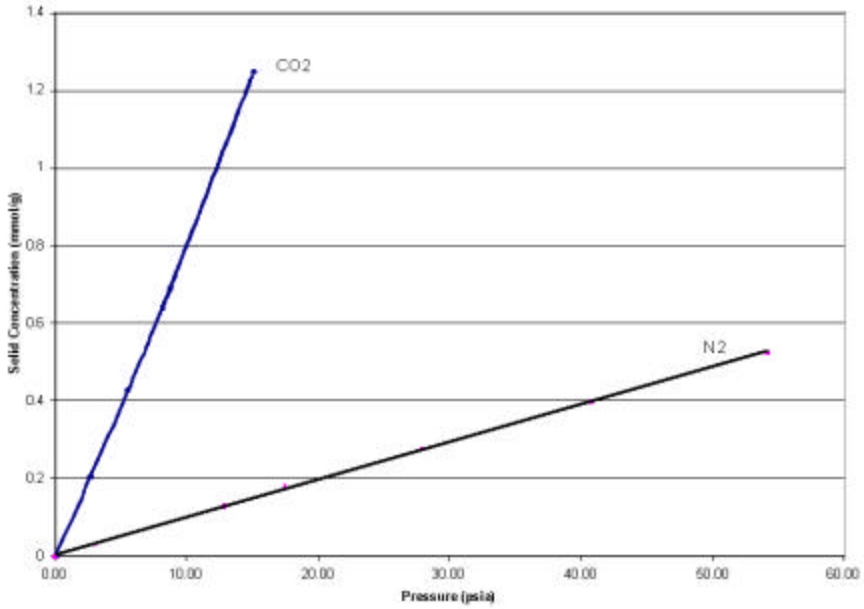

Figure 1.1.1.2.7 *(11)*. Adsorption isotherms for CO_2 and N_2 with SRI high surface area product.

1.1.1.2.8 Conclusion

We have made substantial progress in developing a synthesis process for the copper terephthalate•TED complex. Although the process has not been optimized, our research has identified some of the key parameters to minimize side product formation. We have developed a preferred procedure that gives us high quality product in terms of surface area. In some respects, the product we have obtained appears to be superior to the one we recently received from Dr. Seki. The XRD spectra and TGA profiles of SRI products are very similar to those of Dr. Seki.

In static tests we have shown that the SRI product absorbs CO_2 at room temperature, and because there was no leveling off in the isotherm at the highest pressures tested, the 3-D complex appears to have a very high capacity. High capacity is important because it reduces the overall size of the bed and the attendant compressors of a PSA system, and directly reduces the capital and operating expenses.

In preparation of the next series of dynamic tests in which we monitor the breakthrough of CO_2 through packed beds, we have made pressed disks from the 3-D complex. The disks retain their integrity during normal handling and shipping and thus appear to have adequate mechanical strength for use in a packed bed. The breakthrough tests will help us design a laboratory PSA system, whose performance will be used to design a full-scale system. Capital and operating expenses for this full-scale system will then be estimated by using SRI's Process Economic Program model.

1.1.1.2.9 References

1. Seki, K. et al., U.S. Patent No. 5,998,647, Dec. 1999.
2. Seki, K., Mori, W., *J. Phys. Chem. B.* 2002, *106*, 1380.
3. Seki, K., *Chem. Commun.*, 2001, 1496-1497.
4. Davis, M. E., *Nature* 2002, *47*, 813-821.
5. Seki, K. private communication.

1.1.1.2.10 Publications

No publications have resulted from this work so far.

1.1.1.2.11 List of Acronyms and Abbreviations

ARI	Adsorption Research Inc.
BET	Brunauer Emmett Teller
CCP	CO_2 Capture Project
DMF	N, N-Dimethylformamide
PSA	Pressure swing adsorption
SEM	Scanning-electrom microscopy
SRI	SRI International (Formerly Stanford Research Institute)
TED	Triethylene diamine (also known as [2,2,2,]diazabicyclooctane)
TGA	Thermogravimetric analysis
XRD	X-Ray diffraction

1.2 Pre Combustion Technology

1.2.1 Membrane Studies

1.2.1.1 Sulfur Tolerant Membrane Water Gas Shift Reactor System

1.2.1.1.1 Development of Sulfur Poisoning Resistant Palladium/Copper Alloy Membranes for Hydrogen Fuel Production by Membrane Reaction

Report Title

CO_2 Capture Project - An Integrated, Collaborative Technology Development Project for Next Generation CO_2 Separation, Capture and Geologic Sequestration

Development of Sulfur Poisoning Resistant Palladium/Copper Alloy Membranes for Hydrogen Fuel Production by Membrane Reaction

Report Reference

1.2.1.1.1

Type of Report:	Final Report
Reporting Period Start Date:	February 2003
Reporting Period End Date:	July 2003
Principal Author(s):	Dr. Gokhan Alptekin[1], Dr. Douglas Way[2]
Date Report was issued:	August 2003
DOE Award Number:	DE-FC26-01NT41145
Submitting Organization:	Name of Organization
Address:	[1] TDA Research, Inc. 12345 W. 52nd Av. Wheat Ridge, CO 80033 [2] Colorado School of Mines, Department of Chemical Engineering and Petroleum Refining, Golden, CO 80401

1.2.1.1.1.1 Abstract

Colorado School of Mines (CSM) and TDA Research, Inc. will collaborate for developing a sulfur tolerant, Pd-Cu alloy composite, water-gas-shift membrane reactor which will be used to convert CO in a sulfur contaminated synthesis gas feedstock to pure hydrogen and CO_2. The membrane reactor approach will allow the simultaneous production of a hydrogen permeate stream while maintaining the CO_2 rich stream at high pressure. Pd-Cu alloys have been shown to resist poisoning by H_2S. The fabrication processes developed at the CSM allows preparation of a composite membrane with a micron thick palladium alloy layer, providing high flux and acceptable selectivity at the minimum cost. The advantages of these membranes for processing of sulfur containing synthesis gas will be:

- High H_2 flux
- Sulfur tolerance, even at very high total sulfur levels
- Operation at temperatures up to 500°C
- Resistance to embrittlement and degradation by thermal cycling

This final report discusses our work on the membrane water gas shift reactor research from the CO_2 Capture Project. In the Phase I research, CSM developed various Pd-Cu alloy membranes and characterize them to determine composition, microstructure, and separation performance at high temperature conditions characteristic of operation in a membrane reactor for the water gas shift reaction. First, several candidates were quickly screened and then the best samples were tested in detail to measure mass transfer and kinetic parameters at TDA under representative conditions. In the Phase I work, we also assessed the effects of contaminants, H_2S in particular, and potential of coke formation. Long-term durability of the membranes was evaluated.

1.2.1.1.1.2 Table of Contents

1.2.1.1.1.3 List(s) of Graphical Contents

1.2.1.1.1.4 Introduction

1.2.1.1.1.4.1 Project Description

There is a need to capture the hydrogen available in residual oil feeds and high sulfur feedstocks without releasing CO_2 and sulfur containing gases into the environment. By using a membrane water gas shift reactor, the CO in the syngas from a gasifier can be converted to a hydrogen rich fuel gas stream and a CO_2 rich stream, which can with the minimum of further treatment be compressed and sent to geologic sequestration.

Colorado School of Mines (CSM) and TDA Research, Inc. will collaborate for developing a sulfur tolerant, Pd-Cu alloy composite, water-gas-shift membrane reactor which will be used to convert CO in a sulfur contaminated synthesis gas feedstock to pure hydrogen and CO_2. The membrane reactor approach will allow the simultaneous production of a hydrogen permeate stream while maintaining the CO_2 rich stream at high pressure. Pd-Cu alloys have been shown to resist poisoning by H_2S. The fabrication processes developed at the CSM allows preparation of a composite membrane with a micron thick palladium alloy layer, providing high flux and acceptable selectivity at the minimum cost. The advantages of these membranes for processing of sulfur containing synthesis gas will be:

- High H_2 flux
- Sulfur tolerance, even at very high total sulfur levels
- Operation at temperatures up to 500°C
- Resistance to embrittlement and degradation by thermal cycling

1.2.1.1.1.4.2 Overall Objectives of Proposed Research

The overall objective of the proposed project is to develop the membrane water-gas-shift-reactor technology to proof of concept. In achieving this goal, the key research objective is demonstrating the feasibility of using sequential electroless plating to fabricate $Pd_{60}Cu_{40}$ alloy membranes on porous supports for H_2 separation. Another important objective of the proposed research is the demonstration of the membrane water gas shift reactor in a prototype unit. If results show promise, TDA will carry out the fabrication of a bench-scale membrane reactor and evaluate the combined the performance of the Pd/Cu composite membranes developed by Prof. Way's group and a sulfur tolerant shift catalyst in a single unit. The data generated using the prototype reactor will serve as a basis for detailed engineering and cost analysis of the membrane water-gas-shift reactor. Technological and economic merits of the overall project will also be evaluated.

1.2.1.1.1.4.2.1 Phase I Objectives

The Phase I research plan is designed to provide a fundamental understanding of:

- Optimized membrane structure and Pd-Cu alloy composition
- Effect of temperature and pressure on membrane performance
- Effect of membrane thickness on hydrogen flux
- Effect of H_2S, CO, H_2O on membrane performance

1.2.1.1.1.5 Executive Summary

This final report discusses our work on the membrane water gas shift reactor research from the CO_2 Capture Project. In the Phase I research, CSM developed various Pd-Cu alloy membranes and characterize them to determine composition, microstructure, and separation performance at high temperature conditions characteristic of operation in a membrane reactor for the water gas shift reaction. First, several candidates were quickly screened and then the best samples were tested in detail to measure mass transfer and kinetic parameters at TDA under representative conditions. In the Phase I work, we also assessed the effects of contaminants, H_2S in particular, and potential of coke formation. Long-term durability of the membranes was evaluated. Some of the research results were highlighted as follows:

- A membrane permeation system at TDA was built for extensive sulfur testing on the Pd-Cu membrane. Testing of the membrane under WGSR conditions was also completed using the automated system at TDA.
- A binary gas permeation system was built at CSM for H_2S testing on the Pd-Cu membrane.
- A membrane (#28) with essentially infinite selectivity (H_2/N_2 ~ 70,000) and high flux (0.36 mol/m^2s) has been synthesized for sulfur and WGSR condition testing. The membrane (thickness ~ 12 micron) was supported on an alumina tube.
- A continuous flow through reaction system was built for catalytic study of the Pd-Cu membrane using gas chromatography detection and mass spectrometry. Initial studies showed the Pd-Cu membrane was active for the water gas shift reaction (WGSR). Characterization studies using scanning electron microscopy (SEM) and electron dispersion spectra (EDS) show the presence of Pd and Cu on the top-layer as well as within the support.
- High temperature sealants were tested in an attempt to repair small membrane or support defects.
- Completed binary runs with WGS gases and H_2 at varying temperatures.
- Characterized membranes using EDS and SEM to determine alloy composition and thickness.
- Two separate plating systems were used to eliminate cross contamination of Cu and Pd plating solutions.
- Different (20 nm and 50 nm particle size cut-off) top-layer support tubes have been used to determine the most effective pore size to plate the Pd-Cu membrane.
- Work was done on the stainless steel Pall Accusep? tubes. Palladium was successfully plated on the membrane though some problems with corrosion of the metal support and problems with the design of the welded seals need to be addressed. We are working with engineers at the Pall Corporation to address these problems.
- 2 membranes were tested under CCP protocol WGS conditions with stable properties until addition of $H_2S + H_2O$ combination.
- H_2S testing on the Pd-Cu membranes using binary 1000 ppm H_2S/H_2 mixtures was completed at CSM. Results are qualitatively consistent with those described in the TDA reports. The H_2 flux is inhibited (reduced) compared to pure H_2 values.

1.2.1.1.1.6 Experimental

1.2.1.1.1.6.1 Membrane Preparation and Characterization

The fabrication of the Pd-Cu alloy composite membranes is Confidential Business Information.

1.2.1.1.1.6.2 Improvements In Membrane Preparations

High Temperature Sealants: Most of the membranes tested in the project did not meet the criteria for high hydrogen selectivity. In addition to the defects in the film, the gas leaks from the seals were the major reason for the low selectivity in most of these preparations. A number of possible high temperature sealants were tested in an attempt to seal the leaks and to increase selectivity.

Small defects include cracks in the glaze, cracks in the support or sections of the Pd-Cu film, which did not adhere to the support due to imperfections in the support. These imperfections may include boulders or pinholes in the support. These types of imperfections are shown in Figures 1, 2, and 3. The sizes of the boulders are actually many times the thickness of the actual Pd-Cu film so this may cause obvious problems. These defects may be overcome by synthesizing thicker membranes, but it causes the membrane performance to decline. Some of these imperfections have been identified using SEM.

The high temperature sealants enabled us (at some extent) to use many membranes that have small defects.

Figures 1 & 2. Location of membrane defects & Support defects

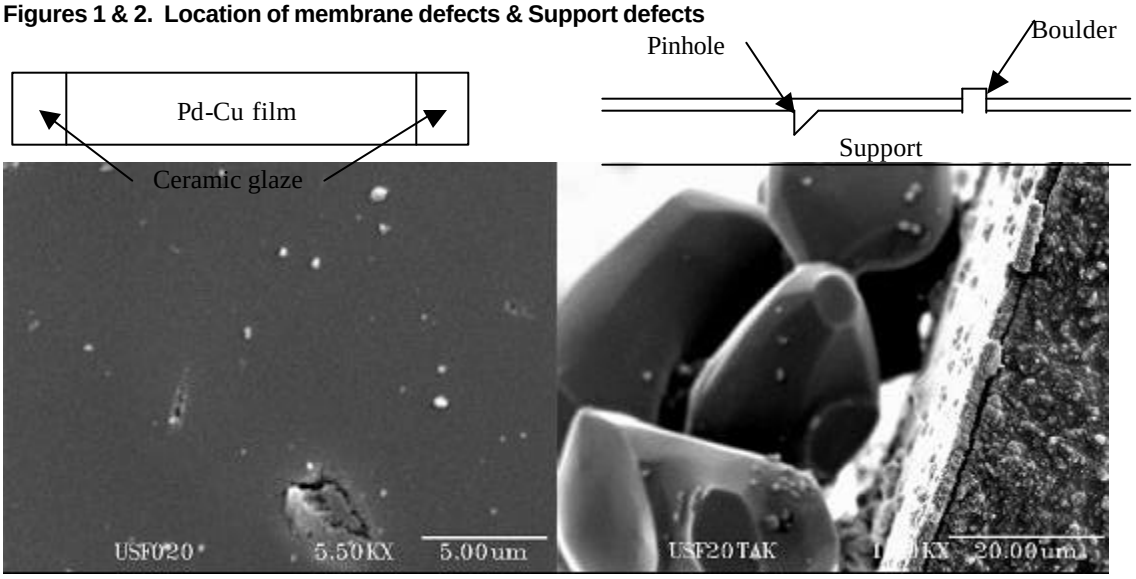

Figure 3. SEM of ceramic support showing holes and boulders, which can cause small defects in the Pd-Cu alloy film.

Through the course of the project, we characterized a large number of membranes using physical and chemical techniques to acquire a fundamental understanding for failure mechanisms. We also characterized few preparations where the stainless steel Accusep tubes were used as the support (Figure 4). Palladium was successfully plated on the zirconia top-layer of the support though problems with corrosion of the stainless steel support still need to be addressed (Figure 5).

1.2.1.1.1.6.3 Membrane Characterization

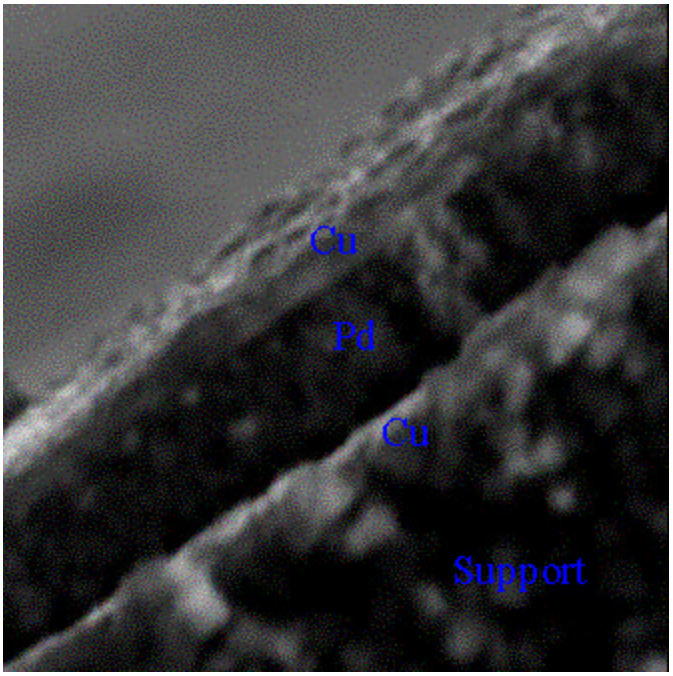

The Pd-Cu alloy membranes are presently being plated on 20 nm and 50 nm pore size zirconia top-layer alumina supports. Thinner membranes can be fabricated on the 20 nm supports with fewer defects. This is probably due to the smaller pore size, which can be filled more readily with the Pd. However, the smaller pore size may mean adhesion strength to the support may decrease and delamination of the Pd film may occur more readily. This was the case when plating the membrane on similar 5 nm pore size alumina top-layer alumina supports. Membranes have also been fabricated on 200 nm pore size alumina supports, but the typical membrane thickness was approximately 10 μm. The hypothesis that higher resistance to H_2 permeation with the smaller pore size needs to be examined.

Figure 4. SEM image of two distinct layers of Cu between a Pd layer before annealing.

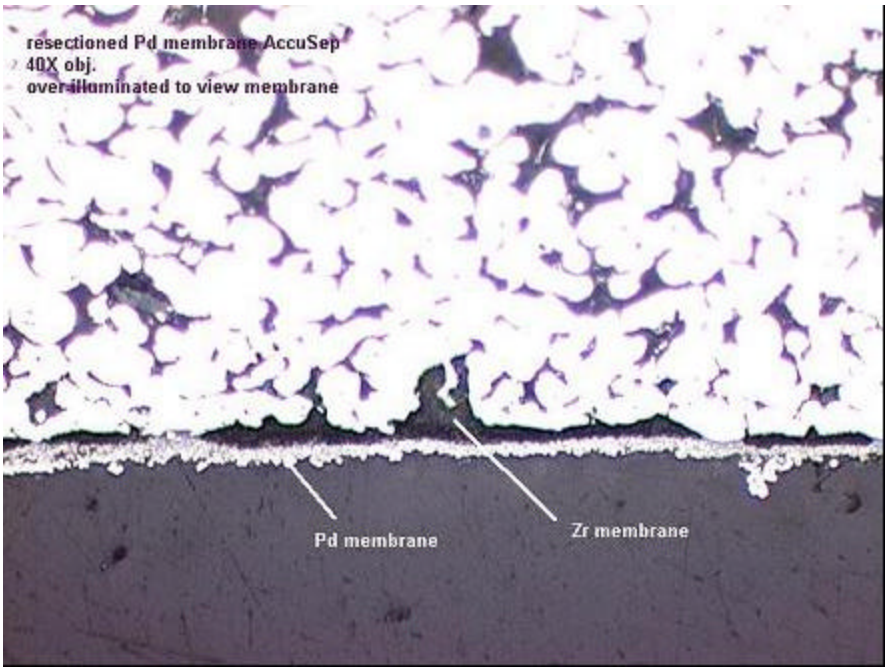

Defects in the zirconia top-layer of the support also present problems when trying to plate a thin uniform metal film less than 5 microns. We are working with Pall to either modify their support or our plating procedure. Finding a feasible stainless steel support would simplify and solve many issues we are presently dealing (i.e., sealing) with the ceramic supports.

Figure 5. SEM of Pall Accusep tube with Pd plated on the zirconia top-layer.

1.2.1.1.1.6.4 Development of an Testing System for Membrane Evaluations

A membrane testing system was constructed at TDA for extensive evaluations of the membranes using representative gas mixtures that involve H_2S. The P&ID of the WGS membrane reactor system is shown in Figure 6.

The separation module is 50.8 cm in length and consists of a 2.5 cm O.D. shell and a 0.6 cm O.D. inner tube both made from SS 316 tubing (0.124 cm thickness). The membrane is centered and attached to the tube by Swagelock fittings. A schematic and photograph of the separation and membrane module are shown in Figures 7 and 8, respectively.

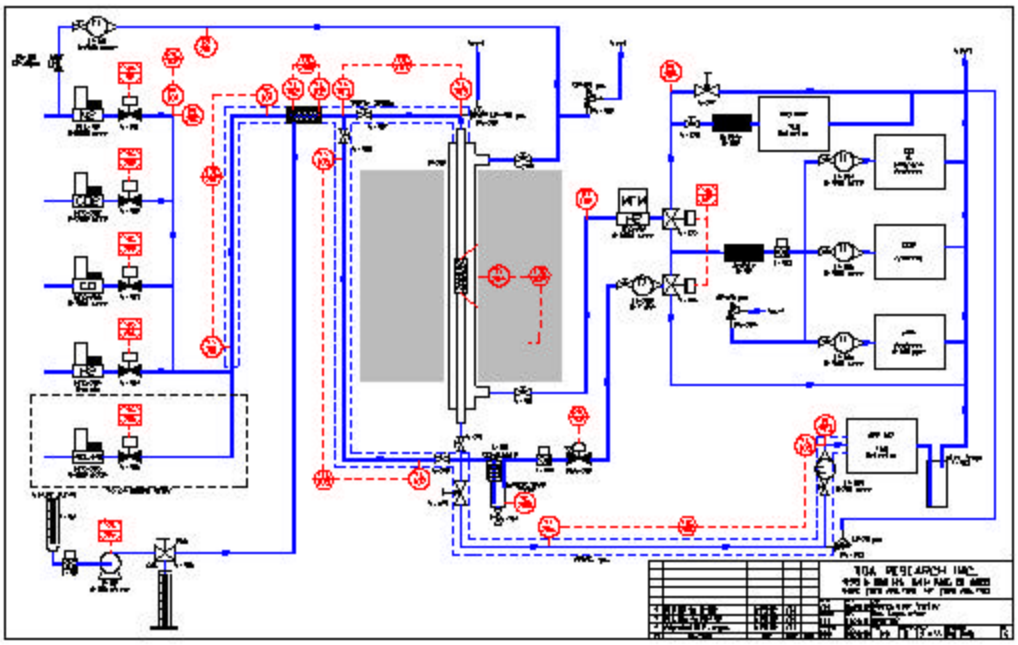

Figure 6. Schematic of the WGS membrane reactor system constructed at TDA.

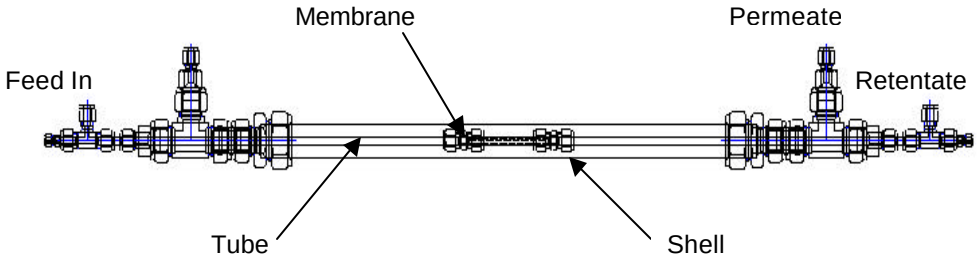

Figure 7. Schematic of membrane reactor with shell and tube.

Figure 8. Photograph of membrane module with shell and tube.

The gases pass through the membrane at temperatures up to 600°C at 300 psig. The pressure of the system was controlled with a Badger pressure control valve located at the downstream of the membrane module. Electronic mass flow controllers were used to introduce the gas streams of H_2, CO, CO_2, and H_2S as well as N_2 used as an inert and sweep gas. Introduction of H_2O into the system was accomplished with a high-pressure liquid pump. The feed gas mixture was either directed through the membrane module or through a by-pass loop for the analysis of the feed gas, as desired. Prior to separation, these gases were heated to about 300°C and mixed at the module inlet.

Figure 9. Membrane module.

The gas stream exiting the module or by-pass loop was then directed into two SRI Model 8610A gas chromatograms (GC) and appropriate gas analyzers, which enabled simultaneous monitoring of both permeate and retentate streams. Following GC sampling, a condenser/desiccant assembly removed all the humidity before these streams were fed to the CO, CO_2, and H_2S analyzers (the analyzers also have CH_4 measurement capability).

Control E/G software was in place to control the apparatus in order to provide unattended operation (including unattended overnight tests). The software controlled the parameters of the

system including reactant flow, furnace temperature, and system pressure, as well as the product gas analyzers and gas chromatograms. Safety precautions were also in place using Control E/G software. In the case of overheating, over pressurization, or a hazardous gas leak, the software automatically followed a procedure for appropriate shutdown of the system.

1.2.1.1.1.6.5 H_2S Analysis

TDA also developed analysis techniques to measure H_2S using a GC and an on-line analyzer. We also identified analytical methods for H_2S measurement at a range of concentrations (Table 1). For the analysis, we used an on-line trace gas analyzer from Zellweger Analytical to measure H_2S concentrations in 0-50 ppm range. A gas chromatogram (GC) equipped with a flame photoionization detector (FPD) was used to measure H_2S concentrations in 100-5,000 ppm range. Because the sensitivity of the FPD detector is reduced at high sulfur concentrations due to over saturation of the detector, the GC was also supplemented with a thermal conductivity detector (TCD) to measure hydrogen sulfide concentrations above 5,000 ppm.

Table 1. Methods for H_2S analysis

Concentration, ppm	Analysis Technique
0-50	On-line trace gas analyzer
50-5,000	GC/FPD
>5,000	GC/TCD

The optimization of the GC methodology and calibration fro H_2S at arrange of concentrations were carried out before each test.

In addition to the extensive multi-flow system at TDA, a binary gas membrane permeation system was built at CSM for testing with H_2S/H_2 binary mixtures. Tests were run to determine the effect of H_2S concentration on membrane selectivity and flux versus time.

1.2.1.1.1.7 Results and Discussion

1.2.1.1.1.7.1 Binary Experiments

During the initial stages of the project, we carried out binary experiments to evaluate the effects of individual WGS components on membrane performance.

Membrane #28 – Infinite Selectivity: The major highlight of the research was the synthesis of a Pd-Cu membrane (#28) that exhibited close to infinite selectivity. In other words, only H_2 can be seen to permeate through the membrane. Nitrogen cannot be detected on the permeate side using a flow meter with a flow rate resolution of 0.01 cm^3/min. This means that the H_2/N_2 ideal selectivity for this particular membrane is at least 70,000. The membrane thickness has been estimated to be approximately 12 µm based on plating time. Though this membrane was thicker than previous membranes synthesized at CSM, the H_2 flux was still a respectable 0.36 mol/m^2 s at 450 °C at a transmembrane pressure of 428 kPa = 50 psig. The pure H_2 flux for membrane #28 is close to those reported by Edlund for commercial Pd-Cu foil membranes with thicknesses ranging from 15 to 25 µm. A plot of the H_2 and N_2 fluxes for membrane #28 are given in Figure 10.

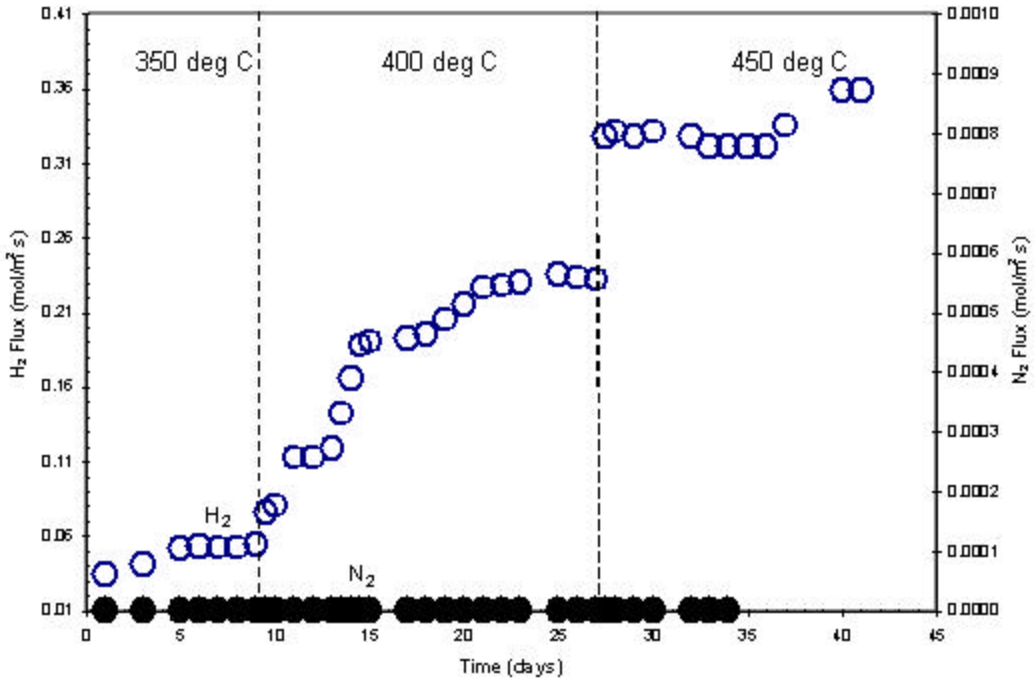

Figure 10. H_2 and N_2 fluxes versus time for a 12 ?m thick Pd-Cu membrane at increasing temperatures and transmembrane pressure of 428 kPa.

The flux in units of moles/m^2•s can easily be converted to cm^3(STP)/cm^2•s by multiplying the moles/m^2•s value by 2.24. For example, the steady-state H_2 flux at 450 °C for the membrane data in Figure 10 is equal to a volumetric flux of 0.81 cm^3(STP)/cm^2•s for a hydrogen feed pressure of 62 psia. The pressure dependence of this membrane has been measured several times during the 45-day permeation test. Curiously, the n value in the hydrogen flux expression below is approximately 1, quite different than the usual Sievert's law expression (square root pressure dependence, n = 0.5) expected for metallic membranes where atomic hydrogen is the permeating species. The flux equation at 450°C for the membrane data is shown below:

$$J = \frac{P}{l}\left(p_{feed}^{n} - p_{permeate}^{n}\right) = 3.12 \bullet 10^{-3} \frac{cm^3(STP)}{cm^2 \bullet s \bullet cmHg}\left(p_f - p_p\right) \qquad (1)$$

The proportionality constant in equation 1 is the permeance, having a value of 3120 GPUs for pure H_2 at 450 °C. A hydrogen permeance of this magnitude is about a factor of 10 larger than those reported for high performance, commercial polyimide membranes. Pd-Cu membranes that are on the order of 1-2 ? m synthesized at CSM can have H_2 fluxes as high as 1.1 mol/m^2 s = 2.46 cm^3(STP)/cm^2•s at similar feed pressures and temperature. However, if the thickness of membrane #28 is really 10 – 15 µm, then its pure H_2 permeability is the highest we have ever measured, close to the Pd-Cu foil membranes commercialized by Edlund.

1.2.1.1.1.7.2 Evaluation of the Effects of WGS Gases on Membrane Performance

In addition to the H_2/N_2 binary experiments, we also tested the effects of CO, CO_2 and H_2O by exposing the membranes to the mixtures of these gases with hydrogen.

Effect of CO_2: We exposed the membrane to a gas mixture of 50% vol. CO_2 in H_2 (balance) at 72 psia, while maintaining a CO_2 partial pressure similar to that provided in the test protocol. Figure 9 presents the hydrogen permeation rate as a function of time. We first measured the permeation rate and selectivity at 350^{o}C, recording a permeation rate of 320 sccm and a selectivity of 22. We then ramped the temperature up 1^{o}C/min to 450^{o}C for a 15 hr overnight testing. As indicated, at 450^{o}C, the hydrogen permeation rate stayed fairly constant, while the selectivity went through a maximum of 55 and then stabilized at 28 (the selectivity is calculated as the H_2/CO_2 molar ratio in the permeate stream).

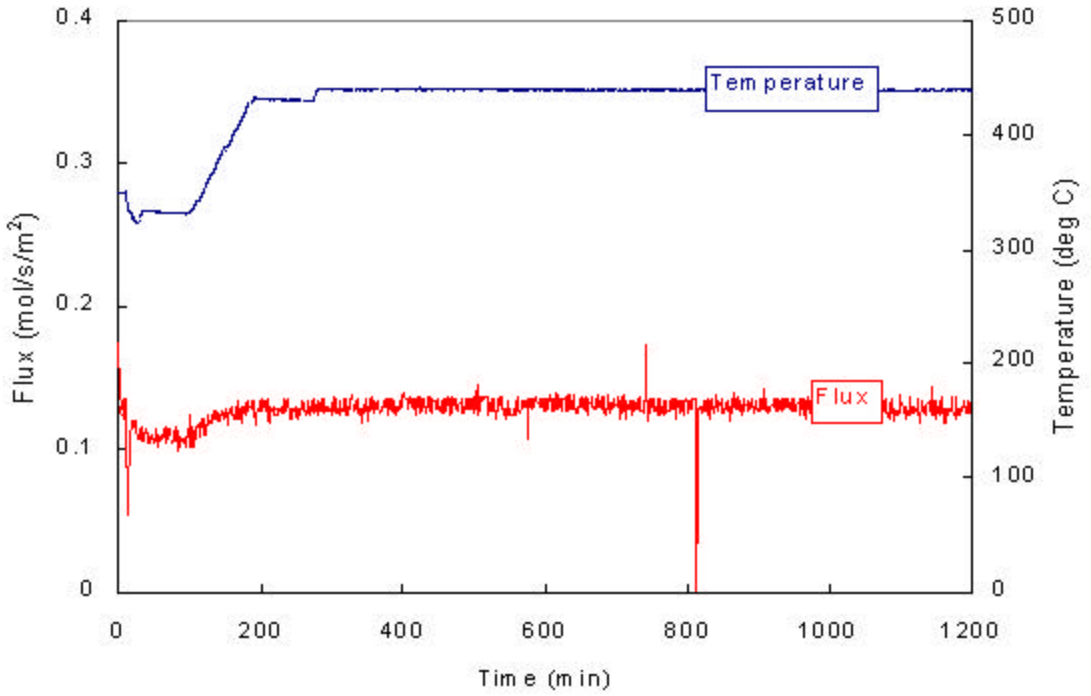

Figure 11. Total flux and temperature versus time using a 50/50 CO_2/H_2 mixture at 72 psia.

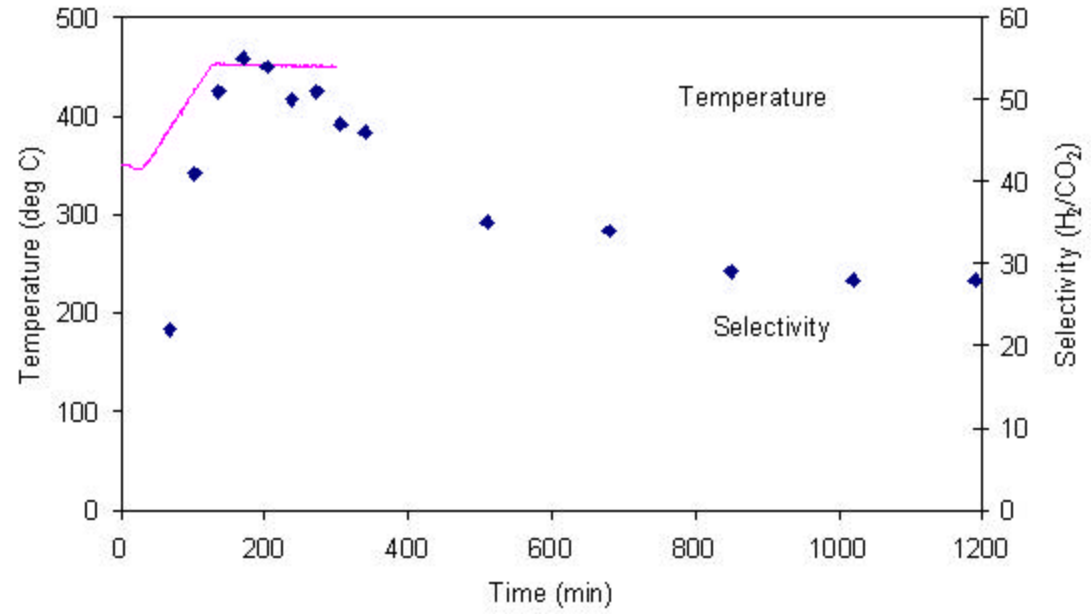

Figure 12. Effect of temperature and time on membrane binary selectivity using a 50/50 CO_2/H_2 mixture at 72 psia.

During this test, we continuously monitored both permeate and residue streams to observe the extent of possible side reactions catalyzed by the Pd-Cu film by using two gas chromatographs and on-line CO, CO_2, CH_4 analyzers. The product gas distribution as a function time is presented in Figure 13.

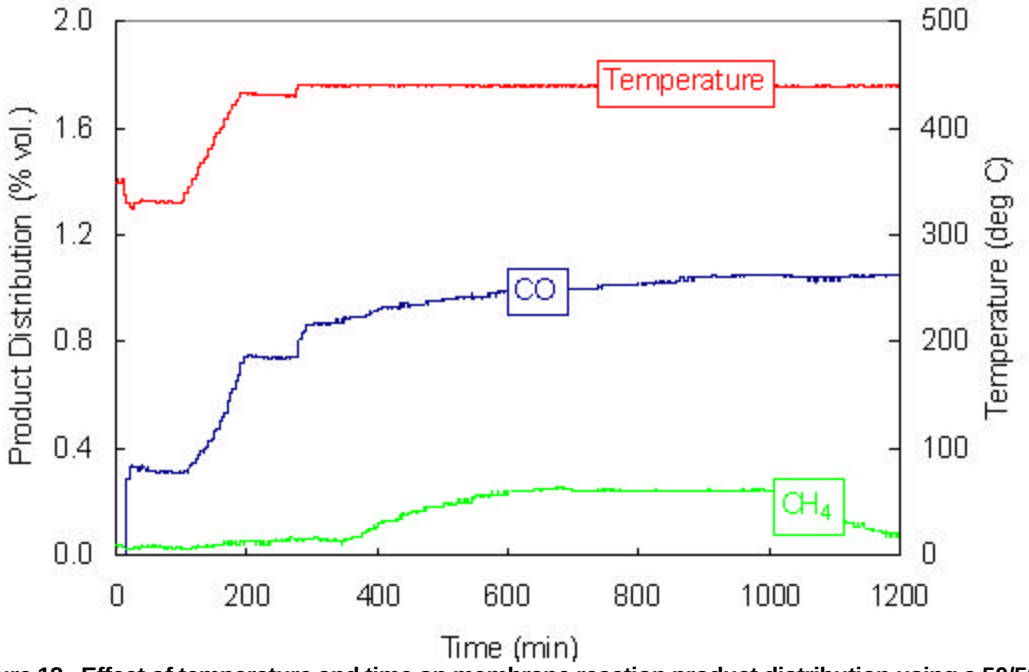

Figure 13. Effect of temperature and time on membrane reaction product distribution using a 50/50 CO_2/H_2 mixture at 72 psia.

Introduction of H_2/CO_2 binary promoted formation small amounts of CO and CH_4, possibly due to reverse water-gas-shift and methanation (Sabatier) reactions:

$$CO_{2(g)} + H_{2(g)} = CO_{(g)} + H_2O_{(g)}$$
$$CO_{2(g)} + 4H_{2(g)} = CH_{4(g)} + 2H_2O_{(g)}$$

In the overall scheme, the carbon conversion (CO_2 conversion into CO and CH_4) was less than 2.5% (the conversion is normalized based on feed flow and assuming a similar flux of these components through the membrane).

Effect of CO: Following the H_2/CO_2 binary, we activated the membrane in hydrogen flow in an attempt to remove any absorbed surface species, until maintaining a stable hydrogen permeation rate. Following hydrogen activation and annealing at 450°C for 10 hrs, we fed 10% CO and H_2 (balance) at 68 psia to provide a CO partial pressure of 7 psia. We carried out the same temperature sequencing as we did for the H_2/CO_2 binary.

As presented in Figure 12, we observed an increase in the permeation rate as a function of time, where the H_2 selectivity stabilized at 30 at 450°C (Figure 14).

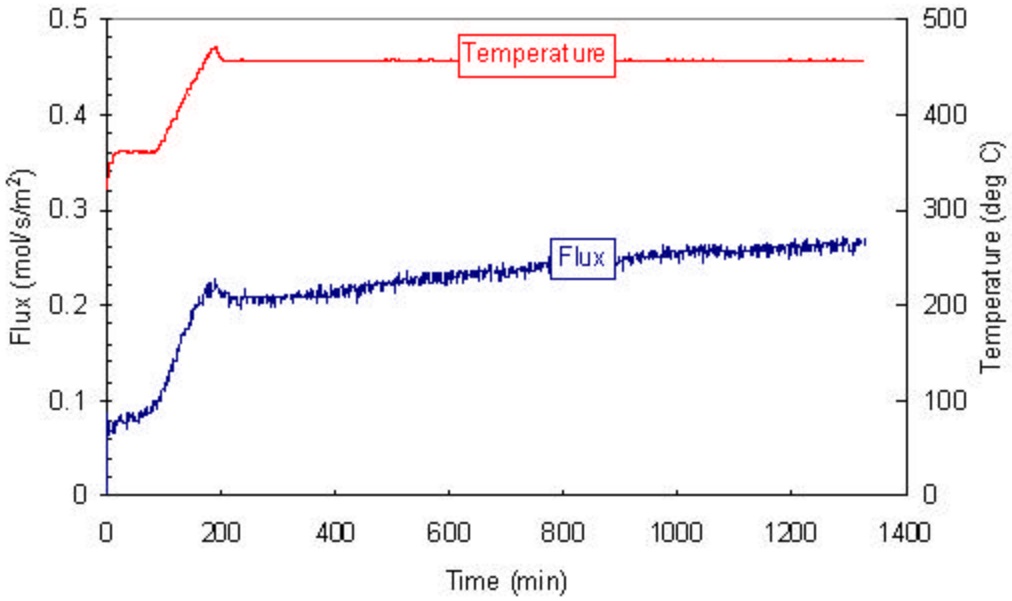

Figure 14. Effect of temperature and time on permeate flux using a 10/90 CO/H_2 mixture at a total pressure of 68 psia.

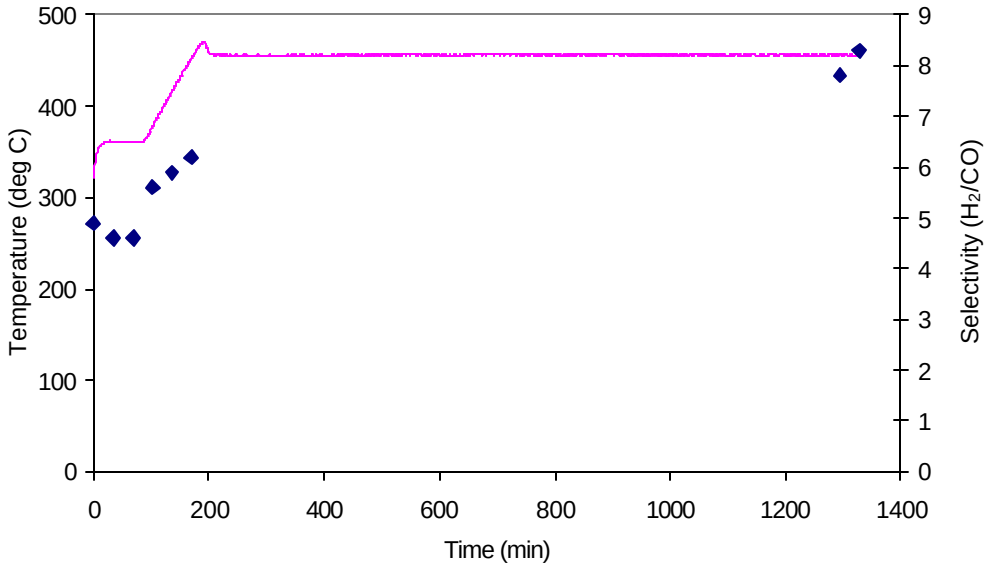

Figure 15. Effect of temperature and time on membrane binary selectivity using a 10/90 CO/H_2 mixture at 68 psia.

The CO_2 and CH_4 presence in the residue stream is indicative of CO conversion (Figure 15). Formation of the CO_2 may be possible due CO disproportionation:

$$CO_{(g)} = C + CO_{2(g)}$$

This reaction is highly undesirable because it also forms a carbon residue, which may cover the membrane surface reducing the flux. However, the extent of this reaction is small evident by the very low CO_2 concentration. We did not observe any decrease in permeation capacity due to inhibition by carbon formation. It is important to note that these test conditions were harsher

(i.e., more prone to coking) than the actual operation, since the presence of high partial pressure of steam will remove any carbon deposits.

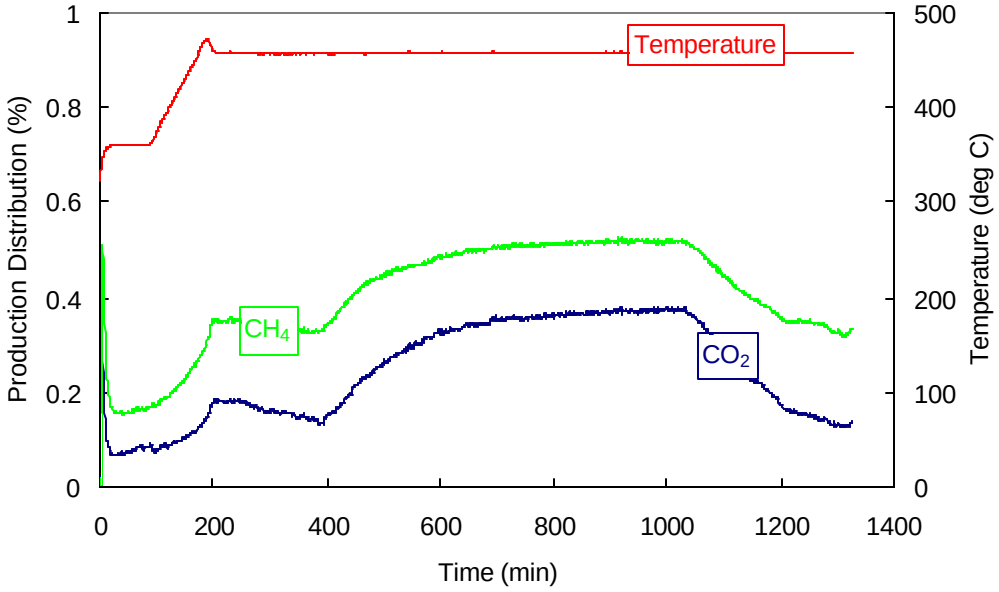

Figure 16. Effect of temperature and time on membrane reaction product distribution using a 10/90 CO/H_2 mixture at 68 psia.

In experiments conducted after the CCP project ended, a 15 micron thick Pd-Cu alloy composite membrane was exposed to a CO_2/H_2 binary mixture for 30 h at 450°C and 1120 kPa. Though the initial permeability of the membrane was only 10^{-8} mol/s/m^2/Pa due to the thickness, the membrane had a hydrogen/nitrogen ideal selectivity of at least 150 and it did **not change** after exposure to the 50/50 hydrogen/carbon dioxide mixture.

Effect of H_2O: Finally, we tested the effect of steam on membrane performance. We carried out a similar membrane activation in hydrogen as described above to restore the initial permeation and selectivity. Following activation and annealing under hydrogen at 450°C, we tested the effect of 7% H_2O/H_2 mixture on sorbent performance. We measured a small decline in the permeation rate by water addition (Figure 17).

We also measured very low quantities of CH_4 and CO in the residue stream, indicating some possible interaction of surface carbon species with steam (Figure 18).

$$C + H_2O_{(g)} = CO_{(g)} + H_{2(g)}$$
$$C + 2\ H_2O_{(g)} = CO_{2(g)} + 2\ H_{2(g)}$$

Presence of a large water partial pressure in the actual operation will be beneficial to the removal of any carbonaceous deposits.

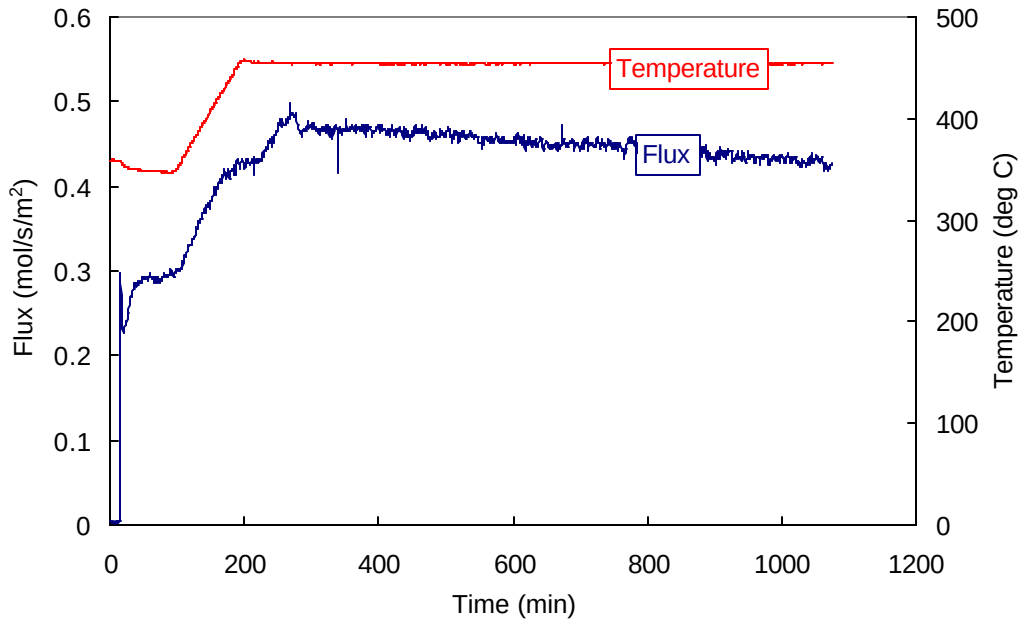

Figure 17. Effect of temperature and time on permeate flux using a 7/100 H_2O/H_2 mixture at a total pressure of 66 psia.

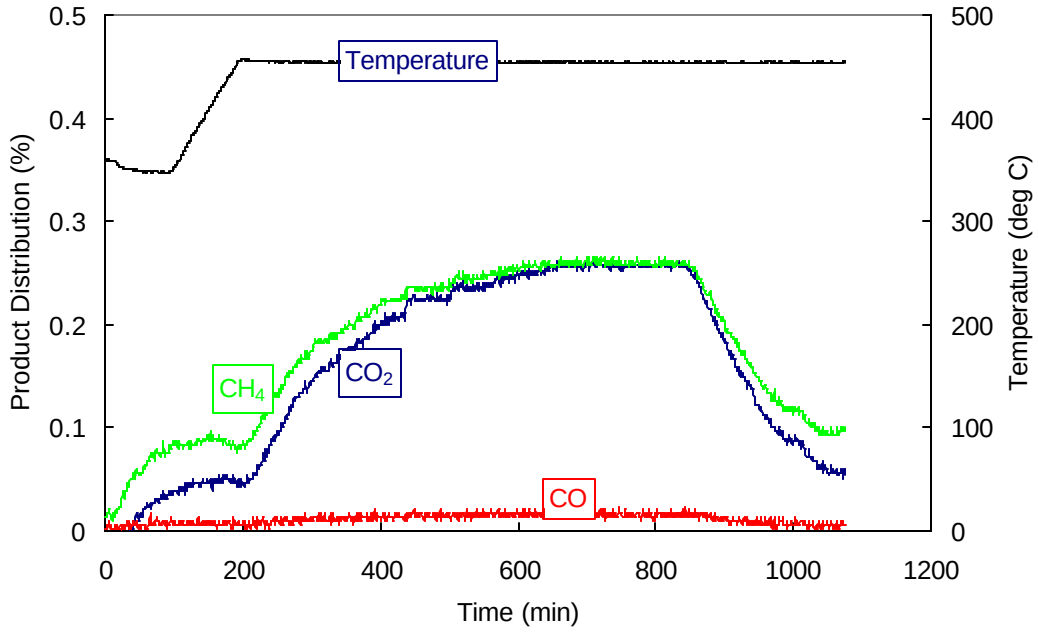

Figure 18. Effect of temperature and time on membrane reaction product distribution using a 7/100 H_2O/H_2 mixture at 66 psia.

1.2.1.1.1.7.3 Non-linearity of Membrane Flux Equations

In the flux equations provided to CCP, it was assumed that the permeance has a linear relationship to the transmembrane pressure difference; as the partial pressure of an individual component increases, the flux through the membrane increases linearly. However, binary

experiments showed that the H_2/CO_2 separation improves as CO_2 concentration increases (i.e., simulating conditions close to the exit of the membrane reactor).

We were surprised with the performance of the thin PdCu membranes yielding high CO_2 concentrations on the permeate side. Ideally, Pd membranes should have infinite selectivity to hydrogen since the separation mechanism is unique to hydrogen (surface adsorption and solution diffusion of atomic hydrogen in the Pd lattice). Unfortunately, it is unlikely to achieve infinite hydrogen selectivity in practical operation due to the presence of defects in the film or in the graphite seals. These defects create passages for other gases causing a decrease in hydrogen purity in the permeate stream. Through the defects, provided that they are small, other gases can transport by Knudsen diffusion based upon the differences in the molecular weight (diffusion rate is inversely proportional to the square root of molecular weight). However, during the binary tests and in the simulation of WGS gases, we noticed that the H_2/CO_2 separation factor was equal to or worse than those calculated for H_2/H_2O and H_2/N_2. Thus, we concluded that mechanisms other than Knudsen diffusion are contributing to the transport of CO_2 across the membrane. We speculate that CO_2 (and CO) may follow a surface diffusion mechanism, in which the gas phase CO_2 first chemisorbs on the surface and then spills over to the permeate side through defects by consequent adsorption and desorption (Figure 19).

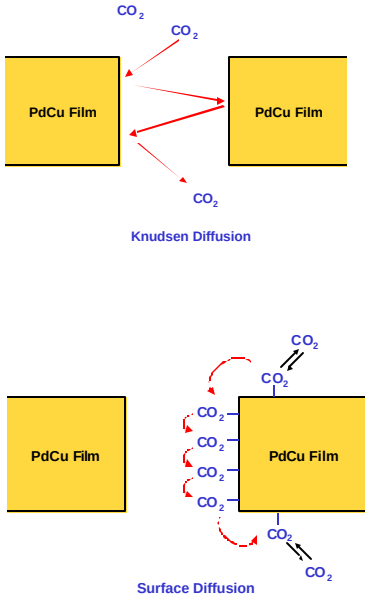

Figure 19. Knudsen diffusion vs. surface diffusion.

Depending on the conditions, CO_2 transport via this type of a mechanism may be faster than Knudsen diffusion, resulting in higher CO_2 levels in the permeate stream in comparison to other gases, such as N_2 or H_2O. Since the inert components do not chemisorb onto the surface, surface diffusion does not occur. On the other hand, CO and CO_2 have a high affinity to the copper surface at the conditions of interest (in fact copper-based catalysts are used for WGS or preferential oxidation of CO due their high affinity to CO even in the presence of high concentrations of H_2). Thus, surface diffusion as a transport mechanism is more probable over the Pd-Cu membranes and the low separation factors for CO_2 and CO can be explained based upon this speculation.

However, it is important to realize that if surface diffusion is a dominant mechanism, the surface coverage of CO_2 (and therefore its diffusion) will not be linearly dependent to the CO_2 partial pressure. Surface coverage can be best explained by Langmuir-Hinshelwood kinetics, and as shown in Figure 20, the CO_2 coverage does not increase linearly with CO_2 partial pressure (this isotherm is generated based on the equation:

$$\text{Surf. Coverage} = k_{ads}[CO_2]/(1 + k_{des}[CO_2])$$

and only used for illustration purpose). Therefore, as the CO_2 concentration increases in the membrane reactor (since H_2 permeates through the PdCu membrane), its flux may not necessarily increase as predicted by the flux equation due to saturation of the surface by CO_2. Therefore, the flux equation developed for CO_2 may not predict the separation performance of the membrane throughout the length of the reactor.

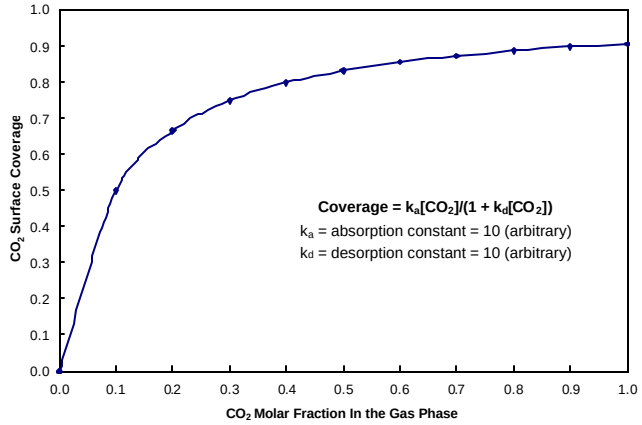

Figure 20. Typical CO_2 surface coverage profile.

Based upon this hypothesis, we carried out few experiments using a $H_2/N_2/CO_2$ ternary mixture and calculated the H_2/CO_2 and H_2/N_2 separation factors over a range of gas concentrations. In these experiments, we observed that the H_2/CO_2 separation factor changes as a function of feed gas concentration (i.e., H_2/CO_2 molar ratio).

In this experiment, after annealing membrane USF-AK-20-22, we flowed a $H_2/N_2/CO_2$ mixture with a molar ratio of 50/25/25 and calculated separation factors of H_2/N_2= 10 and H_2/CO_2= 10 at 450^{o}C (Figure 21). This result is in agreement with the hypothesis. Nitrogen permeation through the membrane occurs presumably via Knudsen diffusion, since it is inert and does not interact with the PdCu membrane. If CO_2 also permeated strictly by Knudsen diffusion, then the H_2/CO_2 selectivity would be higher than H_2/N_2 as predicted by the square root of the inverse of the molecular weights.

We then changed the composition of the feed gas to $H_2/N_2/CO_2$ = 65/25/10 by increasing the H_2 in the feed, while maintaining the same conditions in the reactor (i.e., temperature, pressure). At higher H_2 concentrations, the H_2/CO_2 separation factor decreased to 4 (in a true Knudsen diffusion-based transport mechanism, this should stay the same). However, when we changed the feed composition to $H_2/N_2/CO_2$= 25/25/50, simulating the conditions near the exit of the membrane reactor, we calculated an H_2/CO_2 separation factor of 28. The H_2 selectivity increased 3 times in comparison to the 50/25/25 $H_2/N_2/CO_2$ mixture. We then revisited the initial condition and confirmed the similar hydrogen selectivity observed for the $H_2/N_2/CO_2$= 50/25/25 mixture.

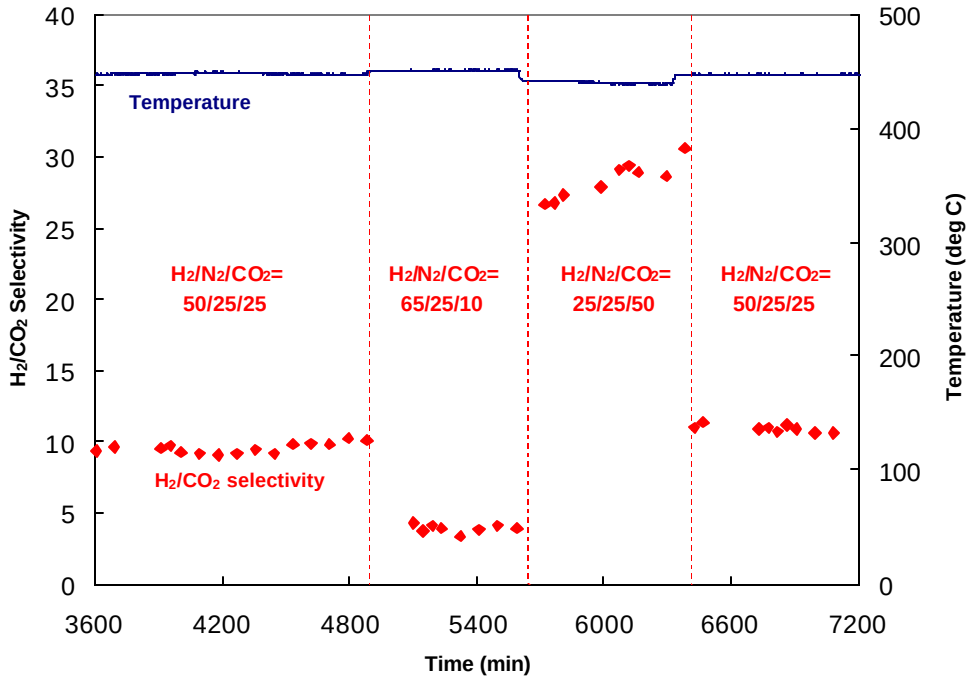

Figure 21. Hydrogen selectivity for different $H_2/N_2/CO_2$ tertiary mixtures.

We believe that a further increase in the CO_2 concentration would generate even better separation factors. Surface diffusion slows down once the CO_2 surface coverage approaches a saturation limit. Near the saturation point, the CO_2 permeation would not increase linearly as predicted by the flux equations provided to CCP. Therefore, it is anticipated that the H_2/CO_2 selectivity, at the end of the reactor, would be higher than that predicted by the flux equation. Although the H_2/CO_2 separation factor of 13 observed using the membrane USF-AK-50-16 is still less than 50, we believe that the PdCu membranes have a potential to meet the objectives and goals of the CCP for carbon recovery (please note that the starting H_2/N_2 selectivity for this membrane was only 18 at 450^{o}C in comparison to 35 for the USF-AK-50-16 membrane). This may be particularly true with the use of thicker membranes with less defects.

1.2.1.1.1.7.4 Effect of Alloy Composition

We investigated the effects of PdCu alloy composition on the performance of the membrane and on membranes catalytic properties. We compared several preparations in an effort to optimize the copper content for the desired application. In addition to the $Pd_{60}Cu_{40}$ alloy composition, we identified that the $Pd_{10}Cu_{90}$ films had some favorable permeation properties.

Membrane USF-AK-20-8 was prepared with an alloy composition of 90% Cu. Due to the high Cu content H_2 flux was low, but ideal H_2/N_2 selectivity was high (Figure 22). A selectivity of 100 was measured. However, when the WGS composition was exposed to the membrane on day 6, the H_2 flux increased 5 times, while still no N_2 flux could be measured.

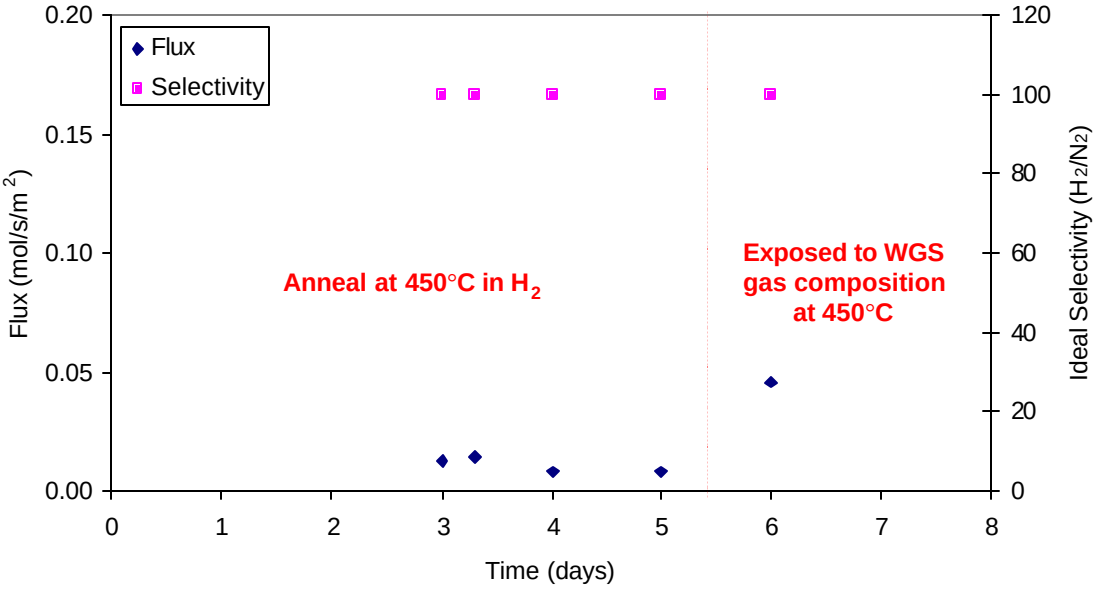

Figure 22. H_2 flux and ideal H_2/N_2 selectivity versus time for membrane USF-AK-20-8.

On day 7, a binary mixture of 50/50 H_2/CO_2 was introduced to the system and 12% conversion of the CO_2 was detected to form CO and H_2O (reverse WGS reaction). Unfortunately, this membrane were not tested for durability in the presence of H_2S because in an overnight test, H_2O saturated the system lines and the membrane had to be removed due to the premature shutdown. We also prepared two membranes with $Pd_{70}Cu_{30}$ alloy composition. Only 2% CO_2 conversion was observed using these membranes USF-AK-50-2 and USF-AK-506, both of which had a Cu alloy composition of approximately 30%. Hydrogen flux in these membranes was lower that that observed for the ones prepared with $Pd_{60}Cu_{40}$ films. The samples with relatively lower copper concentration were also identified as catalytically less active.

1.2.1.1.1.7.5 Membrane Evaluation

1.2.1.1.1.7.5.1 Membrane Evaluation with WGS Gases

We carried out tests to measure the performance of the Pd-Cu membranes under the protocol gas conditions. In this initial set of experiments, we measured the potential poisoning and inhibition effects of combined CO, CO_2 and H_2O gases (excluding H_2S) on membrane performance under the conditions of interest. To be able to demonstrate the full effects induced by these gases, we used a good quality membrane, USF-AK-50-6, that provides not only high flux but also high hydrogen selectivity.

Table 3 describes the conditions that the membrane has been exposed during annealing and ideal selectivity measurements (ideal selectivity is defined as the ratio of the pure H_2 and N_2 fluxes through the membrane at a selected pressure differential) during the 16-day test. Membrane USF-AK-50-6 was annealed in 2% H_2/He at 30 psi for 10 days to assure complete interdiffusion of the Pd and Cu metals. We observed hydrogen selectivity up to 170, and a reasonable flux during the annealing period. Once a stable flux and selectivity maintained, a 50/50 H_2/CO_2 mixture was then introduced to identify the effect of CO_2 (as well as CO and H_2O generated by the side reactions) on membrane performance. We observed an increase in H_2 permeation through the membrane (the flux increased from 0.12 to 0.184 mol/m^2.s, accompanied with an increase from 170 to 250 in ideal selectivity). Following binary experiments, we introduced CO into the reaction gases, while matching the component partial pressures representative of protocol gas. We observed a similar effect on day 14 when CO was introduced with H_2 and CO_2 (an increase in the flux and selectivity compared to ideal flows).

Table 2. Ideal selectivity (H_2/N_2) and H_2 flux versus time at 62 psia and various temperatures and annealing gas conditions for membrane USF-AK-50-6.

Pressure	Temperature	Time	Flux	Ideal Selectivity	Annealing
psig	deg C	day	mol/s/m^2	H_2/N_2	gas
50	400	5	0.097	Infinite	2% H_2/He
50	400	6	0.097	Infinite	2% H_2/He
50	400	7	0.097	Infinite	2% H_2/He
50	450	9	0.118	Infinite	2% H_2/He
50	450	10	0.120	170	2% H_2/He
50	450	11	0.184	250	H_2/CO_2
50	450	12	0.172	250	He
50	450	13	0.153	30	H_2/N_2
50	450	14	0.244	47	$H_2/CO/CO_2$
50	450	15	0.223	250	He
50	450	16	0.184	50	$H_2/CO/CO_2/H_2O$ with He sweep

Finally, we exposed the membrane to a simulated WGS synthesis gas with the composition of 42/19/4/35:$H_2/CO_2/CO/H_2O$ on day 16 for 4 hours at 62 psia and 450°C (Figure 23).

Prior to this experiments, a 42/58 H_2/N_2 mixture was first introduced at 62 psia to the system for 40 minutes to determine a baseline for hydrogen flux in the presence of inert nitrogen. We then replaced N_2, with the $CO/CO_2/H_2O$ combination, while maintaining the same partial pressure across the membrane. As can be seen in Figure 23, the flux through the membrane remained

The hydrogen concentration in the permeate gas averaged at 88% vol.; with 7.0% vol. CO_2, 2% vol. CO and 3.0% vol. H_2O. The H_2 selectivity to CO, H_2O and CO_2 on an individual basis are shown in Figure 20. The H_2/CO_2 selectivity remained constant at 10 whereas the selectivities over CO and H_2O increased with time, shortly after introduction of the WGS gases. No decrease in the selectivity indicates the H_2 permeation was not inhibited by the presence of any of these gases.

constant suggesting no inhibition or fouling of the membrane for the first 4 hours.

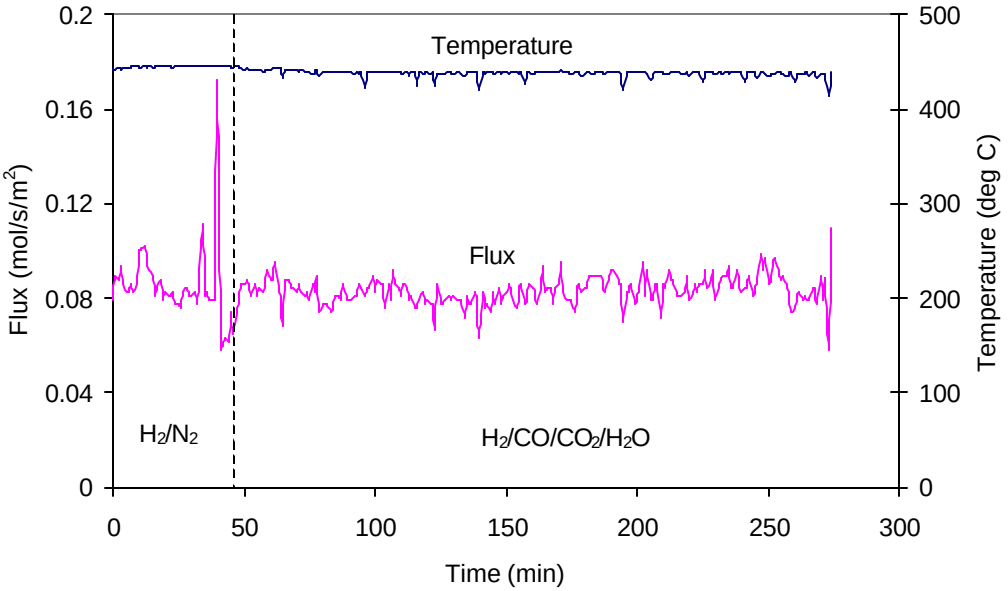

Figure 23. Flux versus time after introduction of WGS synthesis gas to membrane USF-AK-50-6 at 62 psia and 450° C.

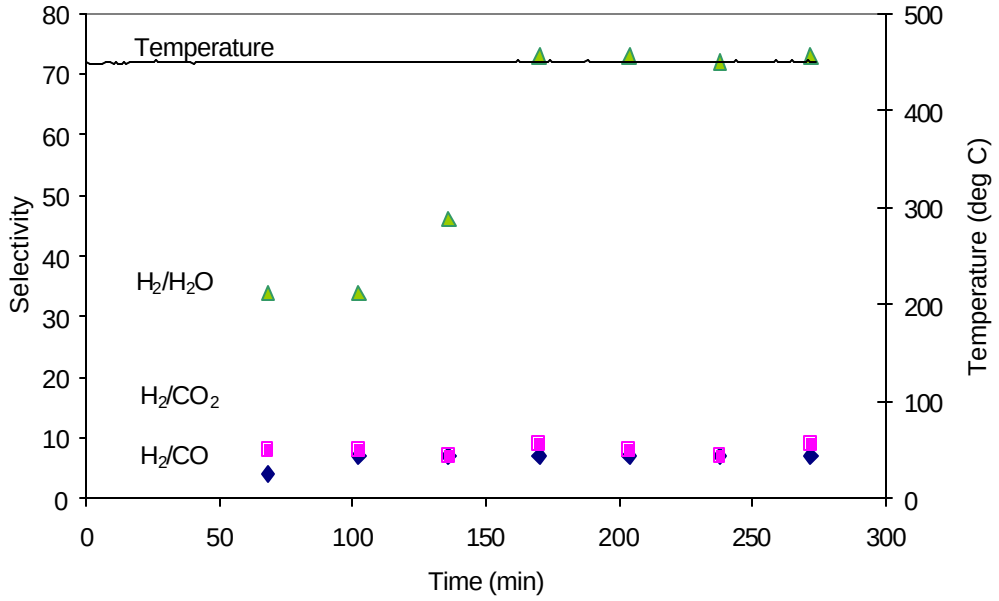

Figure 24. Hydrogen selectivity to CO, H_2O and CO_2 for 4 hours using membrane USF-AK-50-6 at 62 psia and 450° C.

1.2.1.1.1.7.6 Membrane Evaluation in the Presence of Sulfur

We initiated sulfur tests, first by carrying out binary experiments. In the initial tests with H_2S, we used membranes with mediocre performance capability. The objective of these tests was to ensure flaw free operation of the system components in the presence of H_2S and detection and demonstrate the analytical capabilities of the H_2S detection system.

Following the diagnostic experiments, we tested membrane USF-AK-20-9. After annealing in He for 5 days, we exposed it to 100 ppm H_2S in an 8 hr test. Before H_2S exposure, the membrane had a steady state flux of 0.137 mol/s/m^2 and H_2/N_2 ideal selectivity of 23 at 450°C and 40 psig. Although not superior, its performance was satisfactory for initial H_2S testing. Addition of 100 ppm H_2S to 50/50 H_2/N_2 mixture caused a decrease in H_2 flux from 0.137 to 0.081 mol/s/m^2, indicating a ~40% reduction in the hydrogen flux due to sulfur inhibition. As a result of the reduced hydrogen flux across the membrane, hydrogen selectivity also decreased from 23 to 11 during the 8 hr test. However, it was encouraging to observe that after the first one hour of H_2S introduction, the flux through the membrane stabilized, suggesting that the Pd-Cu membranes can operate in an H_2S environment with stable hydrogen flux, even with a decline in its performance.

Following the H_2S experiment, a 20% H_2O/H_2 mixture was used to sweep H_2S from the membrane for 2 hour. The 20% H_2O/H_2 sweep increased the H_2 flux to 0.093 mol/s/m^2 and ideal selectivity to 19. Thus, it is anticipated that in the presence of steam effect of H_2S on sorbent performance will be less severe. Figure 25 presents these results in a graphic form. In addition, we also observed an increase in the ideal selectivity to 28 by purging the membrane with He overnight after the steam exposure increased.

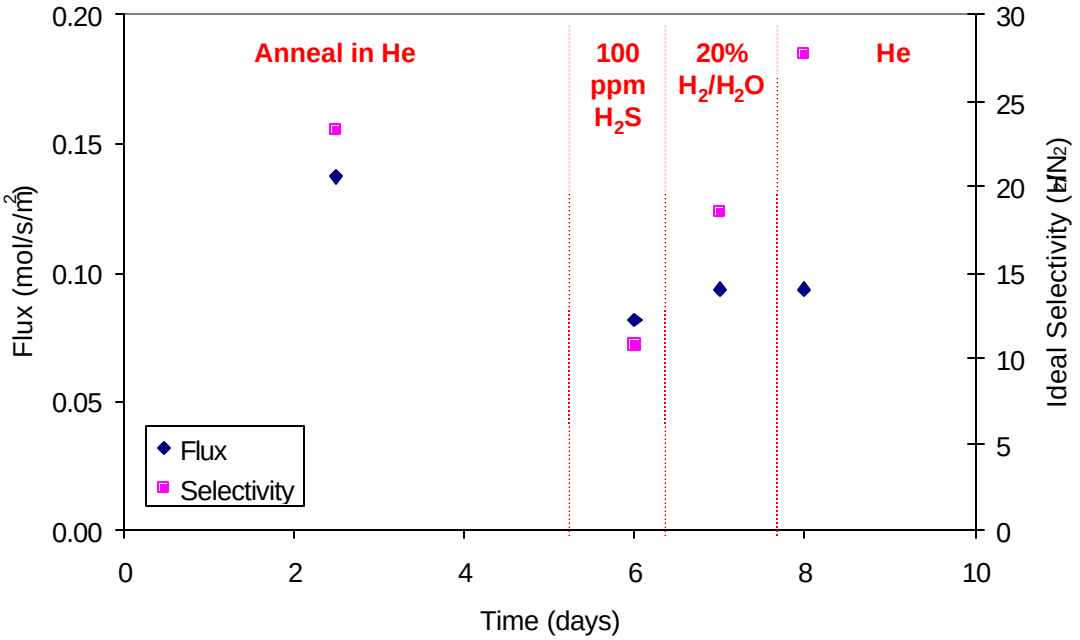

Figure 25. Effect of H_2S exposure on H_2 single gas flux and H_2/N_2 ideal selectivity at 40 psig and 450° C.

We also tested the performance of the Pd-Cu membranes using high sulfur WGS gases. We first tested membrane USF-AK-50-16; it was exposed to a 42/58 H_2/N_2 mixture (the hydrogen concentration matches the protocol conditions) and then to the WGS gases (excluding H_2S) to obtain a baseline for the flux and selectivity in the absence of H_2S. We observed a decrease in selectivity and increase in total flux in the presence of WGS gases in comparison to those of observed in the H_2/N_2 binary (Figure 26). Following the baseline experiments, we introduced 700 ppm H_2S into the WGS gases and initiated a test simulating protocol gas conditions.

With the introduction of H_2S, we observed a sharp increase in flux and a decrease in selectivity to very low levels, close to Knudsen diffusion. These results suggest that the combination of 700 ppm H_2S and H_2O caused significant degradation in membrane performance (i.e. creating defects in the film). We speculate that the combination of H_2O or H_2S gases is causing the problems, since previous work suggest that neither of these gases alone did not deteriorate the membrane performance to such significant extent.

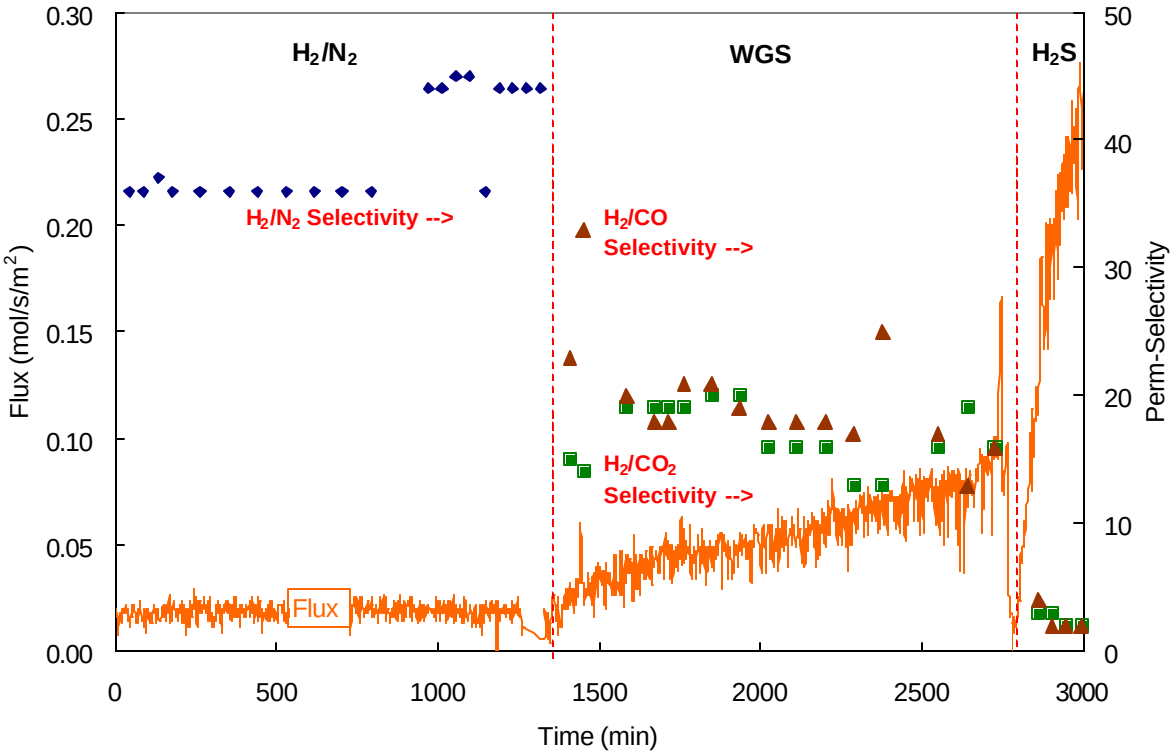

Figure 26. Flux and selectivity as a function of run time for membrane USF-AK-50-16 exposed to H_2/N_2, WGS mixture, and finally WGS mixture + 700 ppm H_2S. T = 350 °C, feed pressure = 60 psig.

To fully understand the effects of sulfur on membrane performance and identify at what sulfur levels that the membrane can be operated, we tested another membrane USF-AK-50-26 in high sulfur environment. In this second set of tests, was first exposed the membrane to a 42/58 H_2/N_2 mixture at where the 60 psig feed pressure and 450 °C to establish a baseline for membrane parameters, hydrogen permeance was 0.0027 mol s^{-1} m^{-2} $psia^{-1}$ (Figure 23) and the H_2/N_2 perm-selectivity was approximately 6 (Figure 24). The initial selectivity was low (H_2/N_2 = 5-7) due to problems with adhesion of the Pd-Cu alloy film to the ceramic support. The poor adhesion has been a recurring problem since late last fall and the cause is under investigation. It is possible the ceramic support manufacturer in France (Exekia) has made some processing changes that changed the surface chemistry of the support. Although the membrane was not high quality (i.e., the separation factor was far below that is required by the application), we exposed it to sulfur at various concentrations ranging from 20 ppm to 630 ppm. The initial tests were carried without any water, using a $H_2/N_2/H_2S$ mixture (42/58/20 ppm). With the addition of 20 ppm H_2S, initially the total permeance decreased from 0.0027 mol s^{-1} m^{-2} $psia^{-1}$ to 0.0018 mol s^{-1} m^{-2} $psia^{-1}$ (Figure 27). However, through the course of the 18 hr test, we observed that the some of the decrease in the flux is recovered and a 0.0022 mol s^{-1} m^{-2} $psia^{-1}$ permeance was established. We believe the decrease in the flux is due to sulfur inhibition effect. It is most likely that the sulfur occupies the sites that are used for dissociative hydrogen chemisorption. As a result of the lower hydrogen flux (i.e., due to the inhibition by sulfur), hydrogen selectivity decreases from 6 to 3.5 in the permeate gas.

After 18 hr operation at 20 ppm H_2S flow, we increased the inlet H_2S concentration to 115 ppm for 8 hours and then to 630 ppm H_2S for another 6 hours. We observed similar trends for 115

and 630 ppm H_2S cases; the initial decrease in the permeance and selectivity with the addition of H_2S was partly recovered and stable values established during the course of the test. After exposure to H_2S, the membrane was swept with N_2 overnight and then we introduced the 42/58 H_2/N_2 mixture into the membrane module, the baseline case, to observe changes in membrane performance. An increase in total permeance and a decrease in H_2/N_2 selectivity can be seen compared to the original binary data.

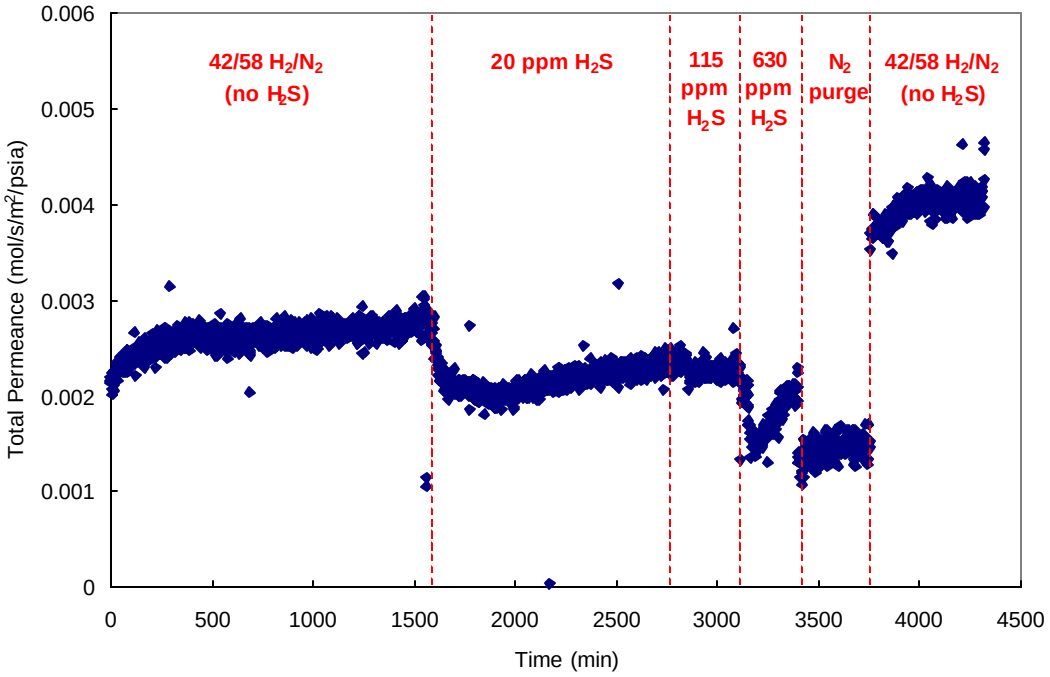

Figure 27. Total permeance vs. time for membrane USF-AK-50-26 exposed to H_2/N_2 and H_2S (20-630 ppm). Feed pressure = 60 psig, T = 450 °C.

During the 72 hr test, we continuously monitored the H_2S concentration in the retentate stream. Figure 29 presents the retentate H_2S concentration as a function of time. It is interesting to note that some of the H_2S was adsorbed by the membrane and (partly by the reactor lines), however, at the end of each test, we observed that the H_2S concentrations in the retentate stream is close to the inlet value. Only for the 630 ppm H_2S inlet condition, we observed higher than expected values in the retentate stream, most probably due to the non-linearity in the GC calibration.

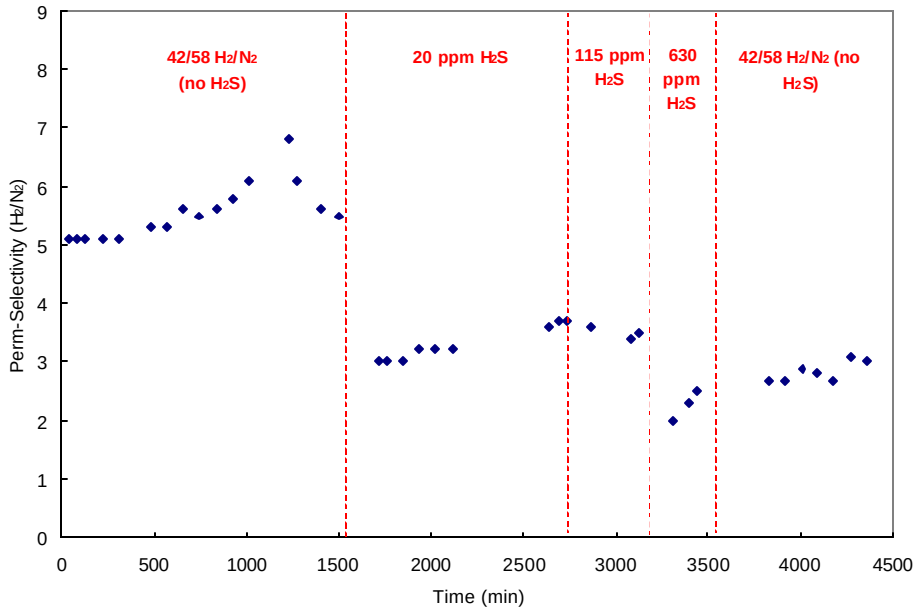

Figure 28. Binary H_2/N_2 selectivity vs. time for membrane USF-AK-50-26 exposed to H_2/N_2 and H_2S (20-630 ppm).

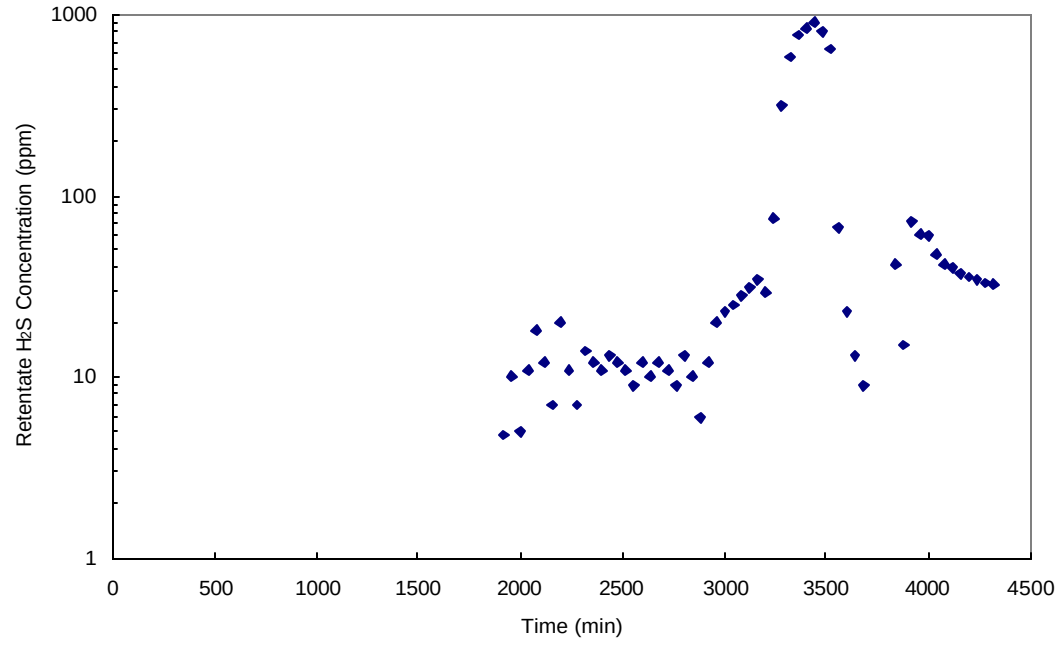

Figure 29. Retentate H_2S concentration vs. time for membrane USF-AK-50-26.

After the tertiary $H_2/N_2/H_2S$ mixture data were taken, steam was introduced at 35% of the feed without H_2S. An increase in total permeance (Figure 30) and a decrease in H_2/N_2 selectivity were detected. A small residue concentration of H_2S (25-40 ppm) was also detected in the H_2S retentate GC. Once again, the small amount of H_2S + H_2O mixture may have created small defects in the membrane which produced the results as seen before with membrane USF-AK-50-16.

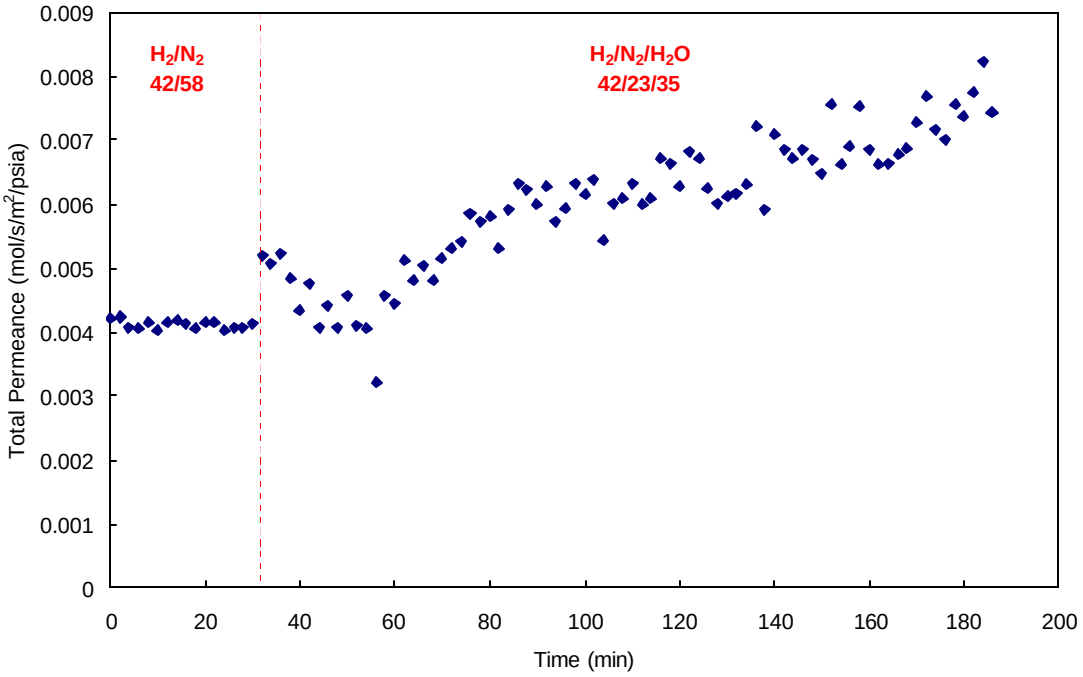

Figure 30. Total permeance vs. time for membrane USF-AK-50-26 exposed to $H_2/N_2/H_2O$ and small residue concentration of H_2S (25-40 ppm).

1.2.1.1.1.8 Conclusion

In the CCP project, TDA and CSM demonstrated that Pd-Cu alloy composite membranes are promising candidates for the WGS membrane reactor application. These membranes can be developed to achieve high hydrogen flux with very high selectivity. Some of the specific conclusions are as follows:

- Through the course of the CCP work, our group prepared thin films on ceramic supports that can separate hydrogen with a flux of 0.36 mol/m^2.s while maintaining an ideal selectivity of 70,000.
- *In this research, may be for the first time, Pd-Cu alloy membranes were tested under WGS reaction conditions with high sulfur concentrations.*
- The binary gas experiments with H_2/CO, H_2/CO_2 and H_2/H_2O showed that hydrogen can be separated from these mixtures without any significant degradation in the membrane performance.
- The binary gas experiments also showed that the Pd-Cu alloy films do not catalyze any undesirable side reactions to any significant extent.
- The membranes exposed to the H_2S-free WGS stream performed reasonably well, achieving H_2/CO, H_2/CO_2 and H_2/H_2O selectivity of 20, 12 and 18, respectively. We observed that the separation factor decreased with the addition of the mixture gases.
- The H_2/H_2S binary gas experiments showed that in the presence of H_2S, the hydrogen flux decreases due to inhibition by sulfur inhibition. Under dry gas streams, where no water vapor was present, a lower (up to 30 to 40% of the original flux) but stable hydrogen flux can be maintained at 20 ppm, 115 ppm and 600 ppm H_2S inlet concentrations. The membrane also maintained its integrity when exposed to H_2S.
- In two attempts, however, the membranes failed when exposed to WGS gases with 630 ppm H_2S (protocol conditions). In these experiments, overall gas flux increased and the separation effectiveness decreased to Knudsen diffusion level.

1.2.1.1.1.8.1 Recommendations

The simulation results provided by Fluor predicted low carbon recovery due to poor membrane selectivity. We are confident that we can fabricate membranes of higher selectivity as seen with membrane #28. Unfortunately, we encountered problems with membrane adhesion to the ceramic supports, which needs to be addressed. We strongly believe that preparation of defect-free membranes with high temperature sealants is key to demonstrate the real potential of these materials. Recommendations for the future work are as follows:

- It is important to note that the simulation results were based on membranes that had already a low selectivity to start with. It is important to identify the reasons that cause low hydrogen separation factors.
- Most of the sealing problems can be eliminated if these films can be prepared on porous stainless steel (PSS) supports. We only made a few attempts to use PSS supports, however, a more through investigation is needed to develop preparation procedures that lead to high performance membranes.
- Preparation of thicker membranes may improve the performance and eliminate the defects in the film to enable the desired separation goals. In support of this hypothesis, after the CCP project ended, a 15 micron thick Pd-Cu alloy composite membrane was exposed to a CO_2/H_2 binary mixture for 30 h at 450°C and 1120 kPa. Though the initial permeability of the membrane was only 10^{-8} mol/s/m^2/Pa due to the thickness, the membrane had a hydrogen/nitrogen ideal selectivity of at least 150 and it did **not change** after exposure to the 50/50 hydrogen/carbon dioxide mixture.

- The fundamental reasons that caused failure of the membrane induced by the H_2S and H_2O combination needs to be understood. It is interesting that only the combination of these components seems to deteriorate the membrane where the single gases do not.
- Films made out of different metal alloys such as Pd-Au are also resistant to copper and may survive under a high sulfur environment and at high steam partial pressures. In particularly, if the failure is due to the copper (i.e., formation of surface species between copper and sulfur that has higher molar volume that cause the delamination of the film), investigation of new sulfur resistant alloys will become more important.

1.2.1.1.1.9 References

No references applicable.

1.2.1.1.2 Development of Silica Membranes for Hydrogen Fuel Production by Membrane Reaction and Development of Mathematical Model of Membrane Reactor

Report Title

CO_2 Capture Project - An Integrated, Collaborative Technology Development Project for Next Generation CO_2 Separation, Capture and Geologic Sequestration

Development of Silica Membranes for Hydrogen Fuel Production by Membrane Reaction and Development of Mathematical Model of Membrane Reactor

Report Reference

1.2.1.1.2

Type of Report:	Final Report
Reporting Period Start Date:	February 2003
Reporting Period End Date:	July 2003
Principal Author(s):	Y.C. van Delft
Date Report was issued:	July 2003
DOE Award Number:	DE-FC26-01NT41145
Submitting Organization:	Energy Centre of the Netherlands
Address:	PO Box 1 NL 1755 ZG, Petten The Netherlands

1.2.1.1.2.1 Abstract

The aim of this project is to develop the water gas shift membrane reactor technology to proof of concept. ECN's tasks are development of tubular microporous silica membranes for use in the reactor, silica membrane testing and development of a software model of the membrane reactor.

Microporous silica membranes have been made according to current standard recipes for immediate use in the test programme. With standard silica membranes the flux criteria of 0.1 mol/sm2bar can be met when no water is present in the feed. However, with water in the feed the flux drops to a value, which is a factor 3 below the target. At the start of the project it was clear the permselectivity criterion of 100 was too high for microporous membranes, a maximum $H2/CO_2$ permselectivity of 39 was measured for standard silica membranes. Selectivity improvement was focused on higher sintering temperatures, but increase of the $H2/CO_2$ selectivity has not been experimentally proven. H2S has no detrimental effect on a standard silica membrane and the H2/H2S selectivity is very high. Under the process conditions, so including water, the stability of the silica membrane is limited to days. For the separation of hydrogen from a mixture with CO_2/CO/H2O the hydrothermal stability has been improved by using modified silica structures by incorporating alkyl-groups (ECN patent pending). The modified silica membrane is stable for more than 1000 hours under simulated steam atmosphere testing.

A software model of the water gas shift membrane reactor has been developed. The model simulates a countercurrent water gas shift membrane reactor with microporous membranes (silica and zeolite) and dense (palladium and proton conducting) membranes and copes with the isothermal and non-isothermal operation of the membrane reactor. The membrane reactor model is implemented as an Aspen Plus User Model (Aspen Plus, version 11.1) and is written in FORTRAN.

1.2.1.1.2.2 Table of Contents

1.2.1.1.2.3 Introduction

The CO_2 Capture Project (CCP) is an initiative of ten major energy and oil companies to develop cost effective technologies for the Capture and Geologic Storage of carbon dioxide. This is to provide control options for CO_2 from the combustion processes operated by these companies and others.

CCP has invited selected organisations to make a proposal for the development of technology to produce hydrogen rich fuel gas. This can be used as a carbon-free fuel in refinery heaters, gas turbines and for power generation from fossil fuel feedstock by means of a water gas shift membrane reactor system. The envisioned application of a water gas shift membrane reactor is to convert the CO in the syngas from a gasifier to produce a hydrogen rich fuel gas stream and a CO_2 rich stream which can be compressed for geological sequestration with minimum further treatment.

The aim of this project is to develop the water gas shift membrane reactor technology to proof of concept. The system is to be designed for operation with sulphur containing feeds from a refinery, such as residual oil, fed to the gasifier. The project is divided into two phases. Phase 1 (12 month activity) involves membrane development and testing on four different membrane materials. The results from this work will be used to estimate membrane and reactor performance, and to determine which of the four membrane types will be selected for further development and application in a laboratory reactor system during phase 2.

ECN's tasks are:

Task 1A: Membrane Development
Development of silica membranes for use in the reactor. ECN will manufacture tubular silica membranes according to current standard recipes for immediate use in the test programme. Specifically for the separation of hydrogen from CO_2/CO/H2O it is foreseen that membrane development is necessary to improve hydrothermal stability by using modified silica structures by incorporating alkyl-groups (ECN patent pending) or halogenide groups or other microporous materials such as zirconia or titania. Membrane materials will be further developed with a focus on WGSMR application. If required according to new process schemes selectivity can be further increased by increasing sintering temperature (smaller pores) of the membrane or modifying the hydrolysis procedure.

Task 1B: Testing of membranes
Silica membrane testing using a model water gas shift composition under simulated operating conditions to determine permeation rate, selectivity, stability, mechanical integrity and resistance to contamination by sulphur, steam and other components of the feed gas.

Task 1C: Modelling
Development of a mathematical model of the membrane reactor with the capability to reflect four membrane types (silica, zeolite, palladium and proton conducting membranes) and to be integrated into process simulation package Aspen. ECN will supply the Aspen membrane software module to Fluor Daniel who may only use the module in and during the project. ECN will help and support Fluor Daniel in using the membrane software module in Aspen and develop relevant process flow sheet options.

The technical progress of ECN in the DOE/WGS5 Water gas shift membrane reactor development study is described in this report. The key developments are given in 1.2.1.1.2.5.1. In Tasks 1A and 1B the progress in membrane development and results of performance tests are described. The water gas shift membrane reactor model for Aspen flow sheeting is described in Task 1C. Finally some conclusions on the membrane development and testing are drawn in 1.2.1.1.2.8.

1.2.1.1.2.4 Executive Summary

The CO_2 Capture Project (CCP) is an initiative of ten major energy and oil companies to develop cost effective technologies for the Capture and Geologic Storage of carbon dioxide. One of the technologies to be developed is the production of hydrogen rich fuel gas to be used as a carbon-free fuel in refinery heaters, gas turbines and for power generation from fossil fuel feedstock by means of a water gas shift membrane reactor system. The aim of this project is to develop the water gas shift membrane reactor technology to proof of concept. ECN's tasks are development of tubular microporous silica membranes for use in the reactor, silica membrane testing using a model water gas shift composition under simulated operating conditions and development of a mathematical model of the membrane reactor with the capability to reflect four membrane types (silica, zeolite, palladium and proton conducting membranes) and to be integrated into process simulation package Aspen.

1.2.1.1.2.4.1 Key Developments

- The maximum H2/CO_2 permselectivity measured at 350°C for standard silica membranes calcined at 400ºC is 39. At a H2/CO_2 permselectivity of 50 the hydrogen permeance is expected to be between 1 and 0.5*10-7 mol/m2sPa (= 0.01-0.02 cc (stp)/sec/cm2 at dP= 1 bar). Selectivity improvement is focused on higher sintering temperatures. Increase of the H2/CO_2 selectivity by increasing the sintering temperature of the silica membranes has not yet been experimentally proven at ECN. Heat treating the modified silica membranes (with built in inert groups) at 600°C instead of 400°C did not increase selectivity. Also the majority of these membranes cracked and further testing was not possible. The hydrogen permeance, derived from the hydrogen partial pressure driving force during gas separation testing with a dry gas mixture is well above 0.1 mol/s.m2bar, which is the target permeance for the application.

- H2/H2S selectivity is 400. Three days testing with H2S has no detrimental effect on a standard silica membrane. Exposition of standard silica membrane to steam at 350ºC shows as expected a decline in permeance and selectivity. In 15 days the H2/CO_2 selectivity decreased from 29.7 to 20.9 and the hydrogen permeance with a factor of 3. Thermodynamic calculations at ECN with FactSageTM show that the hydrothermal stability of zirconia and titania is not expected to be significantly better than standard silica. ECN has focused on the modified silica membranes for improved hydrothermal stability. A modified silica membrane has been on stream in wet gas stability testing for 1000 hours and shows stable and reproducible performance.

- Gas separation with a dry gas mixture showed that from a feed stream containing 35% hydrogen a permeate stream containing 75% hydrogen could be derived. The presence of water in the feed mixtures reduces the hydrogen permeance and hydrogen purity in the permeate compared to the tests without water. Values for Qo (permeance) and Eact (activation energy) to be used as input in the software model have been obtained for the different components in the feed mixture (H2O, H2, CO_2, CO and H2S) through silica membranes.

- A CD-ROM with the installation and sample files and the installation and operation manual of the first version of the water gas shift membrane reactor model has been sent to Fluor end of August 2002. The model is running successfully at Fluor. Help on dealing with error messages and long execution times has been given to Fluor. Programming of the final version with both the Pd alloy and the proton conducting membrane was finished end October 2002. Both the temperature dependent hydrogen permeance and the flux equations of the dense membrane model have been extensively tested. A CD-ROM with the installation and sample files and the installation and operation manual of the final version of the water gas shift membrane reactor model has been sent to Fluor in November 2002.

1.2.1.1.2.5 Experimental

Microporous silica membranes have been made according to current standard recipes for immediate use in the test programme. With standard silica membranes the flux criteria of 0.1 mol/s.m2bar can be met when no water is present in the feed. However, with water in the feed the flux drops to a value, which is a factor 3 below the target. At the start of the project it was clear the permselectivity criterion of 100 was too high for microporous membranes, a maximum $H2/CO_2$ permselectivity of 39 was measured at 350°C for standard silica membranes. Selectivity improvement was focused on higher sintering temperatures, but increase of the $H2/CO_2$ selectivity by increasing the sintering temperature of the silica membranes has not yet been experimentally proven. A value of 9 has been reached for the silica membrane under simulated process conditions. Under these process conditions, so including water, the stability of the silica membrane is limited to days. For the separation of hydrogen from a mixture with CO_2/CO/H2O the hydrothermal stability has been improved by using modified silica structures by incorporating alkyl-groups (ECN patent pending). The modified silica membrane is stable for more than 1000 hours under simulated steam atmosphere testing. H2/H2S selectivity is very high and three days testing with H2S has no detrimental effect on a standard silica membrane. Values for permeance and activation energy to be used as input in the software model have been obtained for the different components in the feed mixture through silica membranes. Thermodynamic calculations showed that the hydrothermal stability of other microporous materials such as zirconia and titania is not expected to be significantly better than standard silica.

A software model of the water gas shift membrane reactor has been developed. The first version of the water gas shift membrane reactor software model with the microporous silica and zeolite membrane has been sent to Fluor end of August 2002. The final version of the water gas shift membrane reactor model with both the Pd alloy and the proton conducting membrane has been sent to Fluor in November 2002. The membrane reactor model simulates a counter-current water gas-shift membrane reactor and describes the non-isothermal and isothermal operation of the membrane reactor. The membrane reactor model is implemented as an Aspen Plus User Model (Aspen Plus, version 11.1) and is written in FORTRAN. A temperature dependent hydrogen permeance has been incorporated. The model is running successfully at Fluor.

1.2.1.1.2.6 Results and Discussion

1.2.1.1.2.6.1 Task 1A: Membrane development

1.2.1.1.2.6.1.1 Standard silica membrane manufacturing

The first 3-6 months the work was focused on 'standard' silica membranes to get an overview of the performance and the stability of the membrane under WGS conditions. For this purpose several batches of tubular silica membranes have been made according to current standard recipes. The silica membranes are made in a batch process, with a maximum of 10 tubes each time. On the outside of alumina substrate tubes with a length of maximum 1 meter porous intermediate layers were coated in order to overcome the surface roughness. A so-called polymeric silica sol was made and coated on top of the intermediate layer. After calcining the membranes are ready for use. The pore size of the membranes is about 5Å and can be optimised for certain applications by e.g. modifying the silica sol or the calcining procedure. The separation layer of these membranes consists of a very thin (<200 nm) hydrophilic amorphous silica film on the outside of a multi-layer alumina support tube (see Figure 3.1).

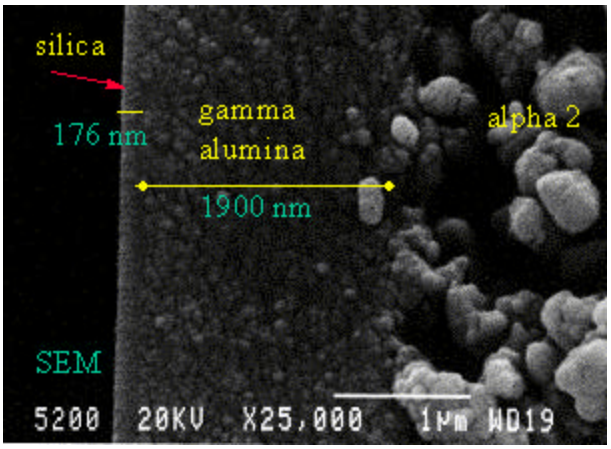

Figure 0.1 Scanning Electron Micrograph of a high-selective silica membrane

The membrane tubes are made at a length of 1 meter and an ID/OD of 8/14 mm. Pieces of 10 cm have been cut from these tubes for use in the test programme of task 1B. An overview of properties of the support and membrane layer is given in Table 3.1.

Table 0.1 Overview of properties of the support and membrane layer

Layer	Coating type	Name	Compound	Thickness	porosity	Pore d50/nm
1	-	Extruded tube	α-Al_2O_3	3000 µm	0.35	4000
2	suspension	alpha 1	α-Al_2O_3	30-50 µm	0.22	180
3	suspension	alpha 2	α-Al_2O_3	30-40 µm	0.34	170
4	Sol-gel	gamma	γ- Al_2O_3	1.5-2.0 µm	0.5	3-5
5	Sol-gel	silica	SiO_2	50- 120 nm	0.5	<1

The quality of batches with tubular silica membranes has been checked by our so-called Helium-1-point test. The Helium-1-point test gives an indication of the defect density of the membrane. By comparing the results of the He-1-point test with gas permeation tests we found that the probability for sufficient gas separation properties is high enough when the 1-point He value is below 100 ml He/min.10cm.3bar. Silica membrane pieces have been selected on He value for use in the test programme of task 1B. Gas permeation tests have been performed with silica membranes with a He-value below 100 units.

1.2.1.1.2.6.1.2 Hydrothermal stability and selectivity improvement

1.2.1.1.2.6.1.2.1 Hydrothermal stability improvement

Specifically for the separation of hydrogen from CO_2/CO/H_2O it is foreseen that membrane development is necessary to improve hydrothermal stability. The approach was taken to investigate the hydrothermal stability of modified silica structures which incorporate alkyl-groups (ECN patent pending). Small batches of tubular modified silica membranes with built in methyl groups have been made according to available recipes. Addition of methyl groups in the silica structure has been done by the addition of and reaction with methyltriethoxysilane (MTES), see Figure 3.2. Calcination temperatures (250 or 400°C), calcination atmosphere (air or nitrogen) and pre-treatment procedures have been varied during fabrication to determine the effect of these processing parameters on the gas separation performance. Pieces of 10 cm have been cut from these tubes for use in the test programme of task 1B. The modified silica membranes have been checked for their suitability and the gas separation performance has been compared with the 'standard' membranes.

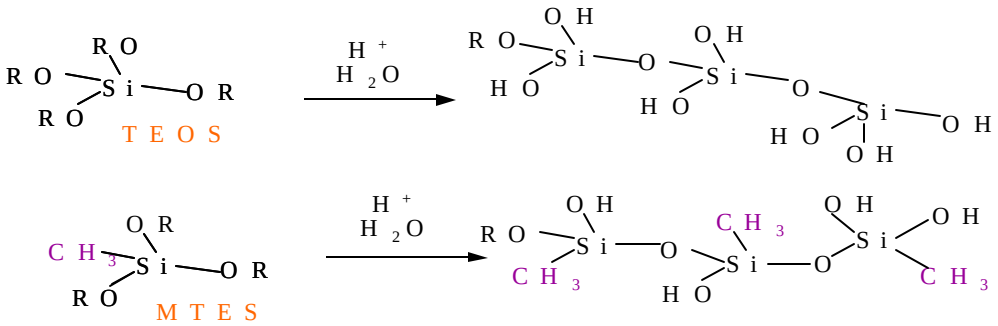

Figure 0.2 Simplified reaction scheme for silica and modified silica membranes

Thermodynamic calculations at ECN with FactSage™ show that the hydrothermal stability of zirconia and titania is not expected to be significantly better than standard silica (Boer, 2002). At high temperature titania reacts with reducing agents such as carbon monoxide, hydrogen and ammonia to form titanium oxides of lower valency (Uhlmann, 1999). Titania reacts with chlorine in the presence of carbon above 500ºC to form titanium tetrachloride.

There are no prototype membranes made from zirconia and titania available which are suitable for hydrogen separation from carbondioxide. This will take a considerable development effort. Furthermore it is generally known that increased calcination temperatures of up to 600ºC will also improve the hydrothermal stability of silica materials. Therefore, regarding the existing time schedule, the CCP pre-combustion team agreed to focus only on the modified silica membranes for hydrothermal stability improvement and on higher calcination temperatures for improved selectivity.

1.2.1.1.2.6.1.2.2 Maximum selectivity standard silica membranes

Standard silica membranes made all in the same way show a variation in hydrogen permeance and H_2/CO_2 permselectivity. In order to know the range of variation an inventory has been made of the twenty-two membranes made and tested in the last two years. Only two of these membranes had a H_2/CO_2 selectivity between 30 and 40 (see Figure 3.3).

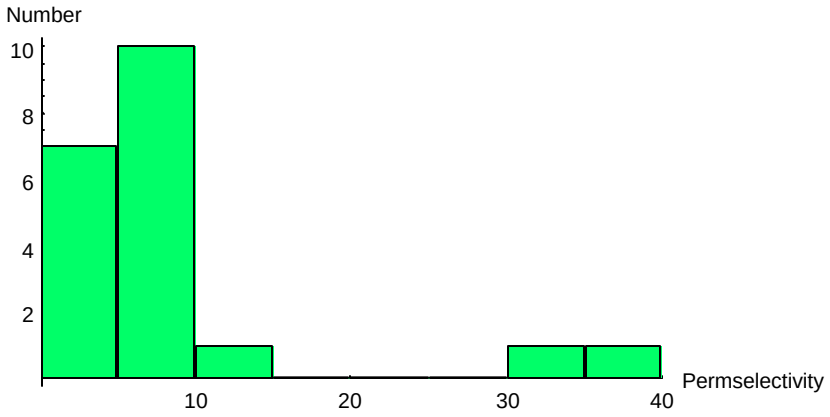

Figure 0.3 Number histogram of H_2/CO_2 permselectivities at 350 ^{0}C and Pav=9.5 bar

The average H_2/CO_2 permselectivity was between 5 and 15 (see Task 1B). The membrane used in the hydrothermal test had a H_2/CO_2 permselectivity higher than average (= 29.7). An overview of the performance of these three standard silica membranes with increased selectivity is given in the Table 0.2. When the membranes have a H_2/CO_2 permselectivity which is a factor 3 to 4 higher than standard they have a hydrogen flux, which is a factor 5 to 10 lower. From this data it is expected that the hydrogen permeance of a silica membrane with a H_2/CO_2 selectivity of 50 would be in the range of 1 to 0.5 x 10^{-7} mol/m^{2}sPa (= 0.01-0.02 cc (stp)/sec/cm^2 at dP= 1 bar).

Table 0.2 Overview performance standard silica membranes

Temperature	350°C	
Membrane type	H_2 flux [cc (stp)/sec/cm^2]	H_2/CO_2 permsel.
Average	0.22-0.67 (0.1-0.3)	5-15
X2M62Si07	0.09 (0.041)	39
X65Si02	0.036 (0.016)	33
XT51Si53	0.084 (0.037)	29.7

H_2 flux between brackets in [mol/m^{2}s], Pfeed= 10 bar, dP= 1bar

1.2.1.1.2.6.1.2.3 Selectivity Improvement

A possibility for increasing the selectivity of the silica membranes would be calcination at 600ºC. In the PhD work of R. de Vos (1998) it was reported that the H_2/CO_2 selectivity increases with at least a factor of 10 when the sintering temperature is increased from 400 to 600ºC. The hydrogen permeance measured at higher temperature (300 in stead of 200ºC) decreased with at least a factor of 3 (seeTable 0.3).

Table 0.3 Hydrogen permeance and H_2/CO_2 selectivity of silica membranes

Membrane	Avg H_2 permeance [mol/m²sPa]	H_2/CO_2 selectivity
Si400 (200ºC) R. de Vos	$1.64\ 10^{-6}$	7.5
Si600 (300ºC) R. de Vos	$6\ 10^{-7}$	70 - 139
Si400 (200ºC) ECN	$5.4\ 10^{-7}$	9 - 13.6
Si600 (200ºC) ECN	$5.1\ 10^{-7}$	7.7
Modified Si250 (350ºC) ECN	$7.6 - 3.1\ 10^{-6}$	4.1 - 4.5
Modified Si450 (350ºC) ECN	$3.9 – 9.3\ 10^{-6}$	4.2 - 5

() between brackets the temperature at which the hydrogen permeance was measured.

Several silica membranes have been made by ECN according to current standard recipes and were sintered at 400 and 600ºC. However, as shown in the table below both silica membrane types gave the same hydrogen permeance and H_2/CO_2 selectivity. Also increasing the sintering temperature of the modified silica membranes did not show an increase of selectivity. Calcination at 600ºC will also improve the hydrothermal stability. In any case increasing the selectivity will cause definitely a decrease of the flux through the membrane, which can be important for the economical feasibility.

1.2.1.1.2.6.1.2.4 Selectivity improvement modified silica membranes

Both the selectivity and the hydrothermal stability of the microporous silica membranes can be improved by:

- A modified sol synthesis procedure by building inert groups into the silica structure, which should result in increased stability but inherently a decrease in selectivity.

- An increase in sintering temperature from 400ºC to 600ºC, which should result in both increased selectivity and stability

The second possibility has been applied to standard silica membranes but has not resulted in increased selectivity as reported by R. de Vos in her PhD work. Modified silica membranes have slightly larger pores and therefore a small decrease in selectivity. The approach is now to sinter the modified silica membranes at 600ºC by which the pores should become smaller and the amount of OH-groups reduces, which should lead to an increase in selectivity of a membrane already incorporating inert groups that improve the stability.

New modified silica membranes have been made. According to the normal manufacturing procedure the modified silica layer were calcined at 400ºC. Then the membranes were built in a test cell, heated to 600ºC and tested with gases. Before and after heat treatment the first membrane (code 3M56MS03) gave a H_2/CO_2 permselectivity of 6.3. So no improvement in selectivity was observed compared with the results of the normal silica membrane. Two other membranes treated in this way showed significantly increased permeance indicating cracking of the layer.

1.2.1.1.2.6.2 Task 1B: Testing of membranes

1.2.1.1.2.6.2.1 Gas permeation tests

'Standard' silica membranes have been tested in single gas (H_2, CO_2, N_2, CH_4) permeation tests at 350°C and a maximum feed pressure of 10 bar. The performance at 350°C, 10 bar feed pressure and a dP of 1 bar for the silica membranes is given in the Table . Silica membranes with a lower selectivity have a high H_2 flux. The test results are comparable with results of silica membranes made in 2001.

Modified silica membranes have been checked for their suitability and the gas separation performance has been compared with the 'standard' membranes. Membranes have been tested in single gas (H_2, CO_2, N_2, CH_4) permeation tests at 350 and 450°C and a maximum feed pressure of 10 bar. The performance at 350 and 450°C, 10 bar feed pressure and a dP of 1 bar for the modified silica membranes is given in the Table 0.4. For comparison also the performance of the standard silica membrane at 350°C is given.

Table 0.4 Performance standard and modified silica membranes

Temperature	350°C		450°C	
Membrane type	H_2 flux [cc (stp)/sec/cm^2]	H_2/CO_2 permsel.	H_2 flux [cc (stp)/sec/cm^2]	H_2/CO_2 permsel.
Modified silica (N_2 calcined)	0.45 (0.2)	7	0.68 (0.3)	9
Modified silica (Air calcined)	0.45-1.79 (0.2-0.8)	4-8	0.23-2.0 (0.1-0.9)	5
Standard silica	0.22-0.67 (0.1-0.3)	5-15	-	-

() H_2 flux in [mol/m^{2}s]

For interaction between the flow sheet modelling and the membrane development early performance data of the silica membrane at 350°C has been sent to Fluor mid-August 2002. The maximum measured H_2/CO_2 selectivity of the silica membrane at 350°C was 15 at that time and first measurements with pure H_2S showed a H_2/H_2S selectivity of 400. Since permeation data on H_2O and CO were not available at that time, the selectivity of the silica membrane for these components compared to hydrogen was estimated to be the same as for CO_2.

1.2.1.1.2.6.2.2 Hydrothermal stability testing

Before hydrothermal testing the prolonged exposition to elevated temperatures was investigated. Thermal cycling of a 'standard' silica membrane from 50 to 350°C under dry He flow shows a slow increase in He permeance in time. The hydrothermal stability for both silica (membrane code B28-11-Si-13 and XT51Si53) and modified silica (5M05MS03 and 6M07MS07) membranes have been tested. In these tests the membranes are exposed to a helium water vapour mixture (70 kPa water with 80 ml/min He) at 350°C. During exposition the He and CH_4 permeability have been measured at certain time intervals.

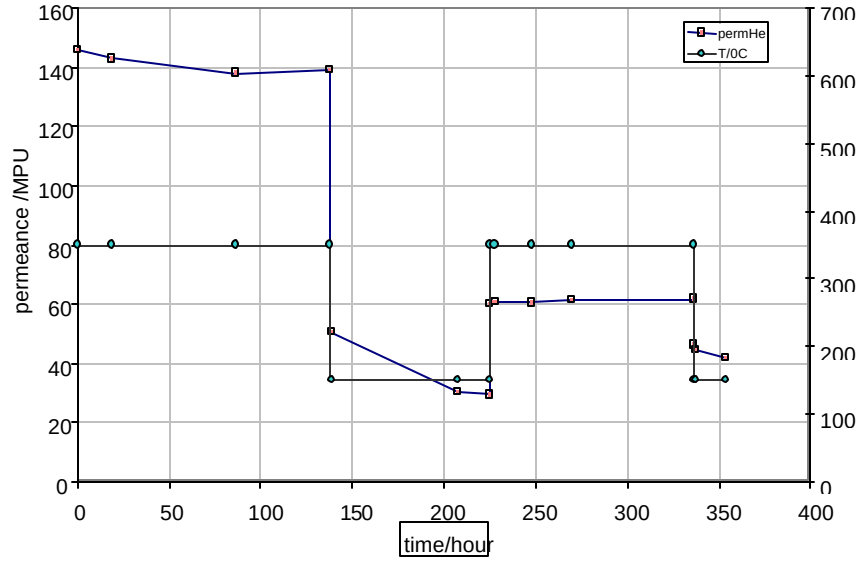

Figure 0.4 Exposition of silica membrane B28-11-Si-13 at 350°C and 150° C (1MPU= 10^8 mol/m^2.s.Pa)

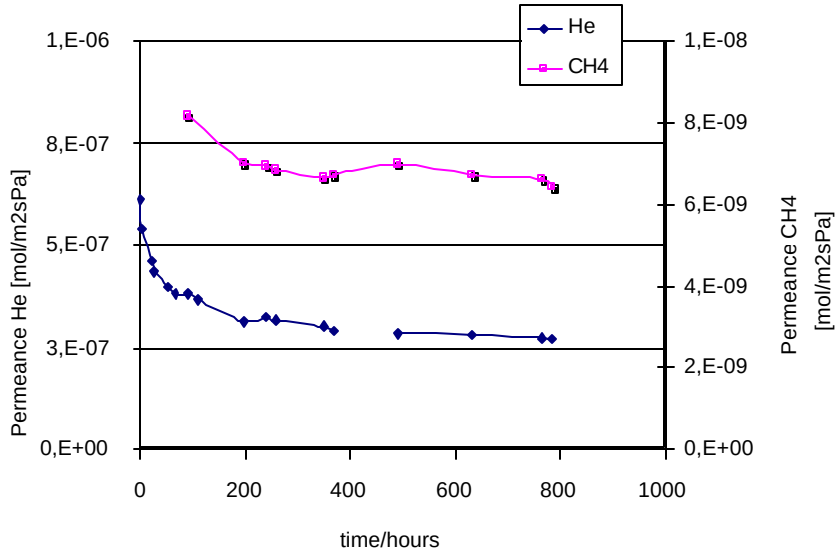

Figure 0.5 Exposition of silica membrane XT51Si53 at 350°C

The results of the measurements using the silica membranes are given in Figure 4.1 and 4.2. The first silica membrane B28-11-Si-13 shows a small decrease in He permeance after 100 hours of water vapour exposition. At longer exposition times the He permeance at 350ºC remains constant. Exposition at lower temperature (150ºC) gives the same He permeance curve in time. The H_2/CO_2 permselectivity decreases after 225 hours of exposition to water vapour (see Table 0.5). The second silica membrane (XT51Si53) shows a similar small decrease in the He permeance in the first 200 hours. The flux/permeance of both helium and methane declined by about a factor of 2. After this time the flux is more or less constant. There is hardly any change in selectivity (48 at the start and 41 after 874 hours for He/CH_4) as both fluxes have decreased. The measurement was stopped according to planning as the modified silica membrane was to be measured.

Table 0.5 Results hydrothermal testing standard and modified silica membranes, 70 kPa water with 80 ml/min He at 350°C

Membrane	Exp time [hours]	Permeance 10^{-8} [mol/m^{2}sPa]				Permselectivity	
		He	H_2	CO_2	CH_4	H_2/CO_2	He/CH_4
Standard silica	0	145	143	17.5	13.6	8.2	10.7
B28-11-Si-13	225	55	96	23.5	97.9	4.1	0.6
Standard silica	0	61.2	37.4	1.3	0.75	29.7	48.6
XT51Si53	239	32.4	-	-	0.7	-	46.6
	368	-	11.2	0.5	0.6	20.9	-
	784.5	27	-	-	-	-	41.9
Modified silica	0	266	-	-	24.9	-	10.7
5M05MS03	230	317	396	97.3	33.3	4.1	9.6

The stability measurement results of the modified silica membranes are presented in Figure 4.3 and 4.4. The first membrane 5M05MS03 shows a slight increase in the permeance after the start of the measurement and after about 200 hours this value is constant. The selectivity He/CH_4 is always 10±1. After about 1150 hours on stream both the helium and methane flux increased and the selectivity dropped. Initial investigation revealed that the sudden flux increase is probably due to crack formation and not by change of the pore system.

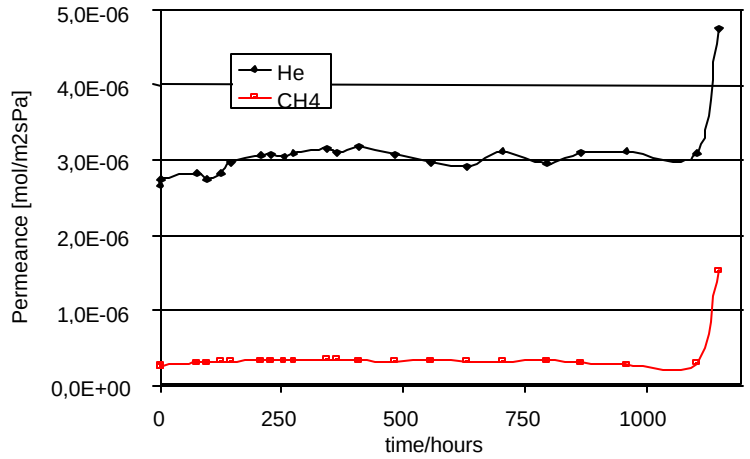

Figure 0.6 Exposition of modified silica membrane 5M05MS03 at 350°C

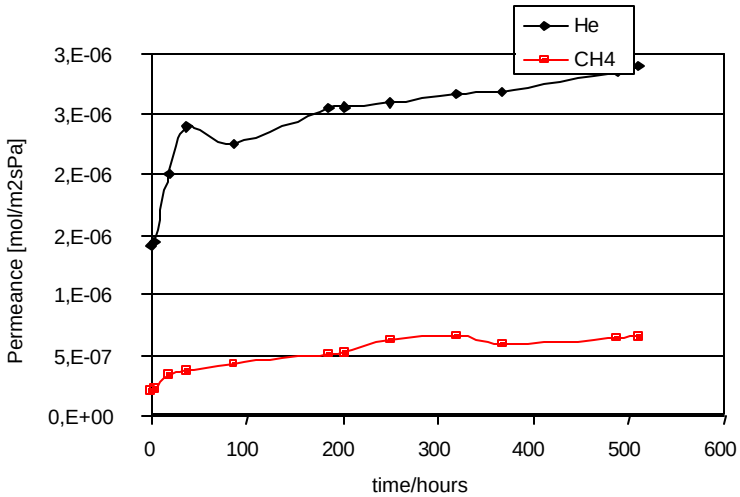

Figure 0.7 Exposition of modified silica membrane 6M07MS07 at 350°C

In the first 50-100 hours the permeance of the second modified silica membrane 6M07MS07 increases by about a factor of 1.5 and then more or less stabilises. The selectivity decreases from about 6.5 to 4.5. The flux stability results are comparable with the first membrane.

1.2.1.1.2.6.2.3 Gas separation tests

1.2.1.1.2.6.2.3.1 Gas separation tests without water

Gas separation tests with the model WGS gas composition have started with the standard silica membrane (T90Si02). With pure gases this membrane had a hydrogen permeance of $1*10^{-6}$ mol/m^{2}sPa and a H_2/CO_2 permselectivity of 13.6 at 350^{o}C measured in the gas permeation test rig. The membrane has been transferred to the high temperature high-pressure test rig for gas separation testing. First measurements are performed **without** water to see the effect of a gas mixture on the hydrogen permeance and the selectivities. The water is balanced in these tests with nitrogen.

Table 0.6 Feed composition for dry gas separation test. Feed flow is 5 l/min

Feed composition [mol %]				
H_2	CO_2	CO	H_2O	N_2
35.0	22.0	2.5	-	40.5

Table 0.7 Permeate and retentate compositions of gas separation tests with T90Si02 (summary).

			Permeate composition [mol %]					Retentate composition [mol %]					H_2 permeance
T [C]	P_{feed} [bar]	dP [bar]	H_2	CO_2	CO	H_2O	N_2	H_2	CO_2	CO	H_2O	N_2	[mol.s^{-1} m^{-2}bar]
256	5	4	74.8	15.6	0.44	-	6.9	26.1	22.6	2.9	-	45.8	0.17
250	10	9	72.4	16.6	0.53	-	8.3	15.3	23.8	3.4	-	54.6	0.14
248	15	14	67.8	18.5	0.71	-	10.9	8.6	23.4	3.7	-	61.1	0.12
345	5	4	75.7	12.6	0.53	-	8.5	25.8	22.9	2.8	-	45.7	0.19
346	10	9	72.5	13.9	0.67	-	10.5	14.5	25.2	3.4	-	53.7	0.14
335	15	14	67.7	16.6	0.88	-	13.4	8.1	25.3	3.6	-	59.8	0.12
431	5	4	76.3	11.5	0.66	-	9.9	25.8	23.5	3.0	-	45.6	0.19
435	10	9	72.4	12.9	0.84	-	12.6	14.2	26.1	3.5	-	53.8	0.15
445	15	14	66.7	15.1	1.11	-	15.9	7.7	26.9	3.9	-	59.1	0.13

In the above table it can be observed that the membrane is capable of producing a hydrogen rich stream containing about 75% hydrogen from a feed stream containing only 35% hydrogen. Carbon monoxide and nitrogen permeate hardly through the membrane.

From the retentate composition it can be observed that there is a significant depletion of hydrogen in the feed. Especially when the driving force is high (dP=14 bar) the feed is depleted in hydrogen from 35% to 8% over a membrane of only 10 cm length. In other words: the hydrogen recovery increases with an increase of the driving force, however, this has to be paid by a decrease in the hydrogen concentration in the permeate.

The hydrogen permeance, derived from the hydrogen partial pressure driving force is well above 0.1 mol/s.m^{2}bar, which is the target permeance for the application. The membrane data show that the hydrogen permeance increases slightly with temperature. Also the nitrogen and carbon monoxide permeance increase with temperature, which indicates for these molecules the main transport is through small pores and not defects, as defect flow is governed by Knudsen diffusion and/or viscous flow which decrease with a temperature increase. The carbon dioxide permeance decreases with temperature probably due to the fact that this molecule strongly adsorbs on the surface and this surface adsorption (and flow) decreases with an increase in temperature. The results of the first dry gas tests were evaluated with the focus on the permeance of the large molecule gasses CO and N_2. As H_2S is even larger and following previous results with pure H_2S, which showed very low H_2S permeances, it was decided not to incorporate H_2S in the gas mixtures. Also the fact that in previous tests it was observed that H_2S had no detrimental effect on the membrane supports this decision.

Gas separation experiments **without water** were repeated with a comparable silica membrane M14Si05b. With pure gases this membrane had a hydrogen permeance of $1.7*10^{-6}$ mol/m^{2}sPa and a H_2/CO_2 permselectivity of 7.5 at 350°C measured in the high temperature high pressure test rig. Feed flows of 5, 10 and 15 l/min have been used in these tests. Only the results of the 15 l/min are presented here.

Table 0.8 Feed composition for dry gas separation test. Feed flow is 15 l/min

Feed composition [mol %]				
H_2	CO_2	CO	H_2O	N_2
37.0	19.2	2.4	-	41.3

Table 0.9 Permeate and retentate compositions of gas separation tests with M14Si05b (summary)

			Permeate composition [mol %]					Retentate composition [mol %]					H_2 permeance
T [°C]	P_{feed} [bar]	dP [bar]	H_2	CO_2	CO	H_2O	N_2	H_2	CO_2	CO	H_2O	N_2	[mol.s^{-1} m^{-2}bar]
250	5	4	83.4	7.5	0.6	-	8.5	35.5	19.7	2.6	-	42.2	0.14
250	10	9	84.2	7.1	0.6	-	8.1	31.9	20.8	2.8	-	44.6	0.13
250	15	14	82.9	7.5	0.6	-	9.0	28.5	21.5	2.9	-	47.1	0.13
350	5	4	86.0	6.1	0.5	-	7.4	34.7	20.0	2.5	-	42.8	0.14
350	10	9	86.4	5.8	0.5	-	7.3	30.4	21.2	2.7	-	45.8	0.15
350	15	14	85.0	6.2	0.6	-	8.2	26.0	22.2	2.6	-	49.3	0.16
450	5	4	86.4	5.6	0.5	-	7.5	35.3	20.0	2.6	-	42.2	0.17
450	10	9	87.2	5.2	0.5	-	7.1	30.2	21.3	2.9	-	45.6	0.18
450	15	14	85.8	5.5	0.6	-	8.1	25.4	22.6	3.1	-	48.8	0.19

In the above table it can be observed that the membrane is capable of producing a hydrogen rich stream containing about 85% hydrogen from a feed stream containing only 37% hydrogen. Carbon monoxide and nitrogen permeate hardly through the membrane. These results compare well with the previous membrane (T90Si02). The hydrogen concentration in the permeate is even higher now, as less depletion of hydrogen on the feed side occurs at the higher feed flow rate used now. From these separation measurements a maximum selectivity of 18 is obtained for H_2/CO_2. The hydrogen permeance, derived from the hydrogen partial pressure driving force is well above 0.1 mol/s.m^{2}bar, which is the target permeance for the application.

1.2.1.1.2.6.2.3.2 Gas separation tests with water

Experiments with membrane M14Si05b were continued, now with water added to the feed. The dry gas feed flow was now 5 l/min instead of 15 l/min in the experiments without water.

Table 0.10 Feed composition for wet gas separation test. Dry gas feed flow is 5 l/min

Feed composition [mol %]				
H_2	CO_2	CO	H_2O	N_2
50.6	26.3	3.2	19.9	0.1

Table 0.11 Permeate and retentate compositions of gas separation tests with water (summary)

			Permeate composition [mol %]					Retentate composition [mol %]					H_2 permeance
T [°C]	P_{feed} [bar]	dP [bar]	H_2	CO_2	CO	H_2O	N_2	H_2	CO_2	CO	H_2O	N_2	[mol.s^{-1} m^{-2}bar]
250	5	4	71.8	14.7	2.1	11.3	0.0	54.7	30.3	3.5	11.6	0.0	0.055
250	10	9	61.8	13.5	1.6	23.1	0.0	52.8	30.3	3.4	13.5	0.1	0.035
250	15	14	59.3	20.3	2.5	17.8	0.0	29.7	19.3	2.2	48.8	0.1	0.050
350	5	4	61.3	4.9	0.6	33.2	0.0	51.4	29.4	3.4	15.8	0.0	0.031
350	10	9	68.1	7.8	0.8	23.2	0.0	50.0	29.1	3.4	17.4	0.1	0.018
350	15	14	60.4	10.2	1.3	28.1	0.0	50.2	28.8	3.2	17.8	0.0	0.013
450	5	4	57.4	2.4	0.5	39.6	0.0	43.0	25.5	2.9	28.6	0.0	0.055
450	10	9	57.0	4.4	1.1	37.4	0.0	41.7	24.7	2.9	30.7	0.0	0.030
450	15	14	49.0	6.2	1.1	43.7	0.0	42.5	25.1	3.0	29.5	0.0	0.021

The above reported measurements have started at 350°C. Then 250 and finally 450°C measurements have been performed. From these measurements and checking of the membrane performance between these temperatures it is clear that the membrane quality (pure silica membrane) decreased already during the measurements at 250°C. Therefore the results of the measurements at 350°C will be discussed only.

The membrane is capable of producing a hydrogen rich stream containing about 70% hydrogen from a feed stream containing 50% hydrogen. The hydrogen permeance, derived from the hydrogen partial pressure driving force has a maximum value of 0.031 mol/s.m^{2}bar. When comparing the measurements at 350°C without water (Table 0.9) with the measurements with water in the feed (Table 0.11) it is clear that both the hydrogen purity in the permeate and the hydrogen permeance are decreased by the water present in the feed stream.

From the above results in the values for Q_o and E_{act} as input in the software model were derived, see Table 0.13. Some corrections and extrapolations have been used for obtaining these numbers. For the moment the temperature range for using these data is from 250 to 450°C. These data have been sent to Fluor.

1.2.1.1.2.6.2.3.3 H_2S permeation

A standard silica membrane has been tested with pure H_2S at different temperatures (only up to 100°C) to determine the permeance and the selectivity of the membrane in feeds containing H_2S. The H_2S permeance is very low (5-6 10^{-9} mol/m^2sPa at 50ºC), which gives a H_2/H_2S permselectivity of more than 400. After three days of testing with H_2S the He flux recovers indicating no detrimental effects on the silica when exposed to H_2S. From these measurements the Q_o and E_{act} values were derived, which are given in the Table 0.12. Included are the values of Q_o and E_{act} for the other main components of the water gas shift mixture. These latter results have been obtained from gas mixture testing for a process without water.

Table 0.12 Data (Qo and Eact) without water

Gas	Qo [mol/m^2sPa]	E_{act} [J/mol]	Permselectivity H_2/gas with gas mixture	Knudsen permselectivity
H_2	4.05E-06	5007	1	1
CO_2	7.78E-08	-2171	18.0	4.69
CO	1.01E-07	1064	26.4	3.74
N_2	8.42E-08	1004	29.6	3.74
H_2S	1.39E-08	1629	150*	4.1

* Calculation based upon permeability of pure H_2S

From measurements including water it is clear that water reduces the permeance of all components. As the permeance of H_2S has not been measured including water (for reason that it can not be detected by GC in the permeate) it is assumed that the H_2S permeance decreases exactly the same as the permeance of N_2 and CO, so by a factor of 2.3. In Table the values for Q_o and E_{act} are given for a water gas shift process mixture with water. For the moment the temperature range for using these data is from 250 to 450°C and for H_2S it is assumed that the measurements up to 100°C can be used for the model parameters up to 450°C.

Table 0.13 Input data (Qo and E_{act}) with water

Gas	Qo [mol/m^2sPa]	E_{act} [J/mol]	Permselectivity H_2/gas with gas mixture from 350°C measurement	Knudsen permselectivity
H_2	4.93E-07	5007	1	1
CO_2	2.41E-08	-2171	9.1	4.69
CO	4.35E-08	1064	8.7	3.74
H_2O	2.50E-06	1663	0.12	3
N_2	3.63E-08	1004	-	3.74
H_2S	6.00E-09	1629	43*	4.1

* Calculation based upon permeability of pure H_2S

1.2.1.1.2.6.3 Task 1C: Modelling

One of the activities of ECN in phase 1 was the development of a mathematical model of the membrane reactor, to be integrated into the process simulation package Aspen Plus, with the capability to reflect four membrane types (silica, zeolite, palladium alloy and proton conductive perovskite membranes). Three Aspen membrane reactor software modules were supplied to Fluor Daniel for use in and during the project. A simplified membrane reactor model was sent to Fluor mid-June 2002 to give Fluor the possibility to run some integrated membrane reactor process flow sheets at an early stage in the project. The first version of the water gas shift membrane reactor model including only the microporous transport model was finished end of August 2002. The final version with also the palladium alloy membrane and the proton conductive perovskite membrane was available in November 2002. In this report a summary is given on the three software modules. First the simplified model and the modelling approach will be described. Some information on the two versions of the water gas shift membrane reactor model and the support to Fluor is given. Finally the different membrane transport models and the water gas shift reaction kinetics incorporated in the final water gas shift membrane reactor model are described. More detailed information is given in (Brandtwagt, 2002; van Delft, 2002; Dijkstra, 2002).

1.2.1.1.2.6.3.1 Simplified Aspen membrane reactor model

To get Fluor started a simplified Aspen membrane reactor model has been made based on a combination of reactor, heat exchanger, splitter and mixers. The purpose of this membrane water gas shift reactor model is to give Fluor the possibility to run some integrated membrane reactor process flow sheets at an early stage in the project. It is not the purpose of the model to give a highly accurate description of the performance of a membrane reactor.

1.2.1.1.2.6.3.1.1 Modelled Process and modelling approach

The model simulates a co-current water gas shift membrane reactor. The working principle of the membrane reactor is given in Figure 5.1.

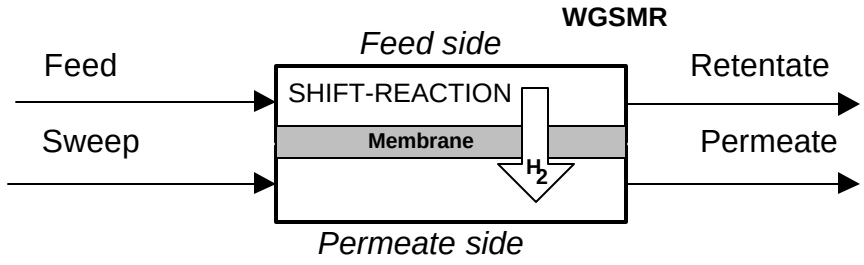

Figure 0.8 Schematic representation of the water gas shift membrane reactor

Reformer gas is fed to the feed side of the membrane. In this part of the reactor a water gas shift reaction takes place. Simultaneously hydrogen diffuses through the membrane, enhancing the shift reaction. A driving force is necessary for the hydrogen diffusion through the membrane, therefore sweep gas is used to lower the hydrogen pressure on the permeate side of the membrane.

The following processes take place simultaneously:
- the water gas-shift reaction $CO+H_2O \Leftrightarrow H_2+CO_2$,
- hydrogen permeates through the membrane, pulling the shift reaction to the right,
- heat exchange.

Aspen Plus is not able to model parallel reaction with permeation directly. Therefore an approach has been chosen using a large recycling stream in which reaction and permeation take place. Due to this large

recycling stream both processes can be considered to take place parallel to each other. Heat exchange is assumed to take place after reaction and permeation. As a result, the effect of sweep gas temperature on the conversion is not taken into account. Other important assumptions are:

- no pressure drop on the feed and permeate side of the membrane,
- no heat loss to the surroundings,
- a thermodynamic equilibrium approach to calculate the shift reaction conversion is used.

1.2.1.1.2.6.3.1.2 Model description

The Aspen Flow sheet model is given in Figure 5.2.

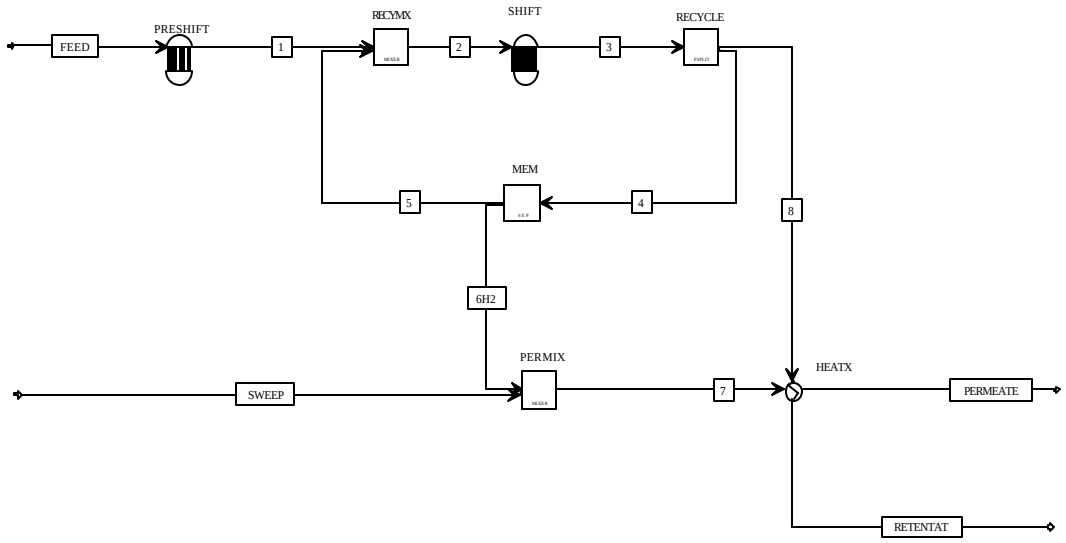

Figure 0.9 Schematic drawing of the model

Feed side:
The FEED stream is led through the PRESHIFT [RGIBSS] block to equilibrate the stream. After it passes the RECYMIX [MIXER] the shift reaction takes places in the SHIFT [RGIBBS] block. Through the block RECYCLE [FSPLIT] a major part of stream is 3 recycled and passes the MEM [SEPARATOR] block, which is the actual membrane. In the MEM block a major part of the hydrogen that is contained by stream 4 is split off, leaving a hydrogen poor stream 5. This hydrogen poor stream is mixed in the block RECYMIX with the FEED stream. Stream 8 is the retentate stream before any heat exchange has taken place. The heat exchange is modelled by the block HEATX [HEATX], where the final RETENTAT stream is calculated.

Permeate side:
The through the membrane diffused hydrogen is represented by stream 6H2. As there has to be a driving force over the membrane in terms of a partial hydrogen pressure, stream 6H2 is diluted by a SWEEP stream in block PERMIX [MIXER] resulting in stream 7. Stream 7 is led to the HEATX block where heat is exchanged with the retentate stream, producing the final PERMEATE stream.

1.2.1.1.2.6.3.2 First version of the water gas shift membrane reactor model

The existing stand alone membrane reactor model has been evaluated and is used as starting point for the membrane reactor model for Aspen flowsheeting. Extra features of the Aspen membrane reactor model are different permeation equations for the four types of membranes and the communication with Aspen.

The public domain solver proved to be not suitable and a stronger commercial solver is used. For using this solver a small fee was paid by ECN. The first version of the water gas shift membrane reactor model, which includes only the microporous membrane, was tested in an Aspen flow sheet. After delivery of the model, support in using the membrane reactor software module in Aspen was given to Fluor. Extra information was given on the programmed water gas shift catalyst and possibilities for Fluor to change the catalyst in the model. Help on dealing with error messages and long execution times has been given.

According to the work plan in the first version (august 2002) of the water gas shift membrane reactor model only the microporous transport model has been incorporated. The model can be used for a first evaluation of the silica and the zeolite membrane performances. Fluor used the membrane reactor model first for evaluating the ECN silica membrane. Comments on the sensitivity runs with the silica membrane have been sent to Fluor. Some guidelines for input variables from the viewpoint of the membrane reactor were given taking into account the trade-off between production rate (= H_2 recovery) and leakage (= carbon recovery) for a microporous membrane. Recommended was to determine input variables like feed and sweep pressures, sweep flow rate and membrane area by the limits of the upstream and downstream equipment of the process and the influence of the variables on the product specs. The optimal point for the trade-off between membrane investments and other investments or operational costs area can be determined by a process cost evaluation.

1.2.1.1.2.6.3.3 Final version of the water gas shift membrane reactor model

The final version of the water gas shift membrane reactor model simulates a counter-current water gas-shift membrane reactor and describes the non-isothermal and isothermal operation of the membrane reactor. The membrane reactor model is implemented as an Aspen Plus User Model (Aspen Plus, version 11.1). Two transport models are available; the microporous model for silica and zeolite membrane reactors and the dense model for Pd-alloy and proton conducting membrane reactors operating below 500ºC. For all membranes an Arrhenius type temperature dependence for the hydrogen permeance is programmed into the final version of the WGSMR model. Both the temperature dependent hydrogen permeance and the flux equations of the dense membrane model have extensively been tested. The model is capable of handling all types of gaseous components, but is restricted to deal with only the relevant components (H_2, CO, CO_2, H_2O, N_2 and CH_4) in reaction and permeation. After delivery of the final model Fluor asked clarification of some features of the software and feedback was given to that.

1.2.1.1.2.6.3.3.1 Gas transport in membranes

The transport of components through the four types of membranes (silica, zeolite, Pd-alloy and proton conductive perovskite membranes) is described by different transport equations. For microporous membranes like the silica and the zeolite membrane a phenomenological, Fick's-type law is used to describe the trans membrane flux of all components:

$$J_i = Q_i(T)\left(P_{i,f} - P_{i,p}\right)$$

in which:

	J_i	flux of component i [mol/m^{2}s]
	P_i	partial pressure component i on the feed (f) and permeate (p) side [Pa]
	$Q_{i,}(T)$	temperature dependent permeance of component i [mol/m^{2}sPa]

The proton conducting membranes under development at Eltron Research Inc. are composites consisting of matrices of both proton conducting ceramic materials and metals which are also capable of high hydrogen flux. For temperatures up to 500ºC the metal matrix will be the major pathway for hydrogen diffusion. Since the active temperature range (300-450ºC) of the water gas shift catalyst is below 500ºC,

the transport of hydrogen through both the Pd-alloy membrane and the proton conducting membrane can be described by:

$$J_{H_2} = Q_{H_2}(T)(P^n_{f,H_2} - P^n_{p,H_2})$$

in which:

	J_{H2}	hydrogen flux through the membrane [mol/m^{2}s]
	$Q_{H2}(T)$	temperature dependent hydrogen permeance [mol/m^{2}sPa^n]
	P_{H2}	partial hydrogen pressure on feed (f) and permeate (p) side [Pa]
	n	coefficient whose value is between 0.5 and 1 [-]

For dense membranes, like the Pd-alloy and the proton conducting membrane, which are in principle 100% selective for hydrogen, the membrane reactor model also accounts for the transport of other components e.g. by leakage through small defects in the membrane or sealing. For the other components (N_2, H_2O, CO, CH_4 and CO_2) the flux equation as proposed by Colorado School of Mines is used in stead of the Poisseuille flow equation. The flux equation is as follows:

$$J_i = Q_i(T)\left(P_{i,f}{}^n - P_{i,p}{}^n\right)$$

in which:

	J_i	flux of component i [mol/m^{2}s]
	P_i	partial pressure component i on the feed (f) and permeate (p) side [Pa]
	$Q_{i,}(T)$	temperature dependent permeance of component i [mol/m^{2}sPa^n]
	n	exponent on partial pressure

For all components and all membranes an Arrhenius temperature dependent permeance is used:

$$Q_i(T) = Q_i^0 e^{\frac{-E_a}{RT}}$$

with:

	Q^0_i	= temperature independent constant [mol/m^{2}sPa]
	E_a	= activation energy for transport [J/mol]
	T	= absolute temperature [K]
	R	= gas constant [J/molK]

1.2.1.1.2.6.3.3.2 Water gas shift reaction

In the membrane reactor hydrogen and carbon dioxide will be produced in the reaction of carbon monoxide and steam; the water gas shift (WGS) reaction. The reaction is a gas phase equilibrium reaction according to reaction scheme:

$$CO + H_2O \Leftrightarrow CO_2 + H_2$$

The reaction is moderately exothermic (ΔH= - 41.1 kJ/mol). The equilibrium constant K_p is defined by:

$$K_p = \frac{c_{H2}c_{CO2}}{c_{CO}c_{H2O}} \qquad [-]$$

with c_i the concentration of component i [mol/m^3]. K_p decreases with increasing temperature, which means that less product will be formed as the temperature rises. A simple expression for the equilibrium constant is (Moe, 1962):

$$K_p = \exp\left(\frac{4577.8}{T} - 4.33\right) \qquad [-]$$

The FeCr catalyst is chosen as a starting point for the kinetic expression in this model (Alderliesten, 1997). The catalyst is active in the temperature range of interest (300-450°C). Furthermore it can

tolerate small amounts of sulphuric components. The reaction rate is described by (Keiski, 1992) using a power law expression:

$$R_{CO} = -k_1 c_{CO}^{0.73} c_{H2O}^{0.55} (1 - b) \qquad [\text{mol/m}^3\text{s}]$$

with β, the reversibility factor: $b = \frac{c_{CO2} c_{H2}}{K_p c_{CO} c_{H2O}}$ [-]

1.2.1.1.2.7 Conclusion

The performance criteria for the membranes were presented by the Pre-Combustion Team during the progress meeting in October 2002 at the Fluor offices. The achieved results of this contract are compared with the set targets in the following tables:

Table 0.14 Results compared with the primary criteria

Criterion	Target	Result
H_2 permeation	0.1 mol/s.m^{2}bar	0.03 mol/s.m^{2}bar (with water in feed) > 0.15 mol/s.m^{2}bar (without water)
H_2/CO_2 permselectivity	100	9 (with water in feed) 18 (without water in feed)
Stability @ $H_2O/CO/H_2S$	95% @ 1 wk	1000 hours
Proof of concept membrane	Availability @ 2 month	Availability @ 1 month

Table 0.15 Results compared with supplemental criteria

Criterion	Result
Process projected 'CO_2 cost' excl. membranes	To be determined by calculations of Fluor
Membrane projected CO_2 cost	To be determined by calculations of Fluor
Membrane development aspects	
Membrane manufacturing & commercialisation	Sulzer Chemtech has license and production line installed
Small series quality assurance	Simple 'wet membrane He-test' has been developed
Sealing aspects	Low-cost, effective sealing (3.5 US$, 600°C, 200 bar) developed
Cost progress	Production line based on robot operation

From Table 0.14 it can be seen that the flux criteria can be met when no water is present in the feed. However, with water in the feed the flux drops to a value below the target. From the beginning it was clear the permselectivity criterion of 100 was too high for porous membranes. A value of 9 has been reached for the silica membrane under simulated process conditions. Under these process conditions, so including water, the stability of this silica membrane is limited to days. A modified silica membrane is stable for more than 1000 hours under simulated steam atmosphere testing.

1.2.1.1.2.8 References

Alderliesten, P.T., M. Bracht (1997): An attractive option for CO_2 control in IGCC systems:water gas shift with integrated H2/CO_2 separation (WIHYS) process- Phase 1: Proof of principle. Final report CEC project JOU2-CT92-0158, ECN-C-97-097, 1997.

Boer de, R. (2002): The chemical stability of ceramic materials for membranes in gas separation applications. Dutch ECN Memo 7.6457-GR02/2, May 2002.

Brandwagt, K., J.W. Dijkstra, Y.C. van Delft (2002): Description of a simplified Water Gas Shift Membrane Model. ECN-CX—02-071, Petten, June 2002.

Delft van, Y.C., J.W. Dijkstra (2002): Water Gas Shift Membrane Reactor Model; Functional specifications. ECN-CX-02-069, Petten, November 2002.

Dijkstra, J.W., G.P. Leendertse, F.W.A. Tillemans, Y.C. van Delft (2002): Water Gas Shift Membrane Reactor in Aspen Plus; Installation and Operation manual. ECN-CX—02-105, Petten, November 2002.

Keiski, R.L, T. Salmi, V.J. Pohjola (1962): Development and verification of a simulation model for a non-isothermal water gas shift reactor: Chem Eng. Journal, 48, (1992), p.17-29.

Moe, J.M. (1962): Chem. Eng. Prog., 58 (1962), p.33.

Ullmann (1999): Ullmann's Encyclopedia of Industrial Chemistry, 6th ed., 1999.

1.2.1.1.4 Development of Dense Ceramic Hydrogen Transport Membranes for Hydrogen Fuel Production by Membrane Reaction

Report Title

CO_2 Capture Project - An Integrated, Collaborative Technology Development Project for Next Generation CO_2 Separation, Capture and Geologic Sequestration

Development of Dense Ceramic Hydrogen Transport Membranes for Hydrogen Fuel Production by Membrane Reaction

Report Reference

1.2.1.1.4

Type of Report:	Semi-Annual Report
Reporting Period Start Date:	February 2003
Reporting Period End Date:	July 2003
Principal Author(s):	M. V. Mundschau, PI; T. F. Barton, C. L. Homrighausen, R. Mackay, S. L. Rolfe, X. Xie, and A. F. Sammells
Date Report was issued:	August 2003
DOE Award Number:	DE-FC26-01NT41145
Submitting Organization:	Eltron Research Inc.
Address:	4600 Nautilus Court South Boulder, CO 80301-3241

1.2.1.1.4.1 Abstract

Research is underway to test the feasibility of integrating dense hydrogen transport membranes with high-temperature water-gas shift reactors. Successful membranes will allow pure, non-polluting, hydrogen to be fed to turbine engines in electric power plants, while simultaneously concentrating CO_2 at very high pressure in a form ready for sequestration. In the first ten weeks of the Phase II study, membranes have already been successfully tested for over 300 hours at 673 K at an absolute pressure of 3.23 MPa (32.3 bar or 468 psi) and a differential pressure of 3.13 MPa (31.3 bar or 454 psi). Tests used a partial pressure of hydrogen in the feed of 0.6 MPa (6 bar or 87 psi), which will be doubled in the near term. The new differential pressure tests double the 15 bar goals met in Phase I. In ambient pressure tests, hydrogen permeabilities up to 2×10^{-7} mol m m^{-2} s^{-1} $Pa^{-0.5}$ (more than ten times better than pure palladium under the same conditions) have consistently been measured in the temperature range 593-733 K. Apparent activation energies under 6 kJ/mol have been measured, which are less than that found for pure palladium (24 kJ/mol). Preliminary economic estimates suggest that at these rates of hydrogen permeation, membranes capable of separating two million metric tons of CO_2 from 0.18 metric tons of hydrogen per year would cost approximately $1.45 million compared to $137 million if pure palladium membranes were used. Membranes have been tested with high-temperature water-gas shift catalysts (90 wt % Fe_3O_4/10 wt % Cr_2O_3, with a minor additive of Cu) and already have been shown to be capable of extracting hydrogen from a water-gas shift gas mixture. A stacked membrane system has been built and performance tested as a first step to scale-up.

1.2.1.1.4.2 Table of Contents

1.2.1.1.4.3 List of Graphical Materials

1.2.1.1.4.4 Introduction

1.2.1.1.4.4.1 Specific Project Goals

The specific goal of the research is to integrate hydrogen transport membranes into water-gas shift reactors and to demonstrate the feasibility of removing sufficient hydrogen through the membranes in order to shift the chemical equilibrium of the water-gas shift reaction: $CO + H_2O \Omega CO_2 + H_2$. In principle, removal of hydrogen through membranes has the potential to shift the reaction essentially to completion, thus maximizing the production of hydrogen and reducing the concentration of carbon monoxide to negligible levels. In addition, such membranes could provide clean hydrogen fuel on one side of the membrane, while leaving concentrated CO_2 at high pressure on the opposite side of the membrane. This would allow economic CO_2 sequestration.

The water-gas shift reaction is exothermic with ?H = -41.1 kJ≅mol^{-1} at standard thermodynamic conditions. This implies that lower temperatures favor production of hydrogen and consumption of carbon monoxide. However, high-temperature water-gas shift catalysts (such as 90 wt % Fe_3O_4/10 wt % Cr_2O_3) typically cannot be run much below 613 K (340EC) due to kinetic limitations. At practical reactor operating conditions of 613-713 K (340-440EC) and 3.5 MPa (35 bar), and economic concentrations of steam, thermodynamics dictates that concentrations of CO cannot be reduced much below 3 to 4 mol % at equilibrium. Removal of hydrogen through membranes will shift the reaction essentially to completion even at high temperatures and allow conversion of virtually all of the residual CO. Hydrogen transport membranes will eliminate the need for low-temperature water-gas shift catalysts (such as Cu/ZnO_2), which are not as robust or as tolerant to sulfur as are the high-temperature water-gas shift catalysts. Membranes will also eliminate the need for heat exchangers required to lower the temperature to about 473 K (200EC) for the low-temperature catalysts.

Technical issues being resolved in the research are as follows: The hydrogen transport membranes would preferentially extract hydrogen from a water-gas shift mixture at an absolute pressure of 3.5 MPa (35bar) containing an input gas of H_2O, CO_2, H_2, CO, H_2S + COS, with balance nitrogen and other impurity gases. Membranes must be stable in this harsh chemical environment, which includes high-pressure, superheated steam in the temperature range of 613-713 K (340-440EC). Feed pressure of hydrogen to turbine engines is preferentially 0.2 MPa (2 bar), so that membranes must be designed to resist a differential pressure of 3.3MPa (33 bar) without rupture or leak. It is desired that the membranes be essentially 100% selective to hydrogen, and possess sufficient hydrogen flux to allow a minimum area to be economic.

1.2.1.1.4.4.2 Overall Project Goals

One CO_2 Capture Project vision for reducing CO_2 emissions from large stationary power plants is as follows: Instead of directly burning coal or other fossil fuel in air to raise steam for running turbine engines, the carbon-based fuel is first converted by reaction with steam or with steam and oxygen to form a mixture of hydrogen and carbon monoxide. Production of H_2 + CO from coal, natural gas, the various fractions of petroleum, and even biomass is thermodynamically favored above temperatures of about 1223 K (950EC) if the proper ratio of C : H : O is maintained in the reaction mixture.

Once the mixture of H_2 + CO is formed, additional hydrogen can be produced by reacting CO with excess steam by the water-gas shift reaction: $CO + H_2O \Omega CO_2 + H_2$. As discussed above, this reaction is economically run at 613-713 K (340-440EC) and 3.5 MPa (35 bar). In the vision of the CO_2 Capture Project, a membrane, which is selective towards hydrogen, separates the hydrogen from the carbon dioxide, excess steam, and other components of the water-gas shift mixture. Removal of hydrogen through the membrane drives the water-gas shift reaction to near completion, consuming essentially 100%

of the carbon monoxide and maximizing the production of hydrogen. The purified hydrogen on the permeate side of the membrane is then fed to turbine engines and is reacted with oxygen to form heat and steam which powers electrical generators. The steam exhaust from the turbine engines can be recycled to reform additional coal or other fossil fuel. Combustion of hydrogen in turbines produces only non-polluting water vapor.

Concentrated CO_2, which remains at the high pressure of 3.5 MPa of the water-gas shift reactor, is essentially the only gas on the retentate side of the membrane (other than excess steam and residual impurities). The concentrated CO_2 at high pressure, can be sequestered by one of the various CO_2 Capture Project initiatives, such as pumping the CO_2 into oil wells to recover additional oil, into coal beds to extract methane, or into other geological features to store the CO_2. Retaining the CO_2 at high pressure on one side of the membrane is a very important feature of this technology, because it reduces the energy and expense which otherwise would be required to re-pressurize tons of CO_2 before it can be pumped into oil wells and other storage reservoirs.

It should be appreciated that by first reforming the coal into CO_2 and H_2 and by consuming the hydrogen separately in the turbine engines, that one avoids diluting the carbon dioxide with large quantities of nitrogen. This would be the case if the fuel were simply burned in air. The extremely large volume of nitrogen which accompanies CO_2 after conventional combustion would make sequestration of the combined turbine exhaust prohibitive or would require subsequent separation of very diluted CO_2 from very large quantities of nitrogen.

It should be appreciated that, in principle, any carbon-based fuel can be steam reformed and/or partially oxidized into a mixture of hydrogen and carbon monoxide. This includes coal, natural gas, heavy and light fractions of petroleum, and even biomass or municipal waste. The H_2 and CO formed from these fuels can then be fed to a water-gas shift reactor to produce additional hydrogen, which again can be purified by a hydrogen transport membrane and fed to turbines. The CO_2 Capture Project vision may be the most versatile for sequestration of CO_2 generated by large stationary sources such as power plants. Of the various CO_2 Capture Project initiatives which have been proposed for the sequestration of CO_2, the above scenario has one of the best chances for success.

Conversion of fossil fuels into a mixture of CO + H_2 (known as synthesis gas or syngas) followed by the water-gas shift reaction, is very well established technology. These reactions have been a standard in the chemical industry for over eighty years and produce millions of tons of hydrogen annually. Thus, in principle, no new technology is required to produce hydrogen from various fossil fuels. The novel and innovative parts of the research involve development, fabrication, and testing of dense hydrogen transport membranes. For the above CO_2 Capture Project vision to become both technically and economically viable, low-cost hydrogen transport membranes must become commercially available. This research addresses the challenges in the development of such membranes.

1.2.1.1.4.4.3 Economic Considerations

If one considers a coal-fired power plant with annual CO_2 emissions of two million metric tons (2.0×10^9 kg), one can calculate the quantity of hydrogen which can be produced from gasification of the coal and estimate the area of membrane which will be required to extract the hydrogen. From the equation: $C + 2H_2O \Omega CO_2 + 2 H_2$, one sees that two moles of molecular hydrogen are produced for each mole of carbon dioxide in the emissions. Using a molecular weight of 44.010 for CO_2 and 2.01588 for H_2, the number of moles of H_2 which will accompany 2.0×10^9 kg CO_2 is: $(2.0 \times 10^9$ kg $CO_2)$(1000 g CO_2/kg CO_2)(1 mol CO_2/44.010g (2mole H_2/mol CO_2) = 9.1×10^{10} mol H_2. This is equivalent to $(9.1 \times 10^{10}$ mol $H_2)$(2.01588g H_2 /mol H_2) = 1.8×10^{11} g H_2 or 0.18 metric tons of H_2.

If one assumes that the membranes now under study can maintain a permeability, P_e, of better than 2.0 x 10^{-7} mol m m^{-2} s^{-1} $Pa^{-0.5}$, and that the flux, J, of hydrogen is given by Sievert=s Law: $J = P_e \cong l^{-1}(p_f^{0.5} - p_p^{0.5})$ where l is the thickness of the membrane in meters and p_f an p_p are the partial pressures of hydrogen in Pa on the feed, f, and permeate, p sides of the membrane, then the number of moles of hydrogen which will pass through 1 m^2 of membrane in one second will be:
$J = (2.0 \times 10^{-7}$ mol m m^{-2} s^{-1} $Pa^{-0.5})(1.3 \times 10^{-4}$ m$)^{-1}(1{,}450{,}000^{05} - 20{,}000^{-05}$ $Pa^{0.5}) = 1.6$ mol $m^{-2}s^{-1}$ if one assumes a membrane thickness of 1.3 x 10^{-4} m needed to resist a differential pressure of 33 bar, a partial pressure of hydrogen in the feed of (0.414)3.5MPa = 1.45 MPa and a partial pressure of hydrogen on the permeate side of 20,000 Pa.

In one year, one square meter of membrane will transport:
(1.6 mol $m^{-2}s^{-1}$)(60s/min)(60 min/hr)(24hr/day)(365 day/year) = 4.6 x 10^7mol H_2 m^{-2}.
To transport 9.1 x 10^{10} mol H_2 per year, the number of square meters of membrane will be:
9.1 x 10^{10} mol H_2/4.6 x 10^7 mol H_2 m^{-2} = 1,978 m^2. For a membrane estimated cost of U.S. \$580.00/m^2, total membrane cost would be (1,978 m^2)(\$580.00/m^2) = \$1,150,000. We estimate that surface catalyst cost would be \$275,000 to give a total of \$1,425,000. The above simplified calculations assume a constant driving force across the membrane, which will not be correct in a stack of membranes, which ultimately reduce the partial pressure of hydrogen in the feed to near zero. More exact calculations are being performed as part of this feasibility study. For comparison, palladium membranes, 127 micron thick would cost nearly \$140,000,000.

Taxation of CO_2 emissions has been a recent viable driving force for developing CO_2 sequestration technologies for lowering CO_2 emissions from North Sea Oil and Gas operations in Norway. Norwegian CO_2 taxes are now 50 Eurodollars per metric ton (> U.S. \$ 60 per ton). Carbon dioxide emissions are now taxed in the Netherlands, Norway, Sweden and Finland. Using a value of two million metric tons of CO_2 per year per power plant, and a tax of U.S. \$60 per ton, the annual tax per power plant would be \$120,000,000. The tax would accrue to 1.2 billion U.S. dollars over ten years. These numbers do not take into account interest lost on principle paid as tax. At this tax rate, the tax would be \$329,000 per day. At this rate, costs of membranes could be recouped in \$1,450,000/\$329,000 per day = 4.4 days. Even if membrane costs were double or triple those estimated, the costs could easily be recouped in only a few weeks. Thus, it is clear that if carbon sequestration systems can be installed and operated below the rate of the tax, that it would be in the economic interest of the power companies to comply with the sequestration initiative.

1.2.1.1.4.4.1 Concepts Behind Dense Hydrogen Transport Membranes

Figure 1.2.1.1.4.4 (1) shows schematically the main concepts of dense hydrogen transport membranes. Hydrogen transport membrane materials developed and tested at Eltron Research Inc., include un-alloyed metals, metal alloys, proton-conducting ceramics, metal-ceramic cermets, and metal-ceramic composites. All of these dense membrane materials transport hydrogen in a dissociated form (i.e. as H^+, H^- or as neutral hydrogen atoms). None of the common dense membrane materials transport hydrogen as molecular hydrogen. Hydrogen molecules, therefore, must first be adsorbed and dissociated on the surface of the membrane facing the hydrogen source.

Some membrane materials such as palladium and palladium alloys, nickel cermets, and many perovskite-based proton conducting membranes possess intrinsic ability to adsorb and dissociate molecular hydrogen. However, if the membrane material does not possess adequate intrinsic catalytic activity for hydrogen adsorption and dissociation, then a hydrogen dissociation catalyst must be added to the surface of the membrane which faces the hydrogen source. Catalysts must remain stable and active in the harsh chemical environment of water-gas shift reactors.

On the hydrogen permeate (or hydrogen sink) side of the membrane, the dissociated hydrogen which has diffused through the membrane, must be recombined to form hydrogen molecules before the hydrogen molecules can desorb from the surface of the membrane. In general, a catalyst which can dissociate hydrogen molecules will also recombine the dissociated hydrogen back into hydrogen molecules. Thus, in principle, the same catalyst can be applied to both sides of the membrane. In practice, the catalysts are optimized for the different environments facing the hydrogen source and sink sides of the membrane. The source side is optimized for maximum adsorption of hydrogen and resistance to catalyst deactivators (from impurities in the water-gas shift reactor), whereas the membrane sink side is optimized for rapid desorption of hydrogen.

Selection of Membrane Materials with High Hydrogen Permeabilities. In Phase I, a number of hydrogen transport membrane materials were investigated.

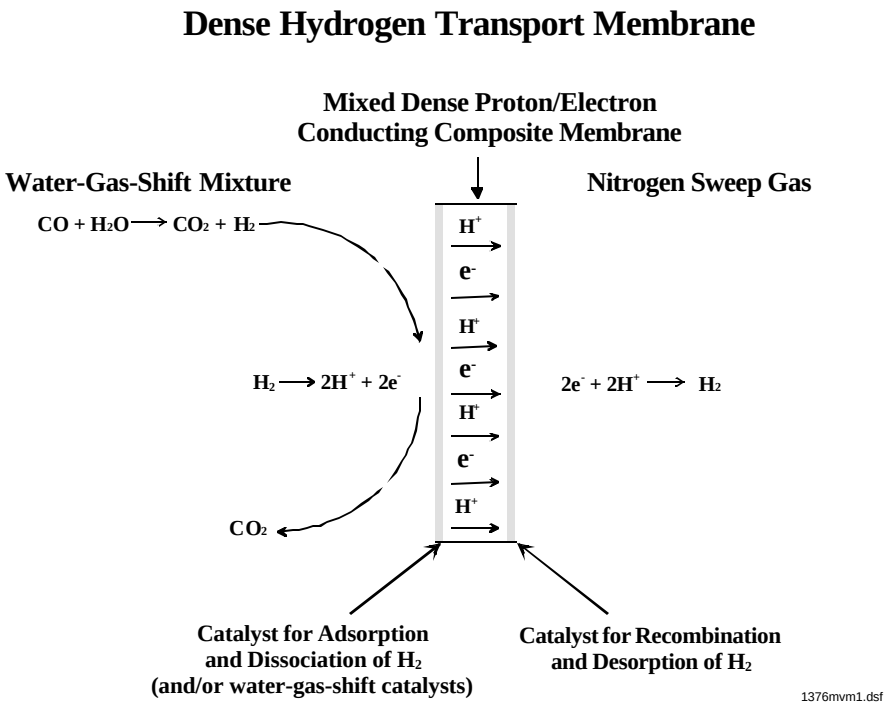

1.2.1.1.4.4 (1) Schematic of a dense high temperature hydrogen transport membrane. The central region consists of a dense material possessing high permeability for hydrogen and essentially zero permeability for other gases. The central layer is also electron conducting. Materials for the central layer may include un-alloyed metals, metal alloys, proton-conducting ceramics, metal-ceramic cermets, and other metal-ceramic composites. Both surfaces of the membrane must possess catalytic activity for the adsorption and dissociation of molecular hydrogen.

1.2.1.1.4.5 Executive Summary

Membranes are being developed and tested which can separate hydrogen from carbon dioxide produced from fossil fuels. The hydrogen, which is collected on one side of the membrane, can be used, for example, as a clean, non-polluting, fuel to run electrical turbines. The pure hydrogen might also be used to power fuel cells or could be used by chemical industry in hydrogenation reactions or in desulfurization of petroleum. On the opposite side of the membrane, carbon dioxide is concentrated at high pressure, in a non-diluted form which will be convenient for sequestration into oil wells for extraction of additional oil, into seams of coal for extraction of natural gas, or into other geologic storage reservoirs.

In principle, all carbon-based fuels, including coal, natural gas, biomass, and various fractions of petroleum can be reacted with steam and oxygen to form a mixture of hydrogen and carbon monoxide called synthesis gas. The carbon monoxide in the synthesis gas can be further reacted with steam to form additional hydrogen and carbon dioxide. Extraction of hydrogen through membranes shifts the chemical equilibrium, which results in the essentially complete consumption of carbon monoxide and maximum production of hydrogen.

In one of the visions of the Carbon Capture Project, fossil fuels, instead of being burned directly in air, are instead reacted with steam and oxygen to produce synthesis gas, which is further reacted with steam to form more hydrogen and carbon dioxide. The hydrogen is extracted through membranes to run turbine engines used in electric power generation, and the carbon dioxide is sequestered. For this vision to become economically viable, low-cost hydrogen transport membranes must be developed which can operate under the relatively hostile chemical environment of water-gas shift reactors which use superheated steam at high pressures and elevated temperatures.

In the Phase II research, which has been underway for approximately 10 weeks at Eltron Research Inc., hydrogen transport membranes are being developed and tested. Under the same conditions, these membranes have ten to one hundred times the hydrogen permeability of palladium membranes, but at a fraction of the cost.

In the Phase II research, high-pressure reactors have been designed, built and tested to operate at an absolute pressure of 3.2 million Pascal (32 bar), with a differential pressure of 3.1 million Pascal (31 bar) across the membranes in the water-gas shift temperature range between 593-713 K. Reactors were designed to operate with a partial pressure of steam on the feed side of the membrane of 1.2 million Pascal (12 bar), a partial pressure of hydrogen of 1.3 million Pascal (13.2 bar), and partial pressures of 570,000 Pascal of CO_2 and 106,000 Pascal of CO, to simulate conditions in industrial water-gas shift reactors.

Membranes, 127 microns thick, have already been tested in preliminary tests for over 300 hours under a hydrogen partial pressure of 0.6 million Pa at 673 K (400°C), and an absolute pressure on the hydrogen feed side of the membrane of 3.2 million Pascal (32 bar), with a differential pressure of 3.1 million Pascal (31 bar) across the membrane. Membranes have successfully resisted the differential pressure without leak and have shown a steady hydrogen permeability of over 2×10^{-8} $mol \cdot m \cdot m^{-2} \cdot s^{-1} \cdot Pa^{-05}$, which is comparable to membranes of pure palladium. In a separate 100 hour test at 3 bar partial pressure hydrogen, absolute pressure of 3.2 million Pascal, and differential pressure of 3.1 million Pascal, membrane disks, 1.5 cm in diameter, were found to distort 0.5 mm at the center due to the pressure. Membranes purged of hydrogen and cooled show only the original metallic phase by X-ray diffraction without evidence of hydrides.

More recent batches of membrane, with improved deposition procedures for membrane catalysts, have consistently shown initial values of hydrogen permeability as high as 2×10^{-7} $mol\ m\ m^{-2}\ s^{-1}\ Pa^{-0.5}$, which is approximately ten times better than pure palladium under comparable conditions. If these values of hydrogen permeability are maintained under water-gas shift conditions, cost of membrane materials and

catalysts is estimated at U.S $1.45 million for a power plant emitting two million metric tons of carbon dioxide annually. For perspective, pure palladium membranes, of similar thickness, would cost U.S. $137 million, at current prices. At carbon dioxide emissions tax rates of U.S. $60 per ton, as in Norway, the annual tax on a power plant with annual carbon dioxide emissions of two million metric tons would be $120,000,000 per year or $329,000 per day. At this tax rate, costs for Eltron membrane materials could be recouped in less than one week, whereas that of pure palladium would require over one year for the materials alone. Eltron's membrane materials thus appear to be economically viable.

In the first ten weeks of the Phase II project, hydrogen transport membranes have already be integrated with beds of commercial high-temperature water-gas shirt catalysts. New ambient pressure reactors were designed, built and tested. A shift in the chemical equilibrium of the reaction has already been observed as predicted by calculations.

1.2.1.1.4.6 Experimental

1.2.1.1.4.6.1 High-Pressure Reactor

Figure 1.2.1.1.4.6 (1) is a schematic of the high-pressure hydrogen separation unit which was designed, built and tested in the first six weeks of the Phase II project. The high pressure reactor was designed to produce a differential pressure across the membrane of 31 bar (3.1 MPa or 450 p.s.i.) in order to meet Phase II goals of 30 bar differential pressure. For sweep gas conditions on the permeate side of the membrane operating at near ambient pressure, the feed gas on the retentate side of membrane operates at an absolute pressure of approximately 3.2 MPa (32 bar or 464 p.s.i.). The reactor was designed to operate at the above pressures between 593-713 K, which is the normal temperature range used in high-temperature water-gas shift reactors (see Twigg, 1997). The reactor is also designed to operate up to 20 bar (2.0 MPa or 290 psi) at higher temperatures, between 975-1075 K.

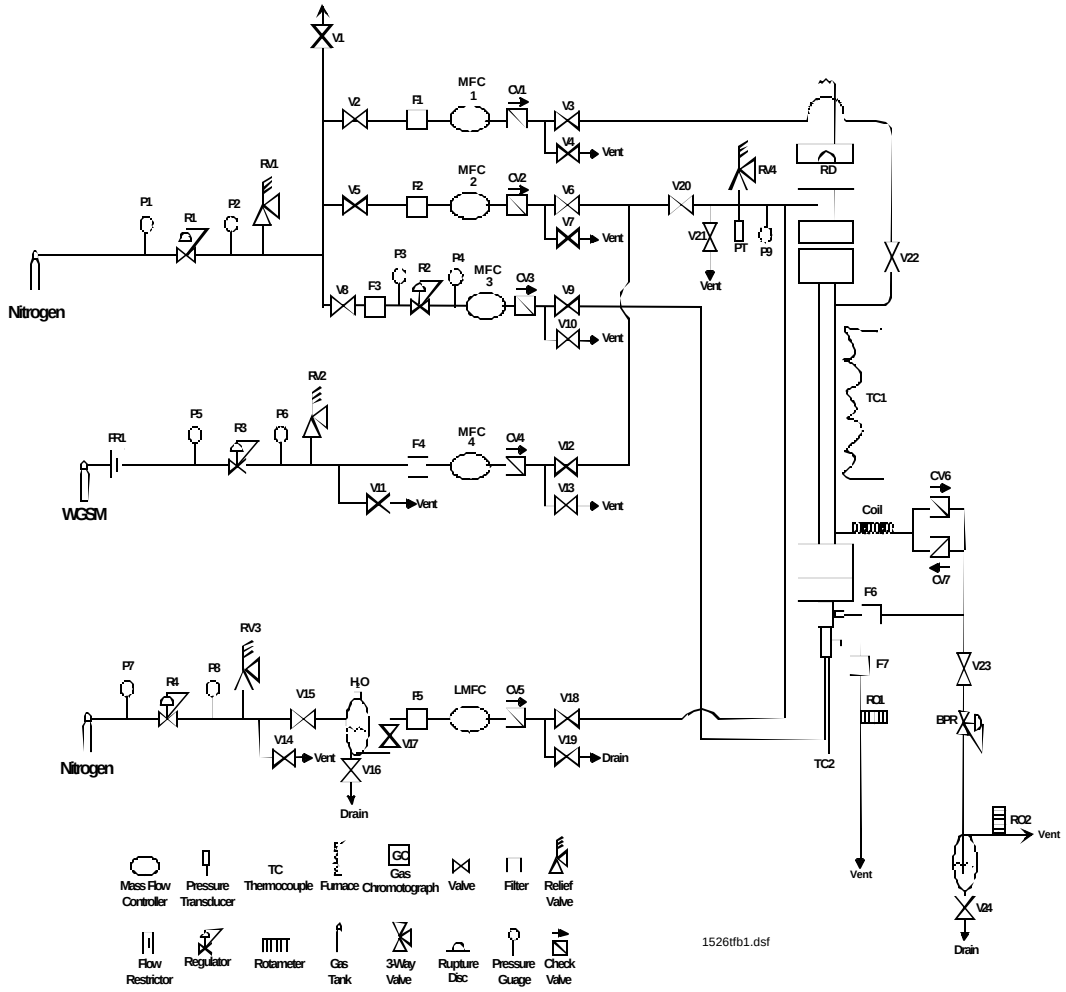

1.2.1.1.4.6 (1) High pressure H_2 separation unit - design configuration.

The top portion of the schematic shows the components of the sweep-gas lines. The schematic indicates nitrogen as the sweep gas, but tanks of argon or helium can replace the nitrogen for leak checks. Auxiliary lines allow nitrogen, argon, or helium gas sources to be fed to the feed side of the membrane, if needed, for high-pressure testing across membranes in inert atmosphere for membrane burst tests, if required.

Inert gas can also be used to dilute the water-gas shift text mixture, or mixtures of hydrogen/helium in the retentate side gas feed, if needed.

The middle portion of the schematic shows the gas lines associated with the water-gas shift gas mixture for the membrane retentate, or feed side. Cylinders of pre-mixed (dry) gas are purchased from AirGas Corporation. Preliminary tests in Phase II are using wet gas mixtures with H_2O, CO_2, H_2, CO, and nitrogen and other impurities. The values may vary slightly depending upon the exact water-gas shift conditions which one intends to model.

The bottom of the schematic shows lines for feeding steam into the feed side of the membrane. Flow of water in the liquid state is controlled with a liquid mass flow controller, calibrated for water. A tank of nitrogen (or other inert gas if needed) is used to pressurize the water and force it into the reactor, where the liquid water is vaporized into steam. Steam is condensed in a water trap, shown on the bottom right, before sending the retentate gas to analysis (vent).

(a) **(b)**

1.2.1.1.4.6 (2) (a) New High Pressure Hydrogen Separation Unit - Eltron Research Inc., and (b) the separation unit with oven. Views of the high pressure reactor which is being used to test stability of catalysts and membranes to at least 32 bar pressure, absolute, 31 bar differential pressure, in a full steam plus water-gas shift reaction mixture containing predominantly, steam, CO_2 and CO at 593-713 K. The facilities at Eltron Research Inc. are one of only a few in the United States with capabilities for membrane tests at these extreme conditions.

Figure 1.2.1.1.4.6 (2) shows views of the high-pressure reactor. A containment facility surrounds the high-pressure unit, and is designed to vent gas, sound alarm, and automatically close valves and shut down gas flow in the event of a catastrophic leak. A rupture disk is installed at the top of the unit, which is designed to burst if design pressures are exceeded. The outer reaction chamber tube walls are constructed of Haynes™ 230 alloy and are lined on the interior with an Inconel™ 800 sleeve.

Appropriate pressure regulators, valves, high pressure mass flow controllers, and check valves are used to deliver feed and sweep gases. Some of these devices are imaged in the photographs. The sweep gas is typically brought in at near ambient pressure. Steam is mixed with the dry gas mixture to give the desired mole fraction of steam in the mixture.

Leak detection is performed by analyzing gas streams by gas chromatography. Analysis of hydrogen permeation rates is performed by measuring hydrogen concentration in the sweep gas by gas chromatography. The gas chromatography instruments are calibrated by standard procedures with hydrogen-helium standard gas mixtures. Mass flow controllers are calibrated for delivery rates and gas flows are corrected to standard temperature and pressure(STP). Helium is added to the feed and is used to leak check the membrane and seals. In general, membranes are discarded if helium is detected in the sweep gas. Data is considered reliable only if leak free to helium, which circumvents need for questionable corrections for mechanical leak compensation. Argon in the feed and sweep is used to leak check system lines for nitrogen leaks from air.

1.2.1.1.4.6.2 Ambient Pressure Reactors

Figure 1.2.1.1.4.6 (3) shows an overview of the experimental bay used in ambient pressure measurements. The ambient pressure stations are used in screening many experimental variables and resolving experimental issues before testing membrane types in the high pressure reactors. The two reactor stations in the center are used for hydrogen flux measurements in dry gas, such as mixtures of hydrogen and helium, CO, and the dry water-gas shift mixture. Long term tests are also run in these reactors. Hydrogen flux is determined from gas chromatography measurements of the concentration of hydrogen which appears in the permeate exhaust. These reactors are used to determine maximum hydrogen flux and hydrogen permeability which can be achieved under ideal hydrogen/helium mixture, to show absence of helium leak in new membrane types, to resolve issues relating to possible catalyst poisoning effects by CO (no poisoning by CO is noted in the temperature range 593-713 K), to resolve issues relating to effects of membrane catalyst deposition methods on hydrogen flux, and to resolve possible issues of interdiffusion between catalysts and membrane materials at high temperatures.

1.2.1.1.4.6 (3) Ambient pressure testing facility - Eltron Research Inc. Left: new reactors for testing membranes with water-gas shift catalyst. Right: reactors for screening membrane catalysts in steam and water-gas shift mixture. Center: reactors used for long-term tests.

The four ambient reactor stations on the right are used to test membranes and membrane catalysts in the water-gas shift mixture with full steam. Hydrogen flux is determined as above from gas chromatography measurements of the concentration of hydrogen which appears in the permeate exhaust. These reactors are used to test and screen new membrane catalysts for stability in steam and to measure effects of catalyst poisoning by sulfur compounds which appear as impurities in the water-gas shift mixture. Liquid water is forced into the reactors by calibrated peristaltic pumps. Water is vaporized by heating tapes surrounding gas lines, and steam is further heated to reaction temperatures within the reactor tube furnaces. Thermocouples suspended a few millimeters from membranes and within the water-gas shift mixture are used to insure that membranes are heated to the proper temperature and that the steam is fully heated. The ambient pressure reactors are used to measure hydrogen permeability as a function of temperature in the steam plus water-gas shift gas mixture and to obtain activation energies and pre-exponential factors for the various types of membrane. Membrane types showing low-activation energies and good hydrogen flux are then selected for high-pressure tests.

The four reactors on the left are used for integrating membranes with high-temperature water-gas shift reactors. Beds of commercial SüdChemie 90 wt % Fe_3O_4/ 10 wt % Cr_2O_3 water-gas shift catalysts are reduced and activated according to the manufacturer=s standard procedure. The four reactors are arranged in series with alternating beds of catalysts and hydrogen transport membranes. The water-gas shift mixture, including steam, can be fed directly to membranes to provide base-line measurements with no catalysts on line. The gas also can be fed directly to the catalyst beds with the membranes off-line to measure baseline shifts caused by the catalysts before extraction of hydrogen. Two membranes and two catalyst beds can be connected in series to measure the effect of removal of hydrogen through the membranes on shifting the reaction. The reactors are also being used to resolve issues of hydrothermal transport of components of the water-gas shift catalysts and reactor wall materials onto membrane surfaces. Guard bed materials are also tested in these reactor to remove impurities in the gas stream which can deactivate membrane catalysts.

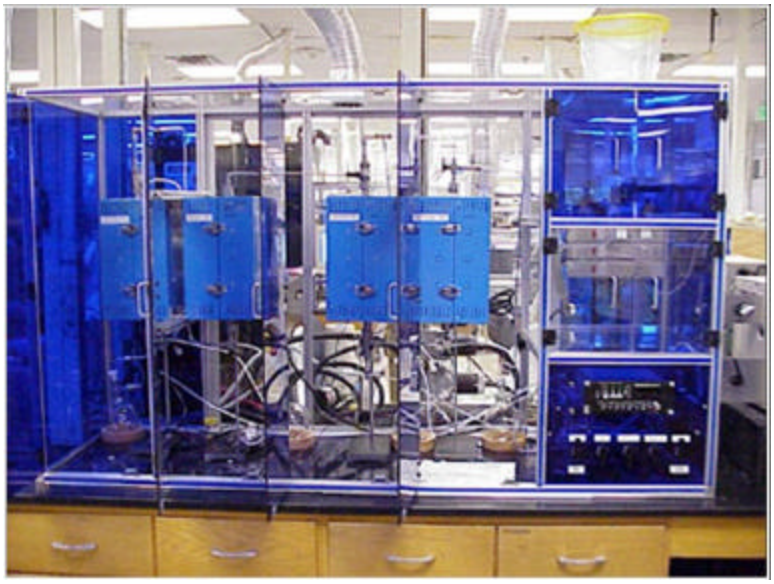

1.2.1.1.4.6 (4) New ambient pressure reactors for testing membranes integrated with beds of water-gas shift catalyst. New system designed and built in month #1. Membranes and catalyst beds connected in series.

Figure 1.2.1.1.4.6 (4) and 1.2.1.1.4.6 (5) show close-up views of the reactor stations used for integration of the water-gas shift catalysts with the hydrogen transport membranes. On the right of Figure 1.2.1.1.4.6 (4) are mass flow controllers and oven controls. On the left are the four reactor tubes, connected in series, surrounded by ovens. Sample collection ports are located before and after each reactor so as to measure gas concentrations for the input and exhaust of each reactor. Samples of input and exhaust gas are fed into gas chromatography instruments for analysis. Figure 1.2.1.1.4.6 (5) shows one of the reactor tubes with the tube furnace opened. Reactors and ovens are surrounded by gas-containment cabinets which are designed to vent gases in the event of a catastrophic leak. Gas detectors are located within the cabinets to sound an alarm in the event of a gas leak.

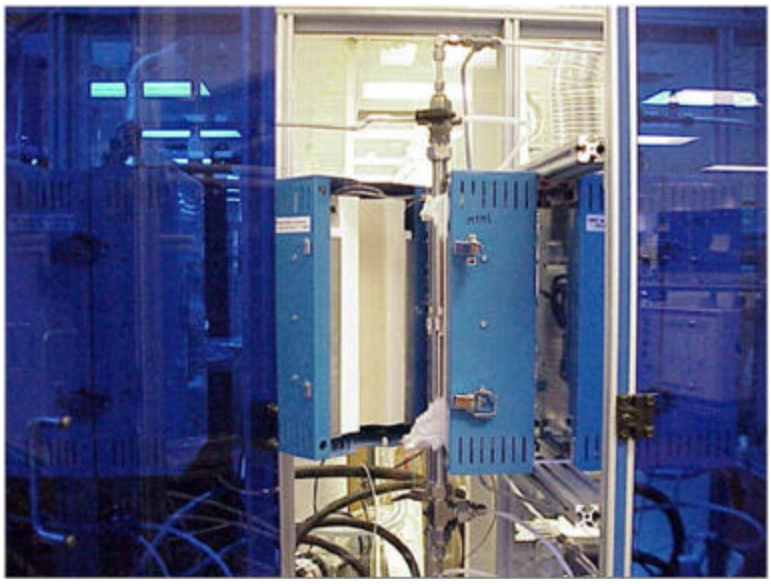

1.2.1.1.4.6 (5) New ambient pressure reactor with oven.

1.2.1.1.4.6.3 Analytical Techniques

1.2.1.1.4.6.3.1 Powder X-Ray Diffraction (XRD) Analysis of Membranes and Catalysts

X-ray powder diffraction data of the commercial catalysts, and membrane materials, before and after use in reactors, was performed using a Philips PW 1830 X-ray diffractometer equipped with a copper anode (? for Cu K_a = 1.542Å). X-ray diffraction analysis of powdered materials and membrane materials is a routine, daily task at Eltron Research. Identification of crystalline phases, including possible impurity phases, is made by comparison of measured peak angles to peak angles catalogued in computer files published by JCPDS- International Centre for Diffraction Data. The data files contain over 50,000 entries of known diffraction patterns. Changes after exposure to the water-gas shift environment, if any, are noted.

1.2.1.1.4.6.3.2 Energy Dispersive X-ray Analysis in Scanning Electron Microscope

Elemental analysis of catalyst and membrane materials are performed using a Princeton Gamma Techniques, Energy Dispersive X-ray (EDX) unit which is housed within a JEOL JSM-5610 Scanning Electron Microscope. Materials are analyzed before and after exposure to the high pressure water-gas shift reaction mixture. Gross impurities acquired on membrane surfaces during exposure to the reaction medium or elements lost due to volatilization by steam are identified. The scanning electron microscope is also used to image membranes and catalysts. Cross sectional images, as well as top and bottom views of membranes are made. The commercial catalysts are also viewed at various magnification before and after use in the reactor.

1.2.1.1.4.6.3.3 X-Ray Photoelectron Spectroscopy (XPS)

X-Ray Photoelectron Spectroscopy is used to detect monolayer level impurities which can adsorb on the catalytic surfaces of the membranes and act as deactivators of catalysts. These impurities can originate with the gas stream, steam, reactor walls, catalyst bed, etc. Monolayer levels of impurities which cannot be detected by EDX usually can be detected by XPS. Typical catalyst poisons searched for include sulfur, phosphorus, silicon, and chlorine. Iron, chromium and sulfur from the beds of water-gas shift catalysts and from reactor walls can be hydrothermally transported by steam to the membrane surfaces and are also sought. Oxidation states of catalysts are also identified by XPS.

1.2.1.1.4.6.3.4 BET Surface Area Analysis

The Brunauer-Emmett-Teller (BET) method is used to measure surface area of the commercial water-gas shift catalysts, before and after use in the reactors. This allow one to determine whether or not the catalysts lose significant surface area during use.

1.2.1.1.4.7 Results and Discussion

1.2.1.1.4.7.1 Analysis of Commercial Water-Gas Shift Catalyst

High temperature water-gas shift catalyst pellets were obtained from Süd Chemie. The composition of this commercial catalyst is reported to be a mixture of approximately 90% Fe_3O_4 - 10% Cr_3O_4. The dark, reddish-brown pellets were cylindrical in shape, ~6 mm diameter by 6 mm high. The density of the pellets was measured to be 1.95 g/cm^3. This compares to density values of between 4.9 to 5.2 g/cm^3 for pure iron oxide, Fe_2O_3 or Fe_3O_4. The catalyst pellets appeared similar to pressed green pellets of unsintered ceramics. Pellets were friable (easily crushed to powder), and the powder was easily attracted to a magnet, consistent with the presence of magnetite (Fe_3O_4). Surface area of the catalyst pellets was measured by gas adsorption and calculated by the BET method. Surface area of the as-received pellet was 105 m^2/g. Surface area measurement of the crushed powder gave a value of 92 m^2/g.

Microscopic examination of catalyst pellets was performed with a Scanning Electron Microscope (SEM) (see Figure 1.2.1.1.4.7 (1)). Very fine, sub-micron size particles were seen, which is typical for fine flocculated precipitates. Inclusions were seen in fair number (see Figure 1.2.1.1.4.7 (2)). Inclusions were identified as graphite particles. We speculate that carbon compounds or graphite may be intentionally added as possible binding agents, or pore formers, or reducing agents for converting Fe_2O_3 into Fe_3O_4.

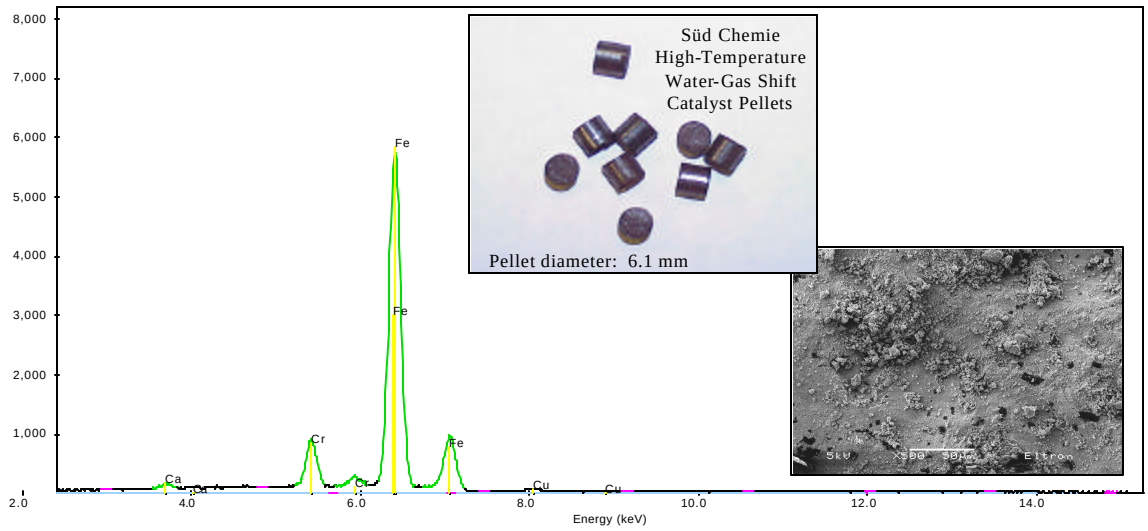

1.2.1.1.4.7(1) Scanning electron microscopy and x-ray energy dispersive spectroscopy analysis of Süd Chemie high-temperature water-gas shift catalyst. Catalyst contains mainly iron and chromium (as oxides). Trace amounts of calcium, copper. Catalyst powder appears to be a very fine (~250 µm diameter) flocculated precipitate. Graphite inclusions are present.

Elemental analysis of commercial water-gas shift catalysts was performed by X-ray energy dispersive spectroscopy in the SEM. The main components were found to be iron and chromium as expected. Minor amounts of calcium and copper were also detected and inclusions of carbon were also found. Copper is a common additive in such catalysts. Powder X-ray diffraction (XRD) was performed on these commercial catalysts (Figure 1.2.1.1.4.7 (4)). Peaks in as-received samples matched with structures of Fe_2O_3 (hematite), Fe_3O_4 (magnetite), and graphite. The peaks were broad, consistent with the small crystallite size. Chromium is known to form a solid solution with iron oxide. There are no separate phases of calcium or copper oxides, suggesting they are either also in solid solution with the iron oxide, are amorphous, or they are present in amounts below the detection limit. A sample heated in air to 1000°C showed an XRD pattern with sharper peaks of the two metal oxide phases, with no graphite present (see Figure 1.2.1.1.4.7 (5)).

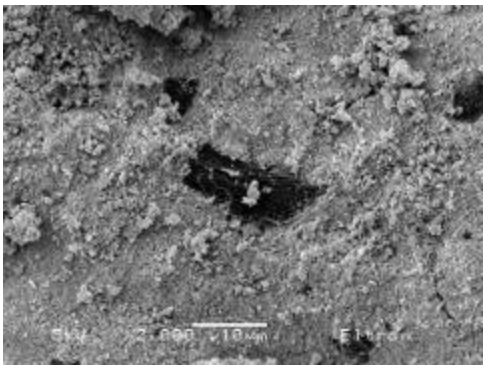

1.2.1.1.4.7 (2) SEM photo of basal surface of catalyst pellet, original magnification 2000X, centered on graphite inclusion.

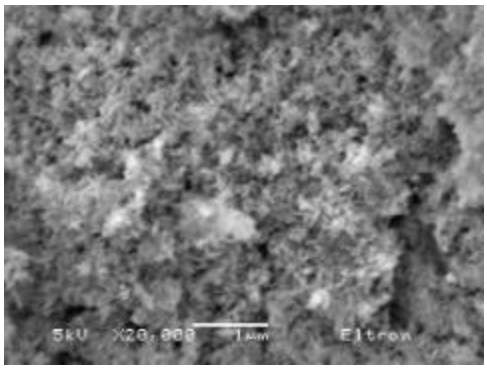

1.2.1.1.4.7 (3) SEM image of basal surface of catalyst pellet, original magnification 20,000X, showing small particle size of iron oxides.

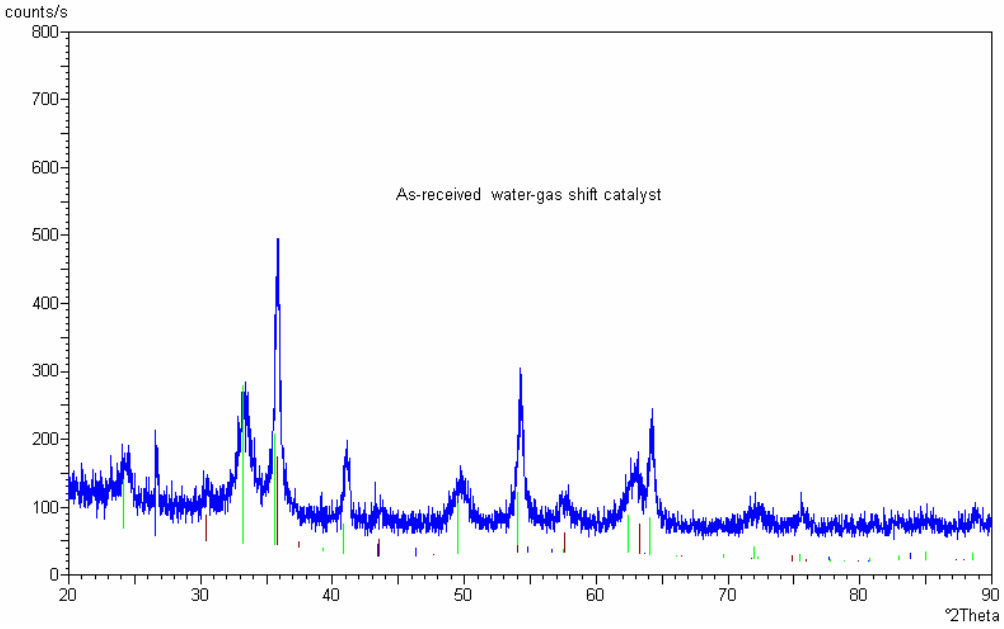

1.2.1.1.4.7 (4) XRD pattern of as-received water-gas shift catalyst. Green lines mark position of peaks corresponding to Fe_2O_3 phase; red lines for Fe_3O_4, and blue for graphite.

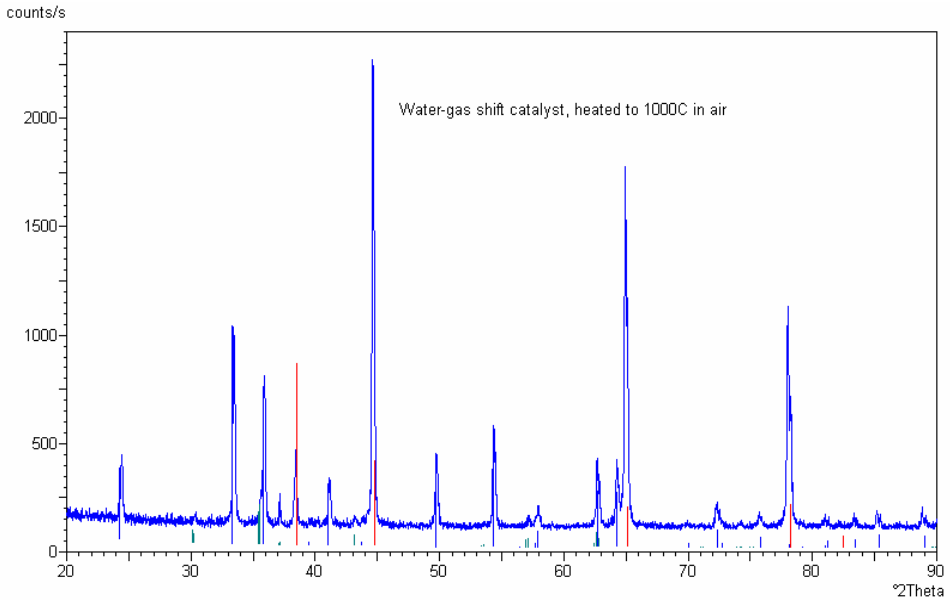

1.2.1.1.4.7 (5) XRD pattern of catalyst powder after heating in air to 1000°C. Blue lines mark position of Fe_2O_3 peaks; green for Fe_3O_4, and red for aluminum sample holder. Peaks have sharpened relative to the as-received pattern, indicating particle sintering at very high temperature. Maximum catalyst operating temperature is 440°C.

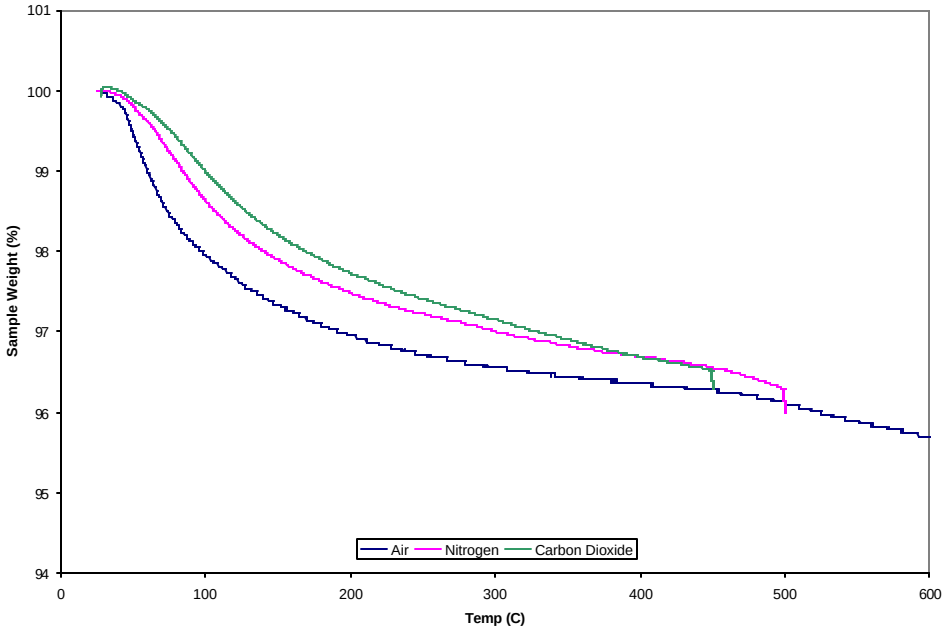

1.2.1.1.4.7 (6) TGA results of catalyst tested in air, nitrogen, and carbon dioxide.

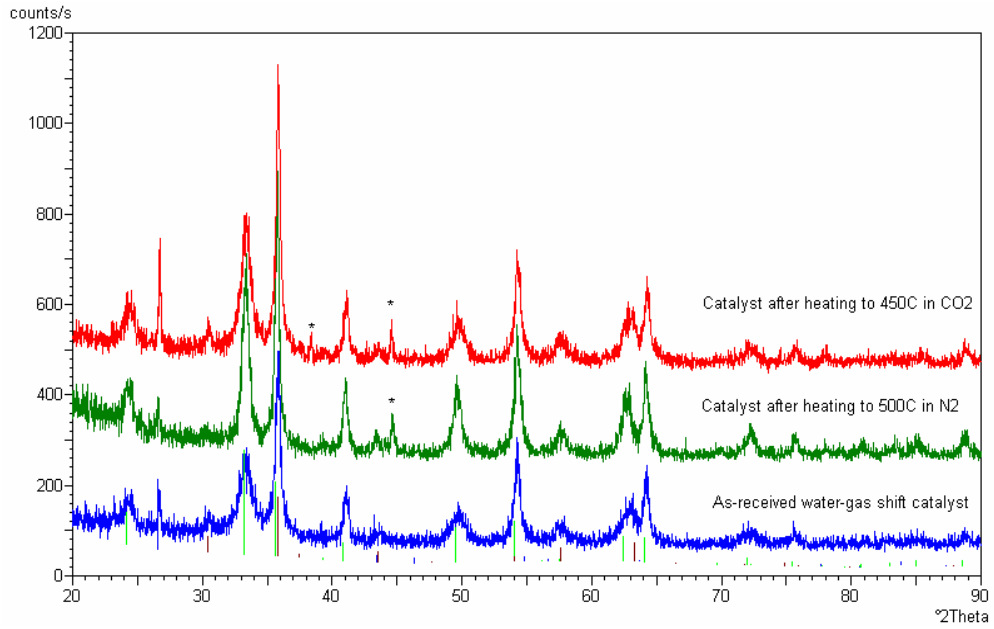

1.2.1.1.4.7 (7) XRD patterns of catalyst powders after testing stability in nitrogen and carbon dioxide.

Some stability tests of these catalysts were performed by thermogravimetric analysis (TGA) and XRD (see Figure 1.2.1.1.4.7 (6)). Thermogravimetric analysis of catalyst powder was performed by heating in air, in N_2, and in CO_2. Weight loss was seen for all three cases. TGA analysis of catalyst powder in air was performed to 900°C. A 2.38% weight loss was seen as a sample was heated to 100°C, and was attributed primarily to desorption of water. An additional 2.23% weight loss was observed between 100°C and 600°C and would likely result from loss of organic binders, but may also be attributed to decomposition of hydrates. Above 600°C, the decomposition or oxidation of carbon occurred and resulted in an additional 1.24% weight loss. Ultimate weight loss was equivalent in both N_2 and CO_2, but rates varied slightly.

XRD patterns were taken of samples heated in nitrogen atmosphere to 200°C, 400°C and 500°C. XRD of each of these samples showed no significant changes, with slight sharpening of peaks only at 500°C (see Figure 1.2.1.1.4.7 (7)), which is beyond the normal maximum use temperature of 440°C. Catalysts were heated to 450°C in 100% CO_2 to resolve issues of possible iron carbonate formation discussed in the literature. No carbonate phase formation was detected by XRD in two spots, and it was concluded iron carbonate formation is not an issue at this time, at least in dry CO_2. Only minimal peak sharpening was observed after heating.

1.2.1.1.4.7.2 Hydrogen Permeation Studies in Ambient Reactors

1.2.1.1.4.7.2.1 A. Effects of Different Catalyst Preparation Methods

In this period, several techniques were tried to improve catalyst coatings on the surfaces of the membrane. Three different treatments were compared. The corresponding hydrogen permeation data of these various membranes are discussed in the following paragraphs.

Table 1.2.1.1.4.7 (1) summarizes the permeation data from the membranes which had no catalysts and which had catalysts deposited by three procedures. As expected, the hydrogen flux through the membrane is not detectable when no catalyst was applied on the surfaces of the membrane. The cleaning process used to clean the surface of the membrane has an important effect on the transport properties of the membrane.

1.2.1.1.4.7 (1)
Hydrogen Permeation Data Through Various Metal Membranes

Membrane Type	Temperature (EC)	H_2 flux ($mL/min \cdot cm^2$)	Permeability ($mol \cdot m/m^2/s/Pa^{1/2}$)
sw-M no catalyst	320	not detectable	NA (very low)
Catalyst / u-M	320	6.0	3.5E-08
Catalyst / *sw*-M	320	15.9	1.4E-07
Catalyst / *Arp*-M	320	17.4	1.6E-07

In summary, the processing techniques involved in depositing hydrogen dissociation catalysts on the membranes exert a significant effect on the transport properties of the membranes. Cleanliness is absolutely essential to obtain the membranes that exhibit excellent hydrogen permeation properties. Taking care during the preparation of the membranes, we have repeatedly been able to achieve high performance of hydrogen permeation in the catalytic membrane reactor (CMR). The permeability of our membranes is 15-20 times better than that of a pure palladium membrane. Earlier permeation data discrepancies (*e.g.*, lower permeability from the Phase I and earlier reports) were the results of using the membranes which were processed with the non-optimized procedure.

1.2.1.1.4.7.2.2 B. Temperature Effect

Hydrogen permeation at various temperatures was examined in this period. Ideally, the temperature effect on the permeability can be used to derive the activation energy of the hydrogen permeation by plotting the *ln(permeability) vs. 1/T*. The slope of the line is related to the activation of the process by the following equation: $E_a = -R \times Slope$, where R is the gas constant 8.314 $JK^{-1}mol^{-1}$. However, the hydrogen permeation that we studied in this program is a complicated process. This involves H_2 absorption and desorption on the respective surfaces, subsequent H_2 dissociation and association on the surface sites, hydrogen dissolution into bulk metal, and hydrogen diffusion through the membrane. Each of these "processes", which may exhibit a different temperature dependency, can be the rate limiting step of the hydrogen transport depending on the specific operating conditions (*e.g.*, temperature, hydrogen partial pressure, catalyst thickness, and presence and types of impurities). Bearing these considerations and literature data in mind, we studied the temperature dependence on several catalyst coated membranes and one palladium membrane. The preliminary results are discussed in the following paragraphs.

In Figure 1.2.1.1.4.7 (8), hydrogen permeability of pure Pd metal as a function of inverse temperature was plotted. The observation that hydrogen permeation increases with increasing temperature is consistent with the literature. From the slope of the fitted linear regression, an activation energy of 14 kJ/mol was obtained based on these experimental data.

(a) (b)

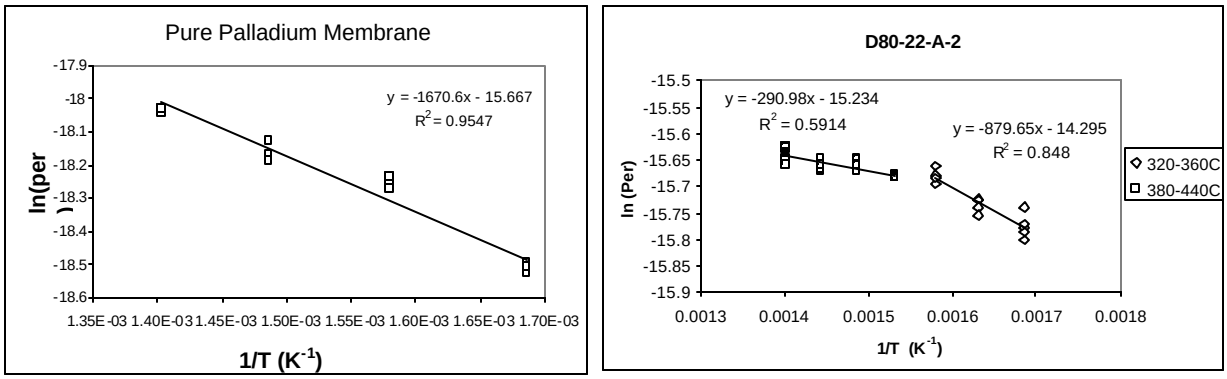

1.2.1.1.4.7 (8) (a) Arrhenius plot of the permeability for hydrogen through pure palladium. An activation energy of +14 kJ·mol^{-1} is found from the slope. (b) Plot for Eltron membrane. Activation energies are 7.31 kJ/mol for low temperature (320-360°C) and 2.42 kJ/mol at high temperature (380-440°C) implying a likely change in mechanism of the rate limiting step.

The results from studying the temperature effect on our composite membranes are not quite as straightforward. We are currently collecting more data in order to comprehensively understand the observed temperature effect. Intuitively, the diffusion either through the palladium catalyst layer or the membrane can be the rate limiting mechanism. Therefore, the apparent activation energy we derived from our permeation data at various temperatures will also be substantially influenced by the catalyst layer thickness and the interfacial interactions between the catalyst and membrane. The preliminary results obtained from our best composite membranes show two distinct slopes in the temperature range of 320-440°C. In the low temperature range of 320-360°C, the permeability increased with increasing temperature, and the apparent activation energy is ~6 kJ/mol. In the high temperature range of 380-440°C, the permeability started decreasing with increasing temperature, and negative activation energies of -7 and -12 kJ/mol were derived from two of the membranes. The temperature of 360-380°C seems to be the optimal range in term of producing the highest hydrogen flux. We are currently not certain of the cause of the decline of the hydrogen flux at the higher temperature range, although it is not unprecedented to obtain a negative activation energy for membranes which dissolve less hydrogen at high temperatures. It is possible that two different mechanisms are dominating the hydrogen permeation at these two different temperature ranges. The lowest permeability we observed from our composite membranes was over 1.5×10^{-7} mol·m^{-1}·s^{-1}·Pa$^{-0.5}$ at 440°C, and the derived activation energies (positive or negative) are rather small. In other words, the hydrogen permeation of our membranes is excellent, and only exhibit slight temperature dependency in the range of 320-440°C. Considering the complex nature of the hydrogen transport through our composite membrane and the variations involved in processing and data collection, more thorough studies on this matter are needed in the future. For the time being, 2.0×10^{-7} mol·m^{-1}·s^{-1}·Pa$^{-0.5}$ is a safe upper estimate of the permeability for the engineering design in the whole operating temperature range (320 to 460°C).

1.2.1.1.4.7.2.3 C. Effects of Using Dry Mixture Gas

Gas cylinders containing an $H_2/CO/CO_2/N_2$ mixture from Airgas Corporation were used as the source of the processing gas. A membrane was tested with this mixture gas as the feed for over 400 hours, and the permeation data were illustrated in Figure 1.2.1.1.4.7 (9). After the feed gas was changed from a H_2/He mixture (66% of H_2) to the $H_2/CO/CO_2$ mixture, the permeability dropped ~ 40% within 2 hours, and continuously decayed at a slower rate over time. At 400 hours, the permeability is only ~ 25% of the original values. This membrane displayed serious discoloration after the usage, and formation of significant amount of carbon black inside the reactor was observed. It was very likely that the following

reactions occurred under this operating condition, and the products, especially carbon, from these reactions seriously reduced the performance on the membrane.

$$CO + 3H_2 \;\; 6 \;\; CH_4 + H_2O \qquad)H = -206.2 \text{ kJ/mol}$$
$$2CO \;\; 6 \;\; C + CO_2 \qquad)H = -172.5 \text{ kJ/mol}$$

It is well known that these undesired reactions can be encountered when operating at low steam ratios in the water gas shift reaction, and the introduction of the steam is necessary to avoid the carbon formation (Twigg, M.Y., 1997). In the presence of full steam, deposition of carbon is not likely to present a problem.

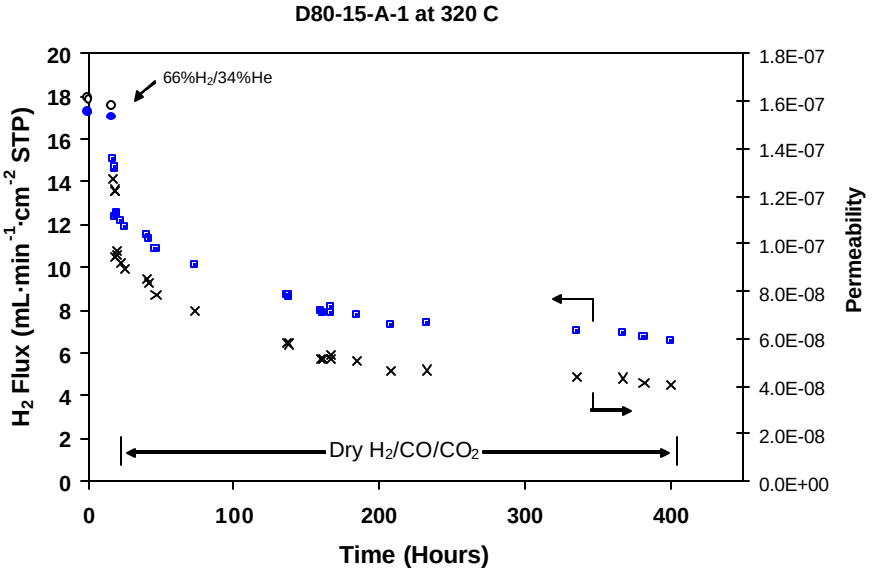

1.2.1.1.4.7 (9) Hydrogen flux and permeability of the composite membrane at 320°C with the dry mixture gas as the feed. (o and ? mark the hydrogen flux and hydrogen permeability for the case of an ideal hydrogen/helium mixture. ¦ and x mark the hydrogen flux and hydrogen permeability in a dry gas mixture containing CO, CO_2, H_2 and N_2. Carbon deposition appears to cause a loss of flux with time, and implies that full steam must be applied to remove carbon.

1.2.1.1.4.7.2.1 D. Hydrogen Permeation with the Full Processing Gas

The specified mole percent gas composition of the full processing feed contains H_2O, H_2, CO, CO_2, and balance of N_2 and other impurities. The steam content in the feed gas was controlled by using a water pump to deliver a calculated amount of liquid water (g/min.) that corresponds to ~37.3 vol% in the feed steam. The necessary amount of water was delivered to a feed line, which was heated to ~300°C with a heating tape, before entering into the membrane reactor. Several membranes were tested in the CMR reactor to study the hydrogen permeation with this processing gas. Figure 1.2.1.1.4.7 (10) plots the hydrogen flux and permeability *vs.* time from one of these membranes. It was clear that hydrogen flux suffered a initial drop right after the addition of steam. This initial sudden decline of the hydrogen flux is likely caused by the reduction of the hydrogen concentration (dilution) and the temperature at the membrane. However, hydrogen permeation slowly recovered to reach a steady state (~ 12 mL/min. cm^2) in 10 hours, and the corresponding permeability is ~ 8.5×10^{-8} $mol.m^{-1}s^{-1}Pa^{-0.5}$ This value is remarkable, and ~9 times better than that of Pd membrane which was operated with an ideal H_2/He mixture. The recovery may imply an initial deposit of impurity onto the surface of the membrane by hydrothermal transport, which is then removed by steam over time.

In summary, we have been successfully operating the hydrogen separation membranes with the true processing gas. The addition of steam in the feed has a negative effect on hydrogen permeation. Permeability dropped to ~50% (in the best cases) as compared with that of using dry gas. We are currently trying to find out the cause of this decline. Besides the cooling effect from the addition of steam, there was some evidence indicating that steam may deposit impurities, such as Fe, Cr, and Ni, from the steel alloy reactor that we are using for housing the membrane. EDX and XPS analysis on the feed sides of several post-run membranes indicated the presence of Fe, Cr, Ni *etc*. metal impurities. In one extreme case, Fe_3O_4 crystals were found on the feed surface of the membrane after long exposure to the steam.

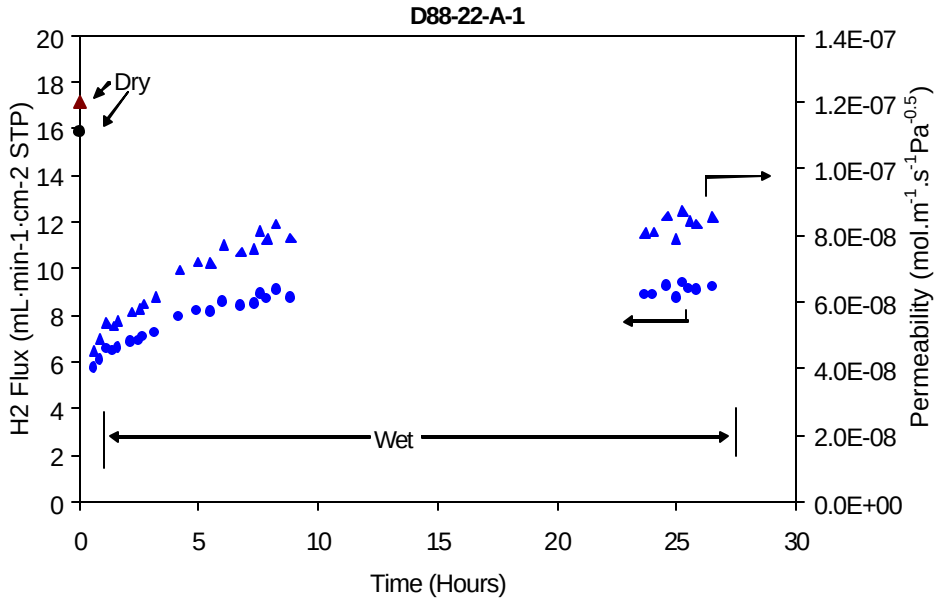

1.2.1.1.4.7 (10) Hydrogen flux and permeability with the full processing gas in the feed. (? and ? are the H_2 fluxes and permeability data, respectively.)

1.2.1.1.4.7.2.1 E. Effect on Hydrogen Permeation by the Up-Stream WGS Catalyst Beds

In this period, we designed and built a membrane reactor with the incorporation of water-gas shift reactors up-stream. The design allows us to collect the hydrogen permeation data with or without the WGS catalyst bed. In a typical experiment, the processing gas is fed first into the membrane reactor directly (bypassing the WGS catalyst bed). When the permeation stabilizes, the catalyst bed is then brought on-line to study the effect of the up-stream catalyst bed on the hydrogen permeation. One example is illustrated in Figure 1.2.1.1.4.7 (11). Moments after the catalyst was brought on line, the hydrogen flux through the membrane increased. This behavior probably reflects an increase of hydrogen concentration in the feed due to the water-gas shift reaction. Based upon equilibrium calculations, for example, the H_2 concentration is expected to increase to 43.4% from 41.4% after the feed stream passes the WGS catalyst at 360°C. The membrane displayed discoloration after use. EDX analysis on the membrane after use often reveals the presence of impurities such as C, S, Si, Cl *etc*. on the feed side of the membrane. It is apparent that steam can transfer many contaminants from the up-stream WGS catalyst bed. Currently, we are working on adding guard beds of high surface area ceramic as a strategy to getter the impurity compounds before they reach the membranes. In addition, the water-gas shift catalysts will be purged for extended periods of time with the water-gas shift mixture to remove the impurities, especially sulfur, before the membranes are brought on-line.

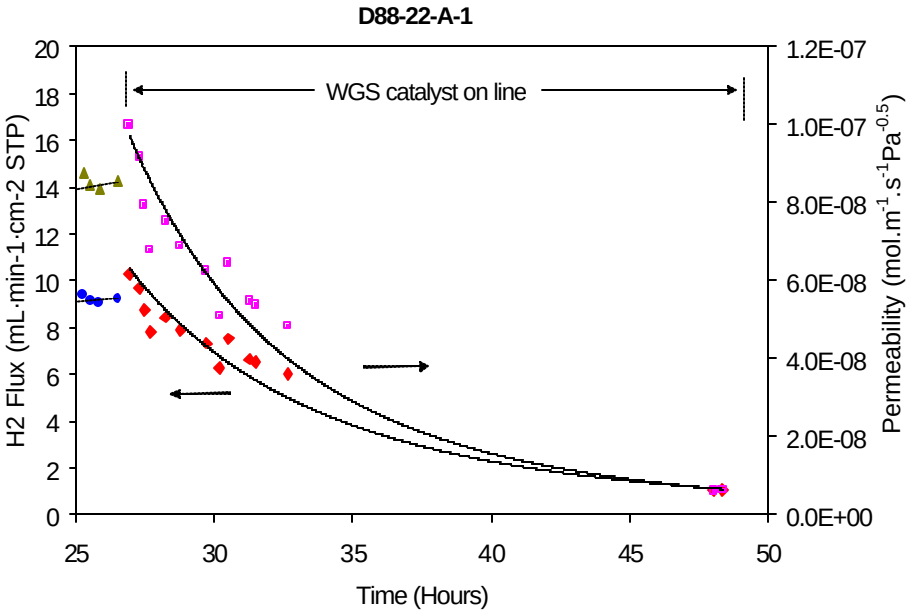

1.2.1.1.4.7 (11) Hydrogen flux and permeability of a membrane with a water-gas shift catalyst bed upstream. (? and ? are H_2 fluxes, and ? and ¦ are the permeability)

1.2.1.1.4.7.3 Stacked Hydrogen Separation Membrane Unit

We have initiated steps towards scale-up of our hydrogen separation membrane unit. Design and fabrication of a stacked separation unit has been completed in order to demonstrate that our membranes may be ultimately amenable to scale-up via a continuous stacked design we have constructed a stacked separation unit composed of two membranes arranged in series. Figure 1.2.1.1.4.7 (12) presents a cross-sectional schematic of the dual stacked hydrogen separation membrane assembly.

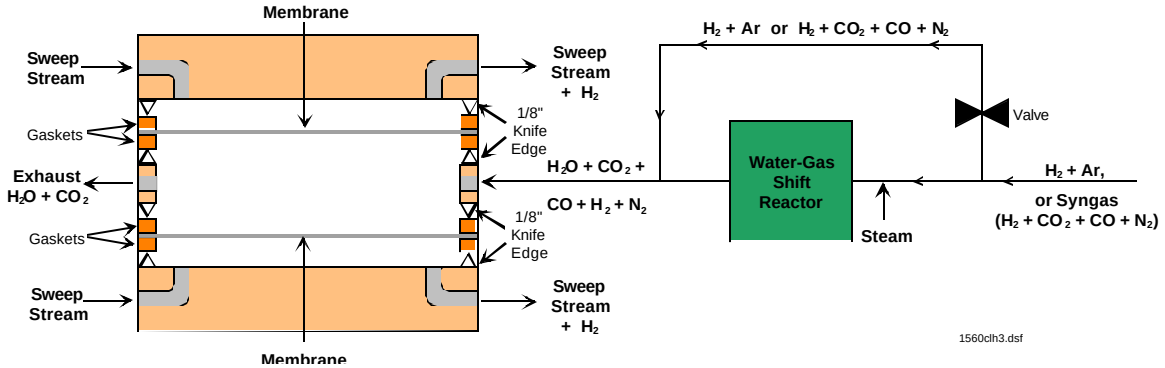

1.2.1.1.4.7 (12) Cross-sectional schematic of stacked hydrogen separation membrane unit.

Two 4.80 cm (1.89 inch) diameter membranes are enclosed in a series of knife-edge flanges. The seal is made by bolting together two identical flanges with a flat metal ring gasket between the knife edges, Figure 1.2.1.1.4.7 (12). The knife-edges press annular grooves in each side of the softer gasket material which fills voids and defects in the knife-edges producing a leak tight seal. Flanges are tapped with 1/4-28 NPT and can be attached directly to a water gas shift reactor or any hydrogen feed stream, as

illustrated in Figure 1.2.1.1.4.7 (12). A feed stream is directed toward the interior of the membrane stack through a centrally located flange. Hydrogen enters the stack between the two membranes and is selectively removed via migration across or through the membrane. Inert gas sweep streams are directed on each side of the membranes in order to efficiently remove hydrogen gas from the stacked membrane unit.

Figure 1.2.1.1.4.7 (13) presents an exploded view of a dual stacked hydrogen separation membrane unit. In this configuration three 1/4-28 NPT flanges are terminated with two individual blank flanges in order to enclose the separation membranes. Flange diameter is 7.00 cm (2.75 inches), membranes are machined to the outside diameter of the copper gasket (4.80 cm, 1.89 inch). Usable membrane area corresponds to the inside diameter of the copper gasket. Inside diameter of the copper gasket is equal to 1.45 inches providing an active membrane area of 10.6 cm^2 or 1.65 in^2 for each membrane or 21.3 cm^2, 3.3 in^2, of total active membrane area combined.

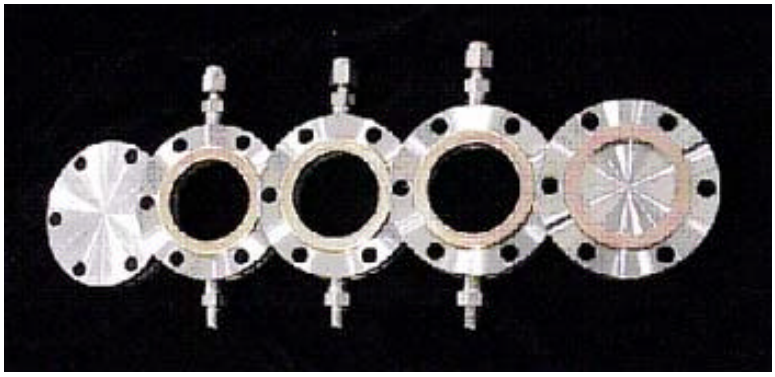

1.2.1.1.4.7 (13) Exploded view of stacked hydrogen separation membrane unit.

Figure 1.2.1.1.4.7 (14) shows a view of the fully assembled unit, this unit has a height of approximately 6.4 cm (2.5 inches) and with a diameter of 7.0 cm (2.75 inches) occupies a total volume of only 176.8 cm^3 (10.79 in^3).

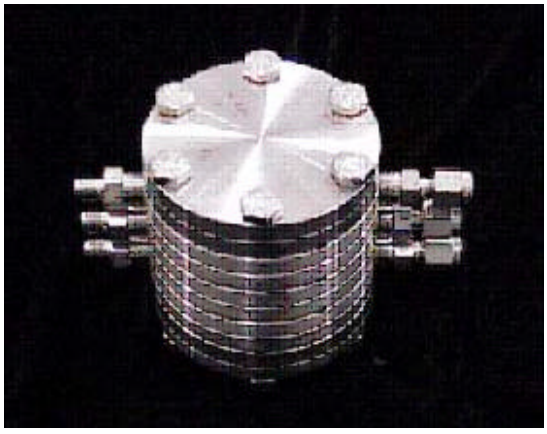

1.2.1.1.4.7 (14) Fully assembled stacked hydrogen separation membrane unit, prior to connection to feed and sweep stream gas sources.

The membrane unit was built to achieve a total hydrogen flux of approximately 213 mL/minute with feed flow rates of 1.7 L/minute and sweep rates of 2.7 L/minute, assuming linear behavior between membrane size, flux and flow rates.

In order to maintain seal or leak integrity and in the interest of safety 0.635 cm (0.25 inch) diameter stainless steel tubing was welded to each of the three tapped CF flanges. The stainless steel tubing is then routed to the exhaust and feed and sweep stream gases. Figure 1.2.1.1.4.7 (15) depicts a fully assembled membrane stack, including 0.635 cm diameter stainless steel gas tubing rising above the ceramic kiln oven. The stack is centered in a ceramic brick kiln oven and routed to source and sweep gases.

Figure 1.2.1.1.4.7 (16) presents the fully constructed hydrogen separation membrane unit with associated hardware. This simple design requires minimal accessories as shown in Figure 1.2.1.1.4.7 (16), bank of flow tubes, ceramic brick kiln oven, thermocouple and temperature control programmer. The unit is thoroughly leak tested prior to each operation.

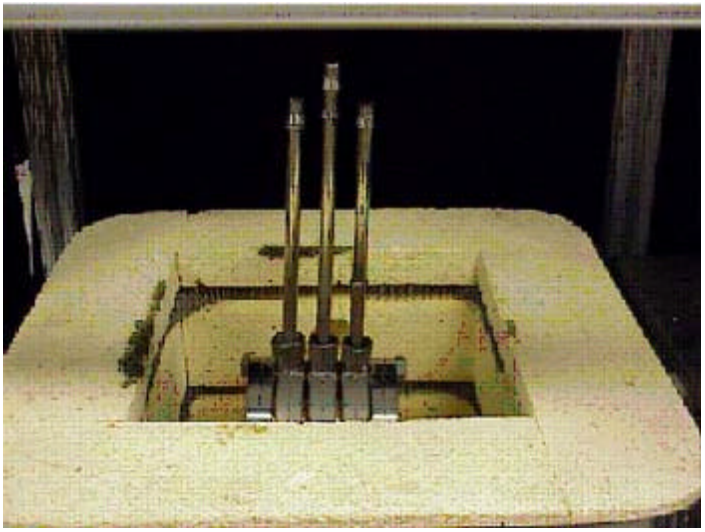

1.2.1.1.4.7 (15) Digital photograph of fully assembled stacked hydrogen separation membrane unit - just prior to use.

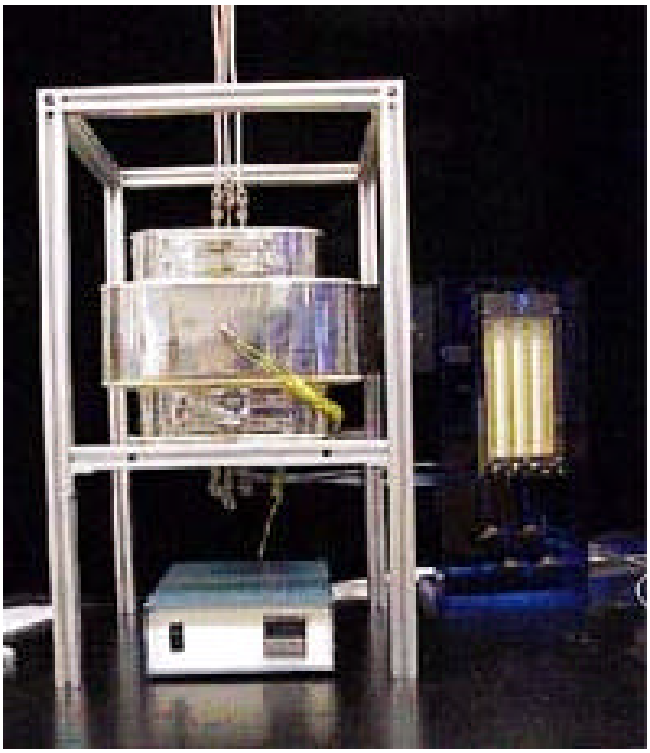

1.2.1.1.4.7 (16) Fully assembled configuration for operation of stacked hydrogen separation membrane unit.

We have operated the stacked separation unit to achieve hydrogen flux values in the same range as the 2.0 cm^2 membrane separation units currently operated by Eltron Research.

These proof of concept experiments are in no way indicative of the potential for total hydrogen flux achieved by units of this general configuration. This is a first design of our separation unit and improvements can definitely be expected. For example, feed stream flow through the stacked unit is directed parallel to the membranes. Rearrangement of flow direction or design of a configuration which reduces laminar flow and increases turbulence will increase hydrogen residence time and undoubtedly increase flux. Experiments were performed in order to verify the effect of increasing hydrogen content in the feed stream upon hydrogen flow or flux on the sweep side of the stacked membrane assembly.

Figure 1.2.1.1.4.7 (17) presents a plot of total hydrogen flow on the sweep side versus volume percent hydrogen on the feed side of the membrane. Volume percent hydrogen on the feed side was varied from 10 to 15 to 20 to a maximum of 30 percent. The plot simply shows the increasing amount of hydrogen extracted by the membrane as a function of increasing hydrogen concentration on the sweep side.

Figure 1.2.1.1.4.7 (18) presents a plot of individual membrane flux as a function of increasing hydrogen concentration on the sweep side again the plot shows an increase in hydrogen flux with an increase in hydrogen concentration. Examination of Figure 1.2.1.1.4.7 (18) also reveals the dependence of permeability upon hydrogen concentration. As the hydrogen concentration increases the permeability also increases as expected.

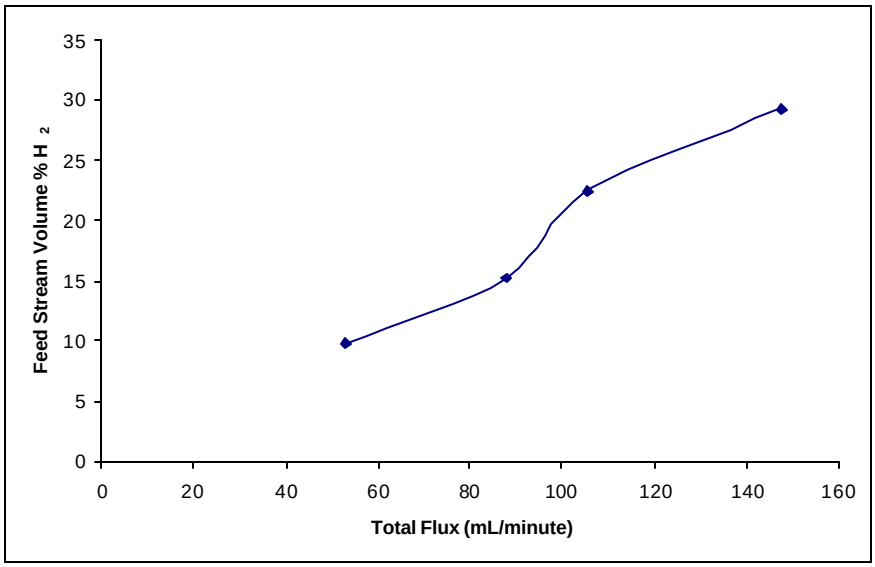

1.2.1.1.4.7 (17) Total flux versus volume percent hydrogen for stacked membrane separation unit.

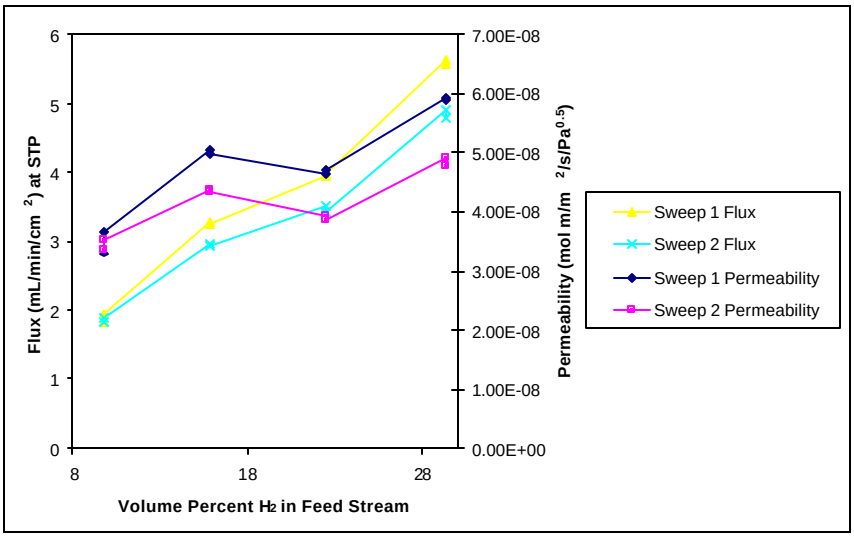

1.2.1.1.4.7 (18) Hydrogen flux and permeability versus volume percent hydrogen in the feedstream for the stacked hydrogen separation membrane unit.

1.2.1.1.4.7.4 Results of High Pressure Tests.

Initial high pressure tests were run for 100 hours at 400°C at a partial pressure of hydrogen of 3 bar at an absolute pressure of 32 bar and a differential pressure of 31.3 bar. After 100 hours, the system was purged of hydrogen and cooled. The membrane disk had distorted slightly over 0.5 mm in the center from the pressure. X-ray diffraction showed complete membrane stability.

Membranes, which were approximately 127 microns in thickness, were successfully tested under differential pressures of up to 31.3 bar (454 psi) and an absolute pressure of approximately 32 bar and a partial pressure of hydrogen of 6.4 bar on the hydrogen feed side of the membrane. Figure 1.2.1.1.4.7 (19) shows hydrogen flux and hydrogen permeability measurements for a membrane, 1.59 cm (5/8 inch) diameter with active surface area of approximately 2.0 cm^2. These preliminary measurements were done with an ideal dry hydrogen/inert gas atmosphere on the hydrogen feed side of the membrane.

Hydrogen flux remained steady for approximately 300 hours, and the membrane did not embrittle or leak under these operating conditions. (The test was terminated after a local power outage at 307 hours.) Tests were run at 673 K (400°C), which is in the middle of the temperature range for the water-gas shift reaction. These preliminary measurements were performed within eight weeks into the Phase II project after designing, building and commissioning the new high pressure system. Membranes will next be tested with the full target partial pressure of hydrogen of 13.2 bar on the feed side of the membrane and then with the full steam and water-gas shift gas mixture.

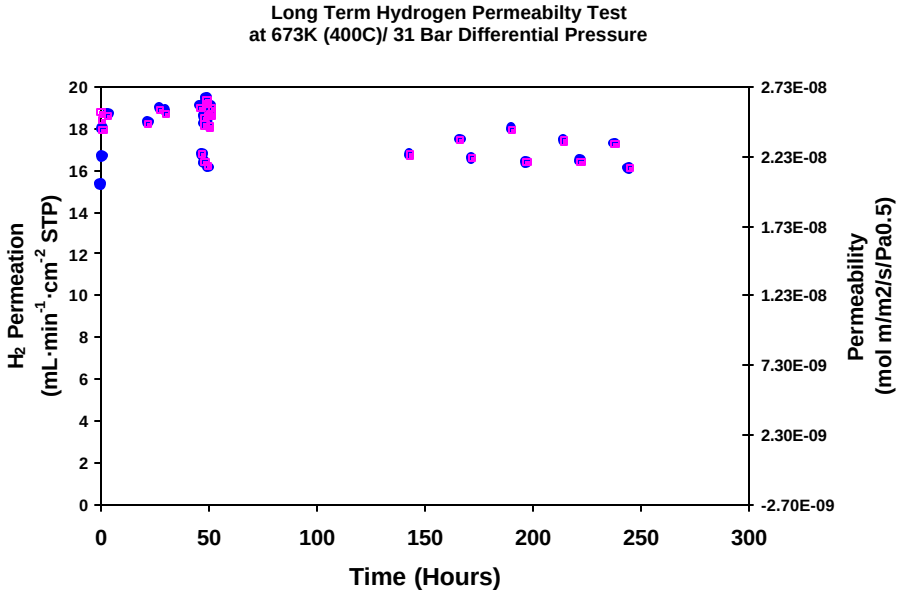

1.2.1.1.4.7 (19) Results of a long-term test measuring hydrogen flux and hydrogen permeability in a high-pressure reactor. A dry 20 mol % mixture of hydrogen plus inert gas was fed to the retentate side of the membrane at approximately 32 bar absolute pressure. A differential pressure of 31.3 bar was maintained across the membrane for over 300 hours at 673 K (400°C). Permeability remains approximately steady at slightly over 2 x 10^{-8} mol·m·m^{-2}·s^{-1}·$Pa^{-0.5}$ for the 300 hour period, which is comparable to membranes of pure palladium. The tests show that a 127 micron thick membrane can resist these differential pressures without leak or hydrogen embrittlement.

1.2.1.1.4.8 Conclusion

It has been demonstrated that Eltron membranes can withstand 31.3 bar differential pressure across them while exposed to 6.4 bar partial pressure of hydrogen. The first project goal of successfully testing to 30 bar differential pressure has thus been met. Initial hydrogen permeabilities of up to 2 x 10^{-7} mol m m^{-2} s^{-1} $Pa^{-.05}$ have been consistently measured in ambient pressure reactors. These values of permeability are approximately ten times *better* than pure palladium membranes run under similar conditions. If these permeabilities can be maintained, membrane costs could be reduced below U.S. $1 million for a power plant emitting 2 million metric tons of CO_2 annually. Membranes have already been integrated with water-gas shift catalysts.

1.2.1.1.4.9 References

Amandusson, H., AHydrogen Extraction with Palladium Based Membranes,@ Dissertation No. 651, Linköping University, Linköping, Sweden, 2000.

Amandusson, H., L.-G. Ekedahl, and H. Dannetun, AThe Effect of CO and O_2 on Hydrogen Permeation through a Palladium Membrane,@ Applied Surface Sci. 153 (2000) 259-267.

Basile, A., A. Criscuoli, F. Santella and E. Drioli, AMembrane Reactor for Water Gas Shift Reaction,@ Gas. Sep. Purif. 10 no. 4 (1996) 243-254.

Benzinger, J. B., AThermochemical Methods for Reaction Energetics on Metal Surfaces,@ in: AMetal-Surface Reaction Energetics,@ edited by E. Shustorovich, (VCH Publishers, Weinheim, Germany, 1991) pp. 53-107.

Criscuoli, A., A. Basile, and E. Drioli, AWater Gas Shift Reaction in a Membrane Reactor: Experimental and Theoretical Results,@ AIDIC Conference Series, Vol. 3 (1997) 1-7.

Criscuoli, A., A. Basile, and E. Drioli, AAn Analysis of the Performance of Membrane Reactors for the Water-Gas Shift Reaction Using Gas Feed Mixtures,@ Catalysis Today 56 (2000) 53-64.

Criscuoli, A., A. Basile, E. Drioli, and O. Loiacono, AAn Economic Feasibility Study for Water Gas Shift Membrane Reactor,@ J. Membr. Sci. 181 (2001) 21-27.

Cusumano, J. A., R. A. Dalla Betta, and R. B. Levy, ACatalysis in Coal Conversion,@ (Academic Press, New York, 1978).

Galasso, F. S., AStructure, Properties and Preparation of Perovskite-Type Compounds,@ (Pergamon Press, Oxford, 1969).

Gaudernack, B. and S. Lynum, AHydrogen from Natural Gas without Release of CO_2 to the Atmosphere,@ Int. J. Hydrogen Energy 23 (1998) 1087-1093.

Henrich, V. E., and P. A. Cox, AThe Surface Science of Metal Oxides,@ (Cambridge University Press, Cambridge, 1996) p. 10.

Lund, C. R. F., AMicrokinetics of Water-Gas Shift over Sulfided Mo/Al_2O_3 Catalysts,@ Industrial & Engineering Chemistry Research 35 (1996) 2531-2538.

Paglieri, S. N., and J. D. Way, AInnovations in Palladium Membrane Research,@ Separation and Purification Methods 31 (2002) 1-169.

Raask, E. AMineral Impurities in Coal Combustion,@ (Hemisphere Publishing Corporation, Washington, 1985).

Twigg, Martyn V., ACatalyst Handbook, Second Edition,@ (Manson Publishing, London, 1997).

1.2.1.1.4.10 Publications

Not applicable.

1.2.1.1.4.11 Bibliography

Riemer, W. F., Editor, ACarbon Dioxide Disposal, Proceedings of the International Energy Agency Carbon Dioxide Disposal Symposium, Oxford 29-31 March, 1993,@ Pergamon Press, Oxford, 1993).

Dinjus, E., Editor, Fifth International Conference on Carbon Dioxide Utilization, Karlsruhe, 5-10 September, 1999,@ (Gesellschaft Deutscher Chemiker, Frankfurt on Main, 1999).

1.2.1.1.4.12 List of Acronyms and Abbreviations

BET	Brunauer-Emmett-Teller (A Surface Area Measure Technique)
CCP	Carbon Capture Project
CF	ConFlat
CMR	Catalytic Membrane Reactor
DOE	Department of Energy
eV	electron Volt
JCPDS	Joint Committee on Powder Diffraction Standards
JEOL	Japan Electron Optics Limited
JSM	JEOL Scanning Microscope
GC	Gas Chromatography
MPa	Mega Pascal
NPT	National Pipe Taper
psi	pounds per square inch
SEM	Scanning Electron Microscope
STP	Standard Temperature and Pressure
TGA	Thermal Gravimetric Analysis
WGS	Water-Gas Shift
XPS	X-Ray Photoelectron Spectroscopy
XRD	X-Ray Diffraction

1.2.1.1.4.13 Appendix - Phase 1 Report

Eltron Research Inc.
4600 Nautilus Court South
Boulder, CO 80301-3241

Final Report

Integrated Water-Gas Shift/Hydrogen Transport Membrane Technology for Simultaneous Carbon Dioxide Capture and Hydrogen Separation

February, 2003

Prepared by
Eltron Research Inc.
on behalf of the CO_2 Capture Project

Final Report

INTEGRATED WATER-GAS SHIFT/HYDROGEN TRANSPORT MEMBRANE TECHNOLOGY FOR SIMULTANEOUS CARBON DIOXIDE CAPTURE AND HYDROGEN SEPARATION

For the Period March 15, 2002 - February 28, 2003

Submitted to

Peter Middleton
BP
Sunbury on Thames, Middlesex, UK

CO_2 Capture Project Consortium and Cofunding from the U.S. Department of Energy under Solicitation DE-PS26-99FT40613 in the category "Applied Research and Development of Technologies for the Management of Greenhouse Gases"

from

Eltron Research Inc.
4600 Nautilus Court South
Boulder, CO 80301-3241, USA

Voice: 303-530-0263
Fax: 303-530-0264
Email: afs@eltronresearch.com

February 28, 2003

TABLE OF CONTENTS

ABSTRACT

Dense nonporous composite membranes, capable of high hydrogen permeability and 100% hydrogen selectivity, were developed and tested at Eltron Research Inc. Matching of the metal and ceramic minimized stress at the ceramic-metal interfaces and maximized the mechanical strength of the cermets. The membranes possessed a permeability for hydrogen near that of pure palladium, but possessed added mechanical integrity. In a second embodiment, methods were developed for sintering fine, sub-micron size particles of ceramic on top of coarser ceramic particles of the same material. The ceramic was designed to have nearly identical lattice constants as palladium.

In order to exceed hydrogen fluxes beyond the limits of palladium, and in order to drastically reduce costs associated with palladium, composite membranes were also produced. Some of these membranes possess values for hydrogen permeability over 10 times that of palladium—but at only a fraction of the cost.

The following are highlights of accomplishments achieved at Eltron Research Inc. during the Phase I Project:

- Composite membranes were developed with 100% selectivity towards hydrogen permeation.

- New ceramics were designed and synthesized to both lattice match and possess similar coefficients of thermal expansion to palladium. Cermets were successfully fabricated and tested and found to have hydrogen permeabilities comparable to pure palladium.

- Low-cost composite membranes were fabricated and tested and were found to have hydrogen flux of 12 $mL \cdot min^{-1} \cdot cm^{-2}$ (STP) corresponding to permeabilities for hydrogen of up to 6.4×10^{-8} $mol \cdot min^{-2} \cdot s^{-1} \cdot Pa^{-0.5}$ at 320°C which is superior to that of palladium under similar conditions.

- Membranes of select elements were successfully operated in high-pressure reactors and remained leak-free to helium up to 15 bar differential pressure and 450• € in hydrogen-helium test mixtures.

- A membrane was run continuously for over three months at 400°C in a hydrogen-helium test mixture, demonstrating long-term stability of the membrane materials towards hydrogen diffusion.

- Various hydrogen dissociation catalysts were screened under the full water-gas shift mixture with steam.

EXECUTIVE SUMMARY

Phase I Project Goals. The overall goal of the Phase I project was to develop and test membranes which are capable of separating hydrogen from high-temperature water-gas shift reactors, containing mole fraction compositions of 43.5% steam, 37.3% hydrogen, 16.5% CO_2, 2.2% CO, 525 ppmv H_2S, and balance of N_2, at absolute reactor pressures of 35 bar and differential pressure of 33 bar. Phase I tests were to be limited to a maximum of 15 bar differential pressure. The initial program solicitation requested tests to be run at 350°C, 400°C and 450°C, which is near the range of typical high-temperature water-gas shift reactors. However, the initial target temperatures were reduced by the Carbon Capture Project Consortium to 250°C, 350°C, and 450°C after the start of the project. The main deliverable of the project was to be data representing key aspects of membrane performance such as activation energies for hydrogen diffusion, pre-exponential factors in Arrhenius plots, and leak rate of components other than hydrogen. The data was to allow mathematical feasibility studies to be performed to determine if membranes are capable of recovering hydrogen at target goals of >95% from water-gas shift mixtures at a target hydrogen purity of >97%, while allowing CO_2 purity and recovery, both of >90%. Membranes would allow high purity hydrogen to be used as a clean fuel for turbine engines in electric power plants, while allowing high pressure CO_2 to be further compressed and sequestered.

Development of Dense Composite Membranes at Eltron Research Inc., Boulder, Colorado. The goal at Eltron Research Inc. was to develop and test dense membranes which are 100% selectively permeable to hydrogen. Dense membranes were selected over porous membranes because of concerns that the high-temperature, high-pressure, steam in water-gas shift reactors would cause excessive hydrothermal transport of silica and other materials used in conventional microporous membranes. Because of the high surface area and surface free energy of the porous membranes, there was concern that there would be a significant thermodynamic driving force for hydrothermal transport of silica on the surface of such membranes leading to plugging of the micro-pores by surface diffusion of silica over time. There were also concerns that only a few pinhole leaks in a porous membrane would lead to unacceptable loss of selectivity, which would be exasperated by the eventual required high absolute pressure of 35 bar and differential pressure of 33 bar.

Membrane Materials Development at Eltron Research Inc. The first strategy explored at Eltron Research Inc. was the development of composite membranes. Cermets are made by sintering together fine powders of metal and ceramic into a dense material. A matrix of ceramic in the cermet acts as a robust mechanical support for hydrogen permeable metals.

In the rational design of cermets, it is desired that the metal and ceramic possess similar coefficients of thermal expansion in order to avoid thermal stress, cracking, and delamination as membranes are successively heated and cooled. In designing metal-ceramic interfaces with a minimum of dislocations, a technique know as lattice matching was borrowed from the semiconductor industry, in which metals and insulating ceramics are commonly combined with semiconductors such as silicon, and in which dislocations and stress at interfaces is highly detrimental to the fabrication, processing, and functioning of semiconductor devices. In lattice matching, materials are selected, which at the atomic level, have similar crystallographic lattice constants and crystallographic symmetry.

Test Results for Cermets. Cermets fabricated by sintering together powders were tested initially from 400-800°C (673-1073 K) under ideal hydrogen-helium mixtures at ambient pressures and were stable and leak-free in this temperature range. Hydrogen permeabilities ranged from 4.44 x 10^{-9} mol•m•m^{-2}•s^{-1}•Pa$^{-0.5}$ at 400°C to 2.18 x 10^{-8} mol•m•m^{-2}•s^{-1}•Pa$^{-0.5}$ at 800°C. Cermets had an activation energy for hydrogen diffusion of 20,600 J•mol^{-1} and a pre-exponential factor, P_0, of 1.22 x 10^{-7} mol•m•m^{-2}•s^{-1}•Pa$^{-0.5}$. The pre-exponential factor for cermets in units of permeance was 3.06 x 10^{-4} mol•m•m^{-2}•s^{-1}•Pa$^{-0.5}$.

Cermets fabricated by sintering together powders were tested initially from 400-700°C (673-973 K) also under ideal hydrogen-helium mixtures at ambient pressures and were stable and leak-free in this temperature range. These materials had hydrogen permeabilities ranging from 3.08 x 10^{-9} mol•m•m^{-2}•s^{-1}•Pa$^{-0.5}$ at 400• C to 5.93 x 10^{-9} mol•m•m^{-2}•s^{-1}•Pa$^{-0.5}$ at 700°C. These cermets had an activation energy for hydrogen diffusion of 10,600 J•mol^{-1} and a pre-exponential factor, P_0, of 2.07 x 10^{-8} mol•m•m^{-2}•s^{-1}•Pa$^{-0.5}$. The pre-exponential factor for these cermets in units of permeance was 7.67 x 10^{-5} mol•m^{-2}•s^{-1}•Pa$^{-0.5}$. For comparison, literature values for thin foils of palladium show permeabilities typically from 1-2 x 10^{-8} mol•m•m^{-2}•s^{-1}•Pa$^{-0.5}$ and activation energies near 24,000 J•mol^{-1}. These hydrogen permeability measurements showed that these cermets were comparable to foils of palladium under similar conditions, but have the advantage that the ceramic phase provides enhanced mechanical support and ruggedness.

Thin Films Deposited on Top of Lattice Matched Porous Substrates. As a second strategy to improve membranes, thin films were deposited onto substrates. It was predicted that lattice-matched substrates would aid nucleation and growth of thin films in analogy to the epitaxial growth of overlayers deposited onto substrates used in the semiconductor industry. Use of electron-conducting substrates was also predicted to be an advantage over using insulating substrates such as alumina, because mobile electrons could aid in the reduction of precursor compounds during membrane preparation.

Fine, submicron size particles were synthesized by the glycine nitrate method. The SEM image in Figure 1 shows a 6-8 micron layer of the fine particles which were sintered to a porous substrate of micron-sized particles. Larger particles were used in the substrate to allow more rapid gas-phase diffusion of hydrogen through the voids between the particles. The sub-micron sized particles were used to support the layers because, in general, smaller pore sizes can be more easily plugged by thinner layers.

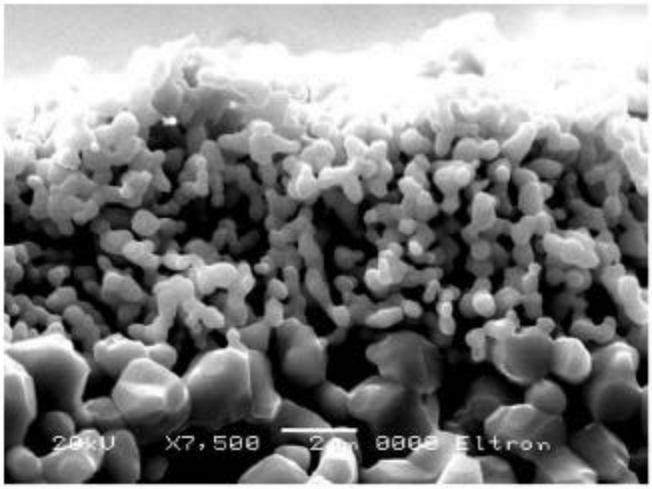

Figure 1. **SEM image shows a fine porous layer of ceramic sintered on top of a ceramic substrate of larger pore size and particle size. The substrate with large pore size allows rapid diffusion of hydrogen and is designed with a thickness to withstand large differential pressures. The fine porous layer acts as a substrate for materials used in the dense composite. Note the 2 micron bar scale showing that pores and particles in the top layer are sub-micron in size.**

Hydrogen Permeability Using Metal-Ceramic Composite Membrane Structures. A number of novel mechanical support mechanisms for these materials were devised and tested. Cermets and composite membranes were designed and fabricated. It was found that some materials could be made to resist up to 15 bar differential pressure without leak up to 450°C and survived over 90 days at ambient pressures at 400°C, under conditions of high hydrogen permeability. Tests were run between 310°C to 450°C for some of the materials at ambient pressures under ideal hydrogen-helium mixtures. Hydrogen permeabilities of between 3.28×10^{-8} mol•m•m^{-2}•s^{-1}•Pa$^{-0.5}$ at 360°C to 5.78×10^{-8} mol•m•m^{-2}•s^{-1}•Pa$^{-0.5}$ at 450°C were achieved. The best membrane yielded a pre-exponential factor, P_0, of 3.65×10^{-6} mol•m•m^{-2}•s^{-1}•Pa$^{-0.5}$, an exponential factor, Q_0, in units of permeance of 0.287 mol•m^{-2}•s^{-1}•Pa$^{-0.5}$, and an activation energy of 24,900 J•mol^{-1}. These values are comparable to palladium, but can be obtained with materials having only a fraction of the cost.

Ceramics were identified to match coefficients of thermal expansion of many of the materials. Use of porous ceramics in the support allowed rapid gaseous diffusion of hydrogen through the pores to the membrane-ceramic interface. Methods were developed for fabricating ceramics with porosity of approximately 40 - 45%. Thickness of the porous ceramic support was approximately 1500 microns (1.5 mm). Permeability of hydrogen at the lowest temperature tested, 320°C, was 6.4×10^{-8} mol•m•m^{-2}•s^{-1}•Pa$^{-0.5}$. Such values are superior even to palladium at similar conditions. The newly developed hydrogen permeable composite membrane materials show great promise because of low cost relative to palladium, higher permeability relative to